

ELECTROCHEMICAL DISCHARGE PHENOMENA IN MANUFACTURING PROCESSES

by

ALLESU KANJIRATHINKAL

ME

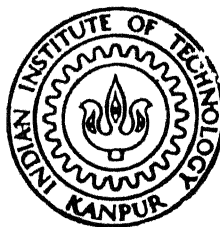
1988

D

KAN

ELE

JH
ME/1988/D
K132e



DEPARTMENT OF MECHANICAL ENGINEERING

INDIAN INSTITUTE OF TECHNOLOGY, KANPUR

DECEMBER, 1988

ME-1988-D-KAN-ELE

13 JUL 1990

TH
671.35
K132 e

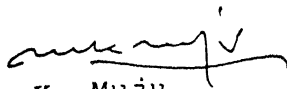
CENTRAL LIBRARY
I. I. T., KANPUR

Acc. No. A108474

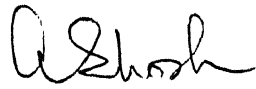
Dedicated To My
Reverend Parents
Smt. E.P. Kochurosa & Sri. K.P. Inasu

CERTIFICATE

Certified that this work entitled "Electrochemical Discharge Phenomena in Manufacturing Processes" has been carried out by Allesu Kanjirathinkal under our supervision and has not been submitted elsewhere for a degree.



M.K. Muju
Professor



Amitabha Ghosh
Professor

Department of Mechanical Engineering
Indian Institute of Technology
Kanpur-208016

ACKNOWLEDGEMENTS

The author expresses his deep sense of gratitude to Prof. M.K. Muju and Prof. A. Ghosh of Mechanical Engineering Department for suggesting the problem and guiding and encouraging me throughout the course of the work.

I am thankful to Mr. V. Raghuram, Research Engineer of the Department for his help in making the electrical circuits and Mr. O.P. Arora for fabricating some circuits for the work.

The author is thankful to the staff of the Manufacturing Science Laboratory M/s R.M. Jha, O.P. Bajaj, B.P. Bhartia, M.P. Sharma, Pannalal, Hirday Ram and Rajesh for their help in making the experimental set-ups.

I express my thanks to Dr. Bansi Lal of the Physics Department for sparing some of his valuable time on experiments with laser and Prof. U.C. Agarwala of the Chemistry Department for clarifying certain points.

The author is grateful to Dr. I.K. Bhat, Mr. S. Mandal, Dr. A.K. Naik and Mr. Joseph John for their suggestions on certain aspects of the work.

I thank Mr. Handoo of ISRO, for suggesting the coating material.

The author expresses his thanks to Mr. K.I. Ramachandran for the help he rendered during the experimentation.

Mr. C.M. Abraham and Mr. Vivek Shukla did the typing of the thesis, M/s S.S. Kushwah and G.K. Shukla has drawn the sketches and Mr. Ravi took the photographs. I am grateful to them all.

I extend my thanks to the administration of Regional Engineering College, Calicut and Ministry of Human Resource Development, Government of India for sponsoring me to pursue Ph.D. study under the Quality Improvement Programme.

My daughter Rose Catharine has kept me awake which indirectly helped to complete this work and my wife Lisy was always with me to help and encourage at every stage of the programme. This work would not have materialised without their contributions.

There are many others left, whose direct or indirect involvement has helped me to complete this research work and made the life at IIT Kanpur a memorable one. I thank them all.

Allesu. Kanjirathinkal

CONTENTS

	Page
Chapter I	
INTRODUCTION	1
1.1 Electricity Assisted Material Removal Processes	1
1.2 Electrochemical Discharges and Machining of Non-conducting Material	8
1.3 Review of Previous Work	9
1.4 Objective and Scope of Present Work	20
Chapter II	
ELECTROCHEMICAL DISCHARGE PHENOMENA AND MACHINING OF NON-CONDUCTING MATERIALS	24
2.1 Discharges in Liquid Dielectrics	24
2.2 Discharge Phenomena in Electrolytes	27
2.2.1 Electrochemical action (without electrical discharge)	28
2.2.2 Electrochemical action with electrical discharge between electrode and electrolyte	30
2.2.3 Electrochemical action with electrical discharges between electrodes	32
2.3 ECD Phenomena and Machining of Non-conducting Materials	36
Chapter III	
EXPERIMENTAL OBSERVATIONS AND DISCUSSIONS	39
3.1 Introduction	39
3.2 Experimental Set-ups	40
3.3 Preliminary Experiments	43
3.3.1 Machining of glass with coated tools	43
3.3.2 External supply of bubbles to the machining zone	44

3.4 Study of the ECD Configuration used for Machining Non-conducting Materials	46
3.4.1 Basic features of the ECD configuration	46
3.4.2a Behaviour of bubbles and voltage-current characteristics in the electrolyte bath without workpiece (negative tool)	49
3.4.2b Voltage-current characteristics in the electrolyte bath without workpiece (positive tool)	55
3.4.3 Potential drop across the tool and the non-machining electrode	56
3.4.4 Effect of electrolyte temperature on voltage-current characteristics	60
3.4.5 Effect of pressure on critical voltage	65
3.4.6 Effect of electrolyte flow on critical voltage	63
3.4.7 Voltage and current profiles with DC (smoothed) supply	69
3.4.8a Waveform of current with DC (full wave rectified) supply (negative tool)	71
3.4.8b Waveform of current with DC (full wave rectified) supply (positive tool)	76
3.4.9a Effect of electrolyte concentration	78
3.4.9b Effect of electrolyte temperature on the nature of discharge phenomena	83
3.4.10 Effect of tool diameter on voltage-current characteristics	84
3.4.11 Test for examining the bulk conductivity of glass	87
3.4.12 Voltage and current characteristics with NaCl and KOH electrolytes	87
3.5 Shifting of Discharge Zone from Tool Tip	92
3.5.1 Visual observation of shifting of discharge zone from tool tip	92
3.5.2 Potential along the hole depth and under the tool	94
3.5.3 Constant rate machining	103
3.6 Experiments Related to Current Density Effects	103
3.6.1 Voltage-current characteristics and waveform of current in a constricted electrolyte passage (plastic partitions)	103
3.6.2 Voltage-current characteristics and waveform of current in a constricted electrolyte passage (glass partitions)	108

	3.7 Experiments Related to Surface Conduction and Interfacial Phenomena of Glass and Other Non-conducting Materials	111
	3.8 Studies on Current Waveform during Machining of Glass and Plastic	119
Chapter IV	PROPOSED MECHANISM OF MATERIAL REMOVAL DURING ECDM OF NON-CONDUCTING MATERIALS	123
	4.1 Introduction	123
	4.2 Proposed Mechanism	123
	4.2.1 Influence of electrolyte concentra- tion and bulk temperature	128
	4.2.2 Influence of type of electrolyte	130
	4.2.3 Tool electrode polarity	131
	4.2.4 Tool shape and size	133
Chapter V	NON-MACHINING APPLICATIONS OF ECD PHENOMENA	135
	5.1 Microwelding of Wires	135
	5.2 Engraving on Glass	140
	5.3 Producing Fine Tapers at Wire Ends	142
Chapter VI	CONCLUDING REMARKS	146
References		148
Appendix		153

LIST OF FIGURES

Figure No.	Title	Page
1.1	Tool size and gap in electrical machining processes	3
1.2	Voltage and current density ranges of electrolyte-system of machining	5
1.3	Generally accepted mechanism of material removal (conducting materials)	7
1.4	Effect of electrolyte and polarity on material removal rate (work: glass) [2]	10
1.5	Effect of electrolyte temperature on removal rate (work material : glass) [2]	11
1.6	Effect of electrolyte concentration on removal rate (work material: glass) [2]	12
1.7	Showing limited machining depth (work material : glass) [2]	13
1.8	Effect of machining voltage on material removal rate (work material : glass) [3]	15
1.9	Effect of temperature of electrolyte on material removal rate (work material : glass) [3]	16
1.10	Effect of concentration of electrolyte (NaOH) on material removal rate (work material: glass) [3]	17
1.11	Limited depth characteristics (work material: glass) [3]	18
1.12	Conductivities of electrolytes [23, 31]	22
2.1	Discharge in liquid dielectrics	25
2.2	Schematics of ECM	29
2.3	Configuration of non-conductor work machining using ECD	37
3.1	Schematics of experimental set-up	41
3.2	Schematics of micro bubble generation	47

LIST OF FIGURES

Figure No.	Title	Page
1.1	Tool size and gap in electrical machining processes	3
1.2	Voltage and current density ranges of electrolyte-system of machining	5
1.3	Generally accepted mechanism of material removal (conducting materials)	7
1.4	Effect of electrolyte and polarity on material removal rate (work: glass) [2]	10
1.5	Effect of electrolyte temperature on removal rate (work material : glass) [2]	11
1.6	Effect of electrolyte concentration on removal rate (work material: glass) [2]	12
1.7	Showing limited machining depth (work material : glass) [2]	13
1.8	Effect of machining voltage on material removal rate (work material : glass) [3]	15
1.9	Effect of temperature of electrolyte on material removal rate (work material : glass) [3]	16
1.10	Effect of concentration of electrolyte (NaOH) on material removal rate (work material: glass) [3]	17
1.11	Limited depth characteristics (work material: glass) [3]	18
1.12	Conductivities of electrolytes [23, 31]	22
2.1	Discharge in liquid dielectrics	25
2.2	Schematics of ECM	29
2.3	Configuration of non-conductor work machining using ECD	37
3.1	Schematics of experimental set-up	41
3.2	Schematics of micro bubble generation	47

3.21	$V_a - i_a$ characteristics (KOH)	91
3.22	Shifting of discharge zone	93
3.23	Schematics of set-up for measuring potential along a hole	95
3.24	Potential variation along the hole	96
3.25	Schematics of set-up for measuring potential below the tool	98
3.26	Potential between electrode and electrolyte with depth of tool	100
3.27	Schematics of side clearance gap	101
3.28	Constant rate machining	104
3.29	$V_a - I_a$ of a constricted passage (electrolyte)	106
3.30	Waveforms of current (Partition: plastic) (a) Full wave rectified supply (b) Smoothed D.C. (c) Blocked condition of hole	107
3.31	Waveform of current and hole enlargement (Partition: glass); (a) Current waveform, (b) Hole enlargement	109
3.32	Current waveforms (plastic and glass partitions) ($V_a \approx 60$ Volts, DC full wave rectified supply) (a) Plastic partition, (b) Glass partition	110
3.33	Conduction through interfacial electrolyte	112
3.34	Electrical conductivities of glass (1) Fused silica, (2) 96% silica, (3) Borosilicate, (4) Soda-lime silica [39]	115
3.35	Wetting of glass (schematics) [41]	118
3.36	Current waveforms while machining plastic and glass (DC full wave rectified supply NaOH (35%) Room temperature $\approx 30^\circ\text{C}$) (a) Machining of plastic, (b) Machining of glass (low Mrr), (c) Machining of glass (Medium (Mrr), (d) Machining of glass (high Mrr)	120 121

4.1	Proposed mechanism of material removal (schematic) (a) Stage a, (b) Stage b, (c) Stage c, (d) stage b (details at b')	124 125
4.2	Process of material removal in machining non- conducting materials using ECD phenomena	129
4.3	Modification of structure (schematic) by K^+ [38]	132
5.1	Voltage vs. electrolyte concentration in micro- welding	137
5.2	Schematics of micro-welding set-up	139
5.3	Thermocouple beads prepared by ECD phenomena	141
5.4	Engraving pen	143
5.5	Engravings on glass slides using ECD phenomena	144
A-1	Pulsed D.C. circuit	154
A-2	High frequency pulse circuit	155
A-3	Schematics of set-up for bubble dia. measurement	158

LIST OF SYMBOLS

C	Capacitance
c_e	Specific heat of electrolyte
C'	rate of hydrogen gas generation
F	Faradays' constant
H	heat required to raise the electrolyte temp. from T_1 to T_b
I	current
I_a	average current
I^*	critical current
i_a	average current density
i^*	critical current density
i_a^*	critical current density (average) DC full wave rectified supply
K_e	conductivity of electrolyte
K_m	conductivity of bubble-electrolyte mixture
m_e	mass of electrolyte
p	pressure
R	resistance
R'	gas constant
R_e	resistance of electrolyte
R_1	resistance of tool-electrolyte interface
R_2	resistance of non-machining electrode-electrolyte interface
S	fringe visibility
s	shift in waveform of current
T_i	initial tem. of electrolyte
T_b	boiling point of electrolyte

V	voltage
V_a	average voltage
V^*	critical voltage
V_a^*	critical voltage (average) DC full wave rectified supply
λ	wavelength of light
α	void fraction
β	angle between laser beams
δ	interference fringe spacing
μ	micro, micron

LIST OF ACRONYAMS

ECD	Electrochemical Discharge
ECM	Electrochemical Machining
EDM	Electrical Discharge Machining
ECDM	Electrochemical Discharge Machining
PAM	Plasma Arc Machining
EBM	Electron Beam Machining
ECAM	Electrochemical Arc Machining
Mrr	Material Removal Rate
USM	Ultrasonic Machining
AJM	Abrasive Jet Machining
WJM	Water Jet Machining
EDD	Electrical Discharge Drilling
DMNC	Discharge Machining of Non-conductors
EMNCM	Electrical Machining of Non-conducting Materials
SMNCM	Spark Machining of Non-conducting Materials

CHAPTER I

INTRODUCTION

1.1 Electricity Assisted Material Removal Processes

Electrochemical Discharge (ECD) is a topic of current interest in the field of machining. It is being applied in machining electrically conducting materials and seems to be applicable in the machining of non-conducting materials also. The various methods of electrical machining are Electrochemical Machining (ECM), Electrical Discharge Machining (EDM), Electrochemical Discharge Machining (ECDM)*, Plasma Arc Machining (PAM) and Electron Beam Machining (EBM). Except ECDM, all other processes can be used only with conducting materials. The most important feature of electrical machining (like other unconventional machining processes) is that the hardness and strength of work material is not an important parameter deciding the machinability; whereas in conventional methods of machining, the tool material must be harder than the work material. The machining of materials having high hardness, toughness, brittleness and heat-resistant characteristics poses serious problems in conventional methods.

* ECDM of conducting materials is generally known as Electrochemical ARC Machining (ECAM).

Use of electricity for controlled removal of metals dates back to 1935, when Jacquet applied the electrolysis phenomenon for the production of polished surfaces in metal specimens. In 1939, W. Gussell (USSR) proposed a method of machining by the combination of chemical and mechanical means. The process envisaged by him had many features almost identical to the present day practice of ECM. In 1941, Burgess (USA) also demonstrated the possibility of applying electrochemical means for machining metals and alloys.

Priestly, an English scientist was the first to detect the erosive nature of the electrical discharges. However, the first metal cutting machine based on the principle of electrical discharge erosion was built by Lazarenko and Lazarenko (USSR) in 1943. The electrical circuit for spark generation developed by them was in use for several years.

ECDM has a very recent origin. In 1968, attempts had been made to use this phenomena for drilling non-conducting materials. Literature is available on ECDM of conducting materials from 1970 onwards. The name ECDM is used because it has features of both ECM and EDM. It is believed that, a portion of the ECM phase is converted into EDM phase in such processes. A voltage, higher than that commonly used in ECM, is the main factor that decides whether the process is ECM or ECDM.

The size of the tool and the work-tool gap used in ECM, EDM and ECDM are compared in Figure 1.1. ECM has the highest work-tool gap of 100 to 300 μm , followed by ECDM of conducting

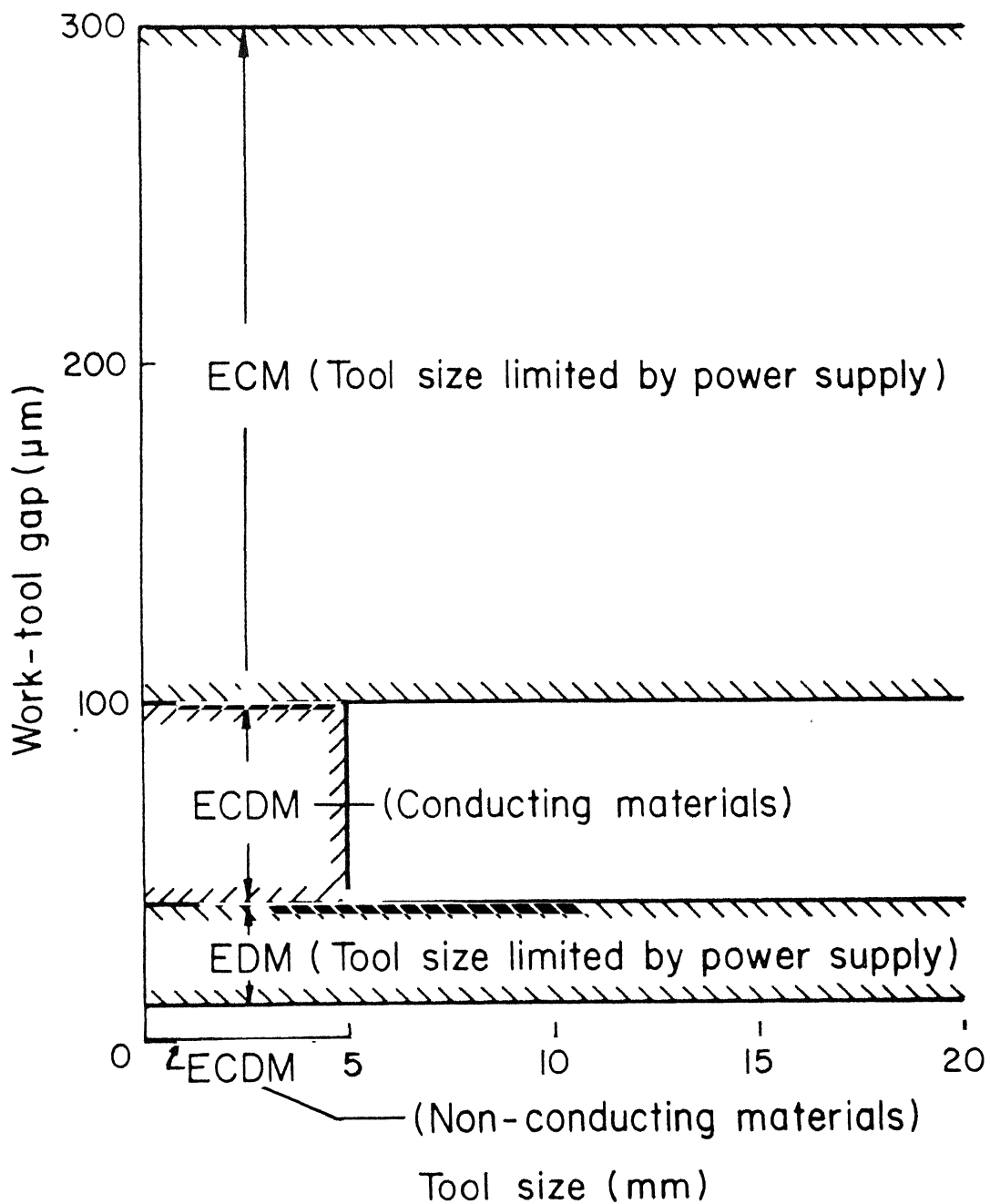


Fig.1.1 Tool size and gap in electrical machining processes

materials. EDM works with a small gap of 10 to 40 μm . In ECDM of non-conducting materials, the tool-work gap is almost zero, as the tool is in contact with the work (Section 2.3). ECM and EDM can use tools of very large size. Probably the limitation comes from the power supply and process control restrictions. In ECDM (conducting materials), only small diameter tools are used so far (Section 2.2.3). The size limitation on the tools used in ECDM of non-conducting materials is discussed in Section 4.2.4. It is obvious from the above data that discharges are produced in dielectric, the medium used in EDM, under very small work-tool gap; whereas in electrolytes, the medium used in ECM the discharges can be produced even at higher work-tool gap.

Figure 1.2 illustrates the voltage and current-density ranges that are used in the various electrolyte systems of machining. The usual range of voltage in ECM is from 8 to 20 Volts. Under the above voltage range, ECM produces satisfactory metal removal rate (mrr), surface finish and accuracy. ECDM of conducting materials works at the voltage range of 20 to 40 Volts. High current densities of the order of 800 amps/cm^2 are attained in this process and mrr obtained are very high compared to those during ECM or EDM. The machining of non-conducting materials by ECDM takes place at voltages of 30 to 120 Volts depending on the type of work, diameter of tool, and electrolyte type and concentration. In comparison with machining of conducting materials, the current densities are very low because of the non-conducting nature of the work, even with

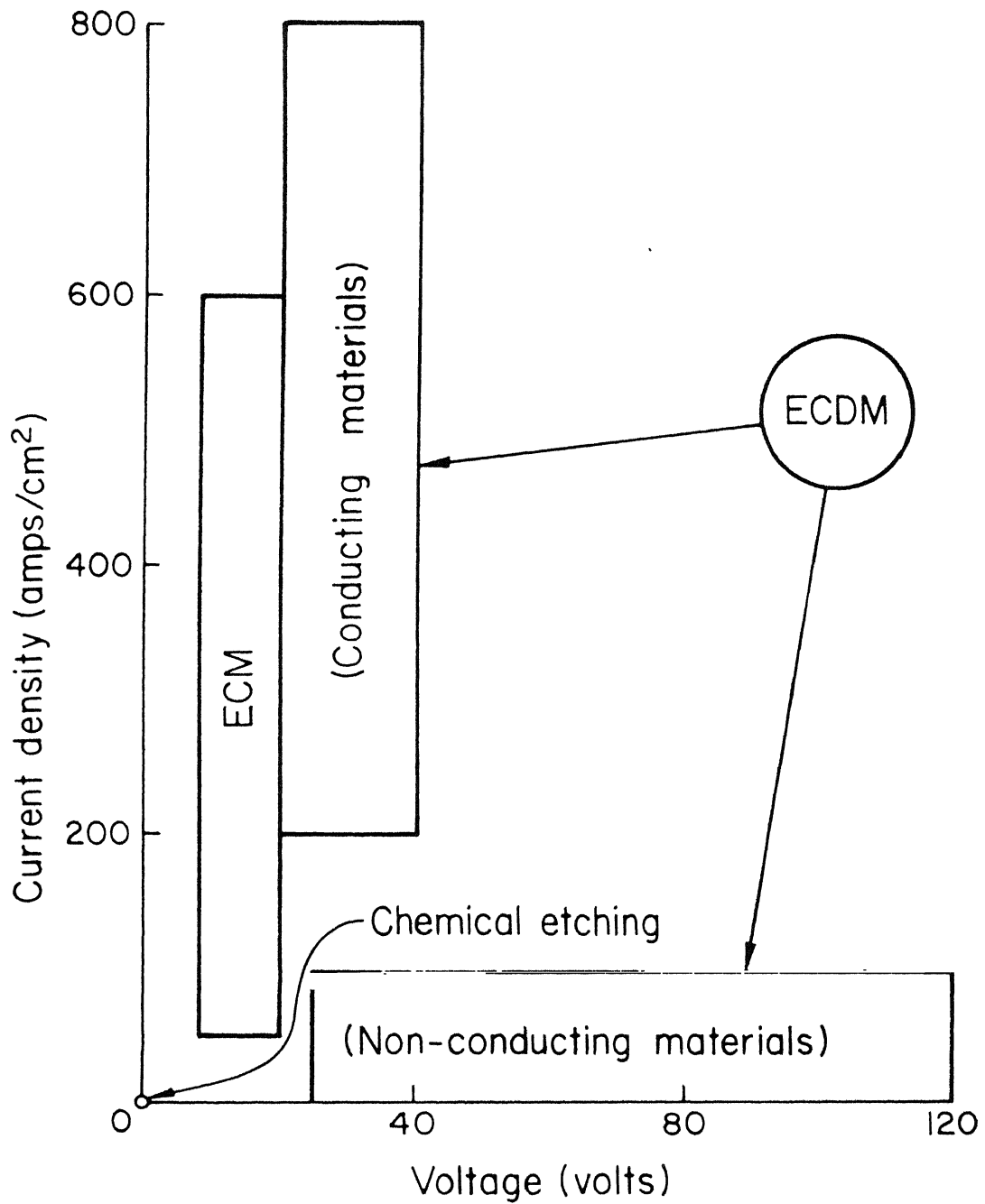


Fig. 1.2 Voltage and current density ranges of electrolyte-system of machining

higher voltages of machining. The chemical etching, on the other hand, neither needs any external voltage nor has any current density criterion. Being a process of zero voltage and zero current-density, chemical etching takes a position in the graph at the origin of the z-y axis. It is an established fact that for EDM and ECM there are accepted theories for the mechanics of material removal. In ECM, the metal is removed ion by ion (anodic dissolution) according to Faraday's laws of electrolysis. EDM, basically is a thermal process and the material removal is effected by thermal melting and vaporization assisted by mechanical shock and cavitation. In ECDM of conducting materials the material removal is assumed to be due to the combined effect of ECM and EDM; the anodic dissolution is assisted by thermal melting, vaporization, mechanical shock and cavitation. However, the electrical discharges in ECDM (conducting materials) has an arc character whereas in EDM, sparks are dominating in the removal process. Figure 1.3 indicates the above comparison.

The mechanism of material removal by ECD in non-conducting materials, by and large, is not clear. All the researchers have considered it as a combination of EDM and chemical action. The discharges through the bubbles, generated out of chemical reaction and some vapour layer formed during the process, is believed to be causing the melting and vaporisation of the material. The voltages used are quite high compared to that in

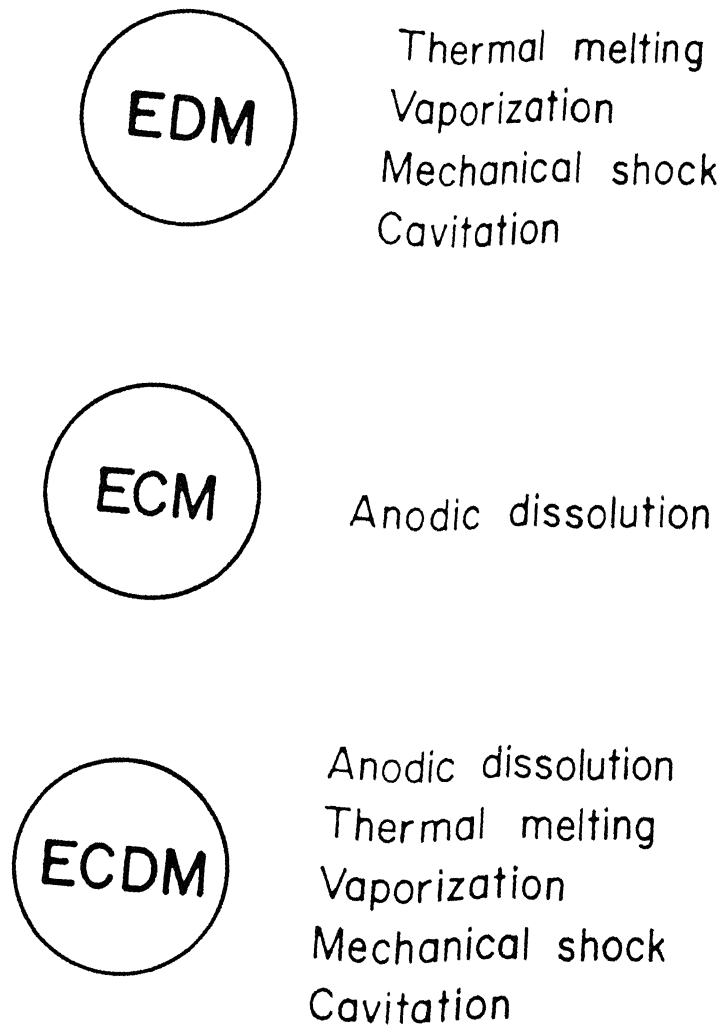


Fig.1.3 Generally accepted mechanism of material removal (Conducting materials)

ECM depending on the work material. The main difference of the process from that of machining of conducting material is that, in this case the tool is touching the work.

1.2 Electrochemical Discharges and Machining of non-Conducting Material

Electrical discharges are produced in electrolytes when a sufficient voltage gradient exists along a non-conducting phase in the electrical path. Gas bubbles, generated due to the chemical reactions in the electrolyte, have much importance in this context. Local boiling of the electrolyte also leads to the formation of a non-conducting phase. High voltage gradients are formed across these non-conducting phases and electrical discharges are produced. Normally the discharge originates at one of the electrodes through the above mentioned non-conducting phase but it can grow to bridge the electrodes, if the electrodes are spaced close enough.)

Non-conducting materials can be machined using ECD with proper combination of voltage, electrolyte and concentration.) The configuration of such a process is discussed in Section 2.3. A variety of non-conducting materials can be cut using this process. Considering the set-up cost, this system of machining can compete with other methods of machining of non-conducting materials such as Ultrasonic Machining (USM), Abrasive Jet Machining (AJM), Water Jet Machining (WJM) etc., especially in certain types of materials.

1.3 Review of Previous Work

Limited literature is available in the area of machining of non-conducting materials using ECD phenomena. Kurafuji's and Suda [1] drilled holes up to a depth of 0.31 mm in glass specimen using NaOH electrolyte (15% concentration) at a cell voltage of 34 Volts.) The process was tested with different electrolytes and tool materials. The mechanism of material removal was far from clear and it was thought that NaOH attacked glass chemically and the process received a Chemical-Machining label thereby. But at the same time since large number of hydrogen bubbles gathered around the tool, electrical discharges were fired through these hydrogen bubbles and the process was also viewed as a kind of EDM. They named the process as Electrical Discharge Drilling (EDD). Cook et al [2] conducted experiments with ECD for machining glass and other non-conducting materials and found that mrr in glass depends on voltage, electrolyte temperature and concentration as shown in Figures 1.4, 1.5 and 1.6. They also suggested that the increase in mrr could be due to the increase in the conductivity of the electrolyte under higher concentration and temperature. Drilled depths showed a limiting character as illustrated by Figure 1.7. The depth did not increase further after reaching a limiting value, however long might the machining time be. Most of the experiments were done with a positive tool and NaOH (35%) as electrolyte. They suggested that the material removal could be due to thermo-mechanical, chemical, field effects or due to some unknown effects.

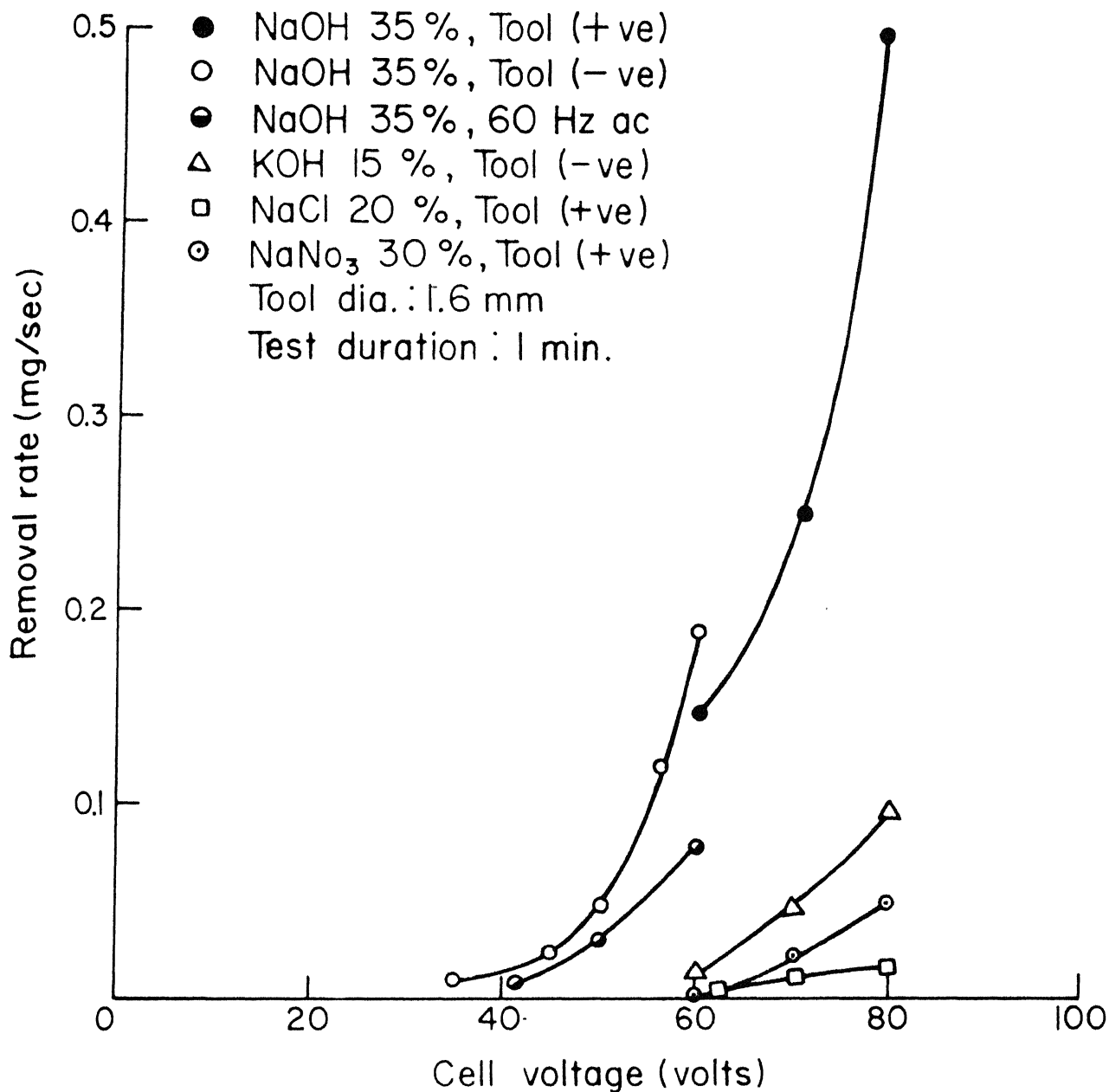


Fig.1.4 Effect of electrolyte and polarity [2] on material removal rate (work: glass)

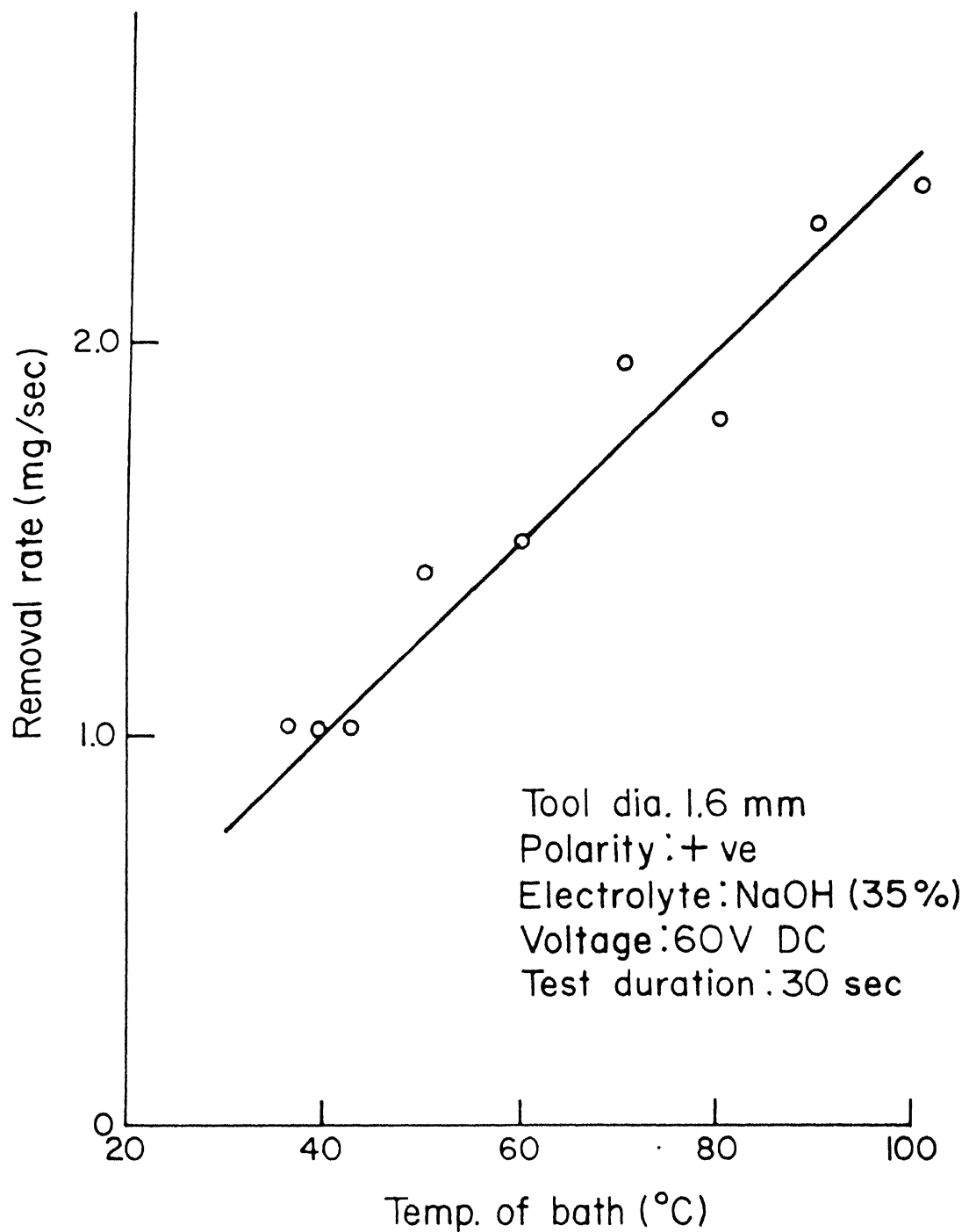


Fig.1.5 Effect of electrolyte temperature on removal rate (work material:glass) [2]

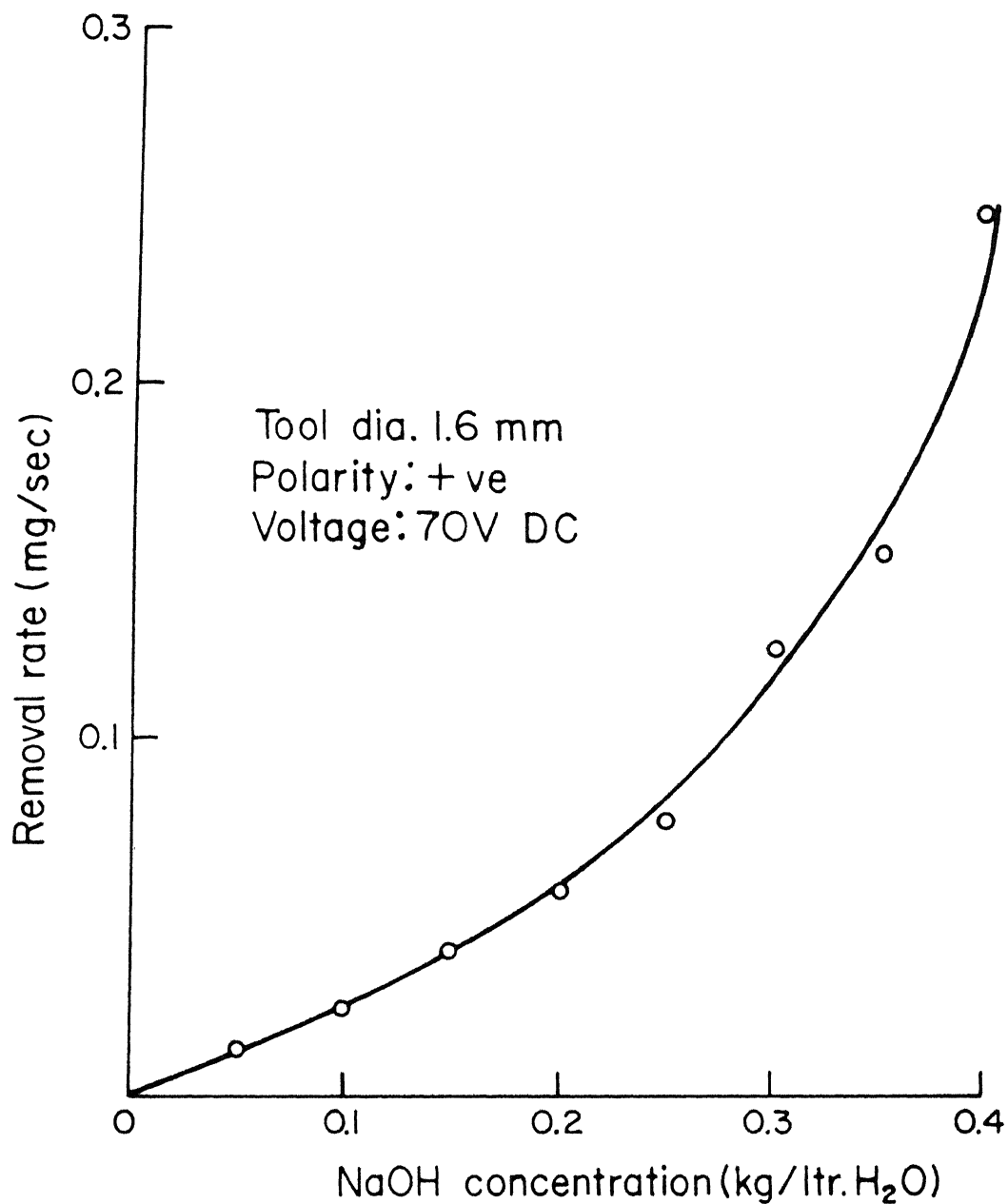


Fig.1.6 Effect of electrolyte concentration [2] on removal rate (work material: glass)

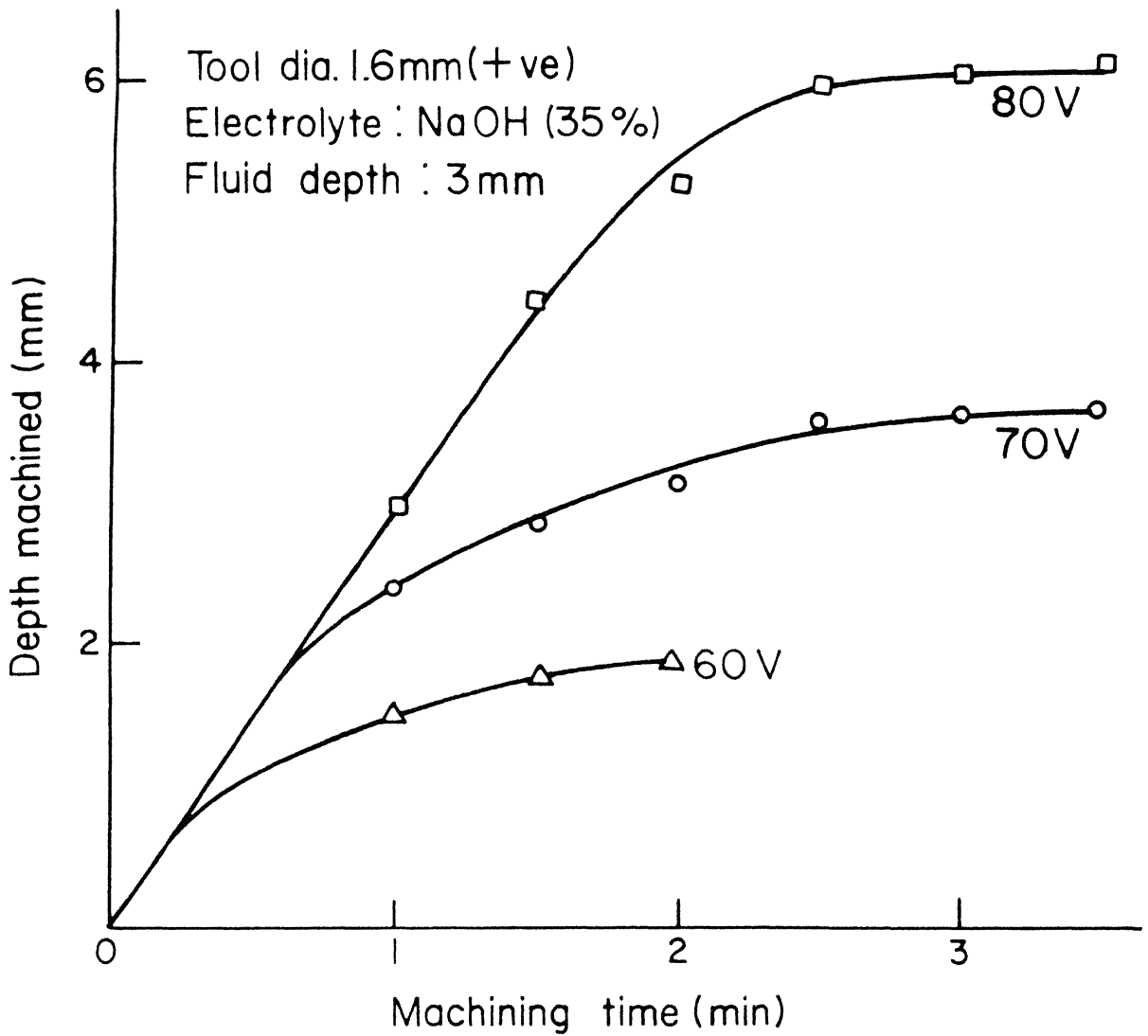
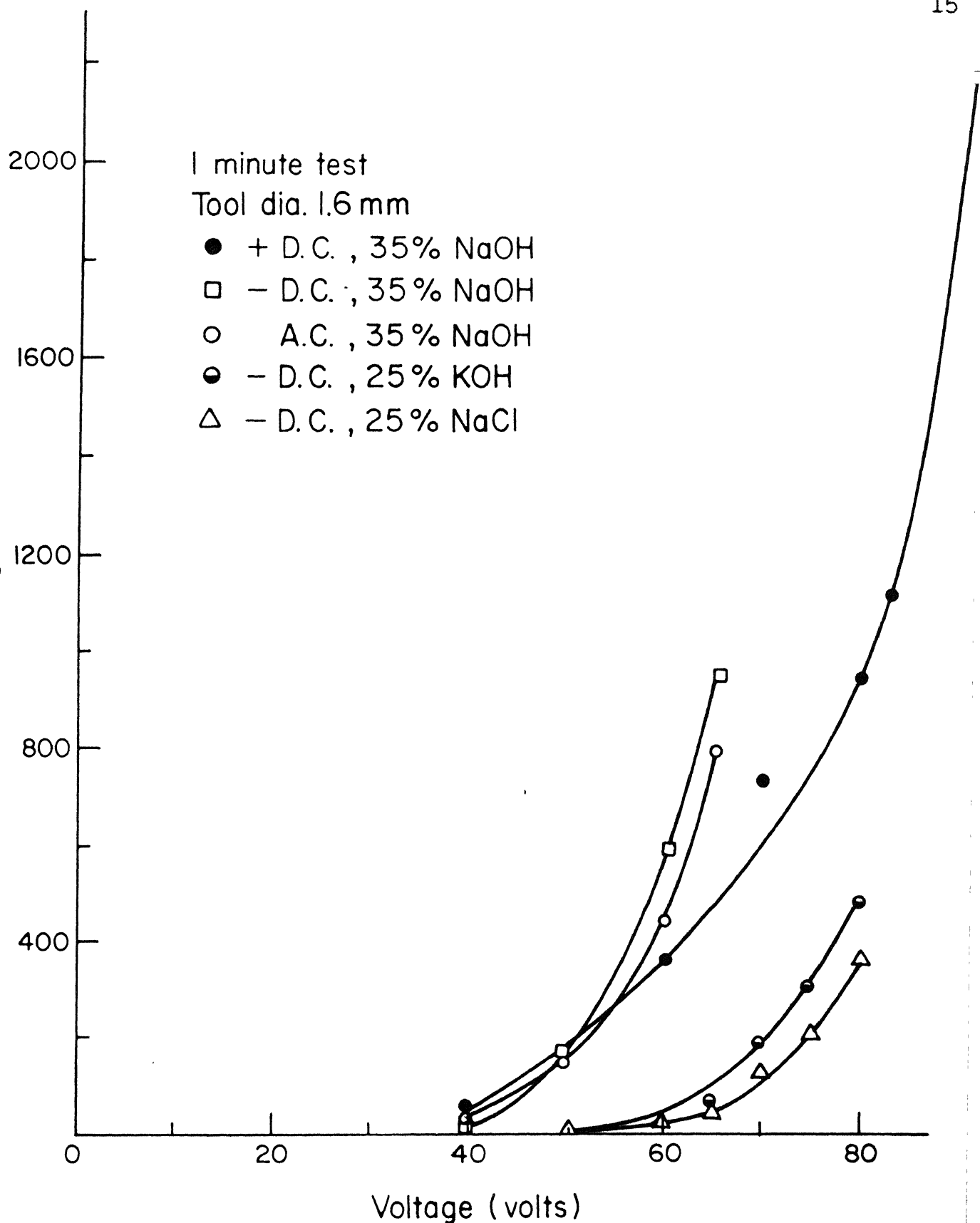


Fig.1.7 Showing limited machining depth [2]
(work material : glass)

The process was named as Discharge Machining of Non-Conductors (DMNC). Umesh Kumar [3] carried out experiments with glass and other non-conducting materials using ECD process. He mainly concentrated his experimentation with a negative tool because of the problem of wear encountered by a positive tool. The results obtained by him are shown in Figures 1.8, 1.9, 1.10 and 1.11. Mrr in glass showed an increase with negative tool also as with increase in temperature and electrolyte concentration. Mrr obtained by him also showed an upward trend with machining voltage. He found that the corner reproducibility of the process was very good and the Mrr and finish obtained were comparable with those obtained by ultrasonic machining. The discharge vanished from the tool under flowing electrolyte condition. Limiting depth obtained by him using a negative tool are as shown in Figure 1.11. Hollow tools gave better machining performance. The mechanisms suggested by him were thermo-mechanical and electrochemical actions. The process was named as Electrical Machining of Non-Conducting Materials (EMNCM). Tsuchiya et al [4] used wire-electrochemical discharge for machining of glass and ceramics. The cutting technique of wire EDM combined with the ECDM of non-conducting materials has been the basis for the machining. They used specimens of 1.2 mm thick with NaOH and KOH electrolytes. A supply of 25 Hz frequency (rectangular pulse) with 80% duty factor gave high mrr. They found that the cutting rate increased with increasing duty factor and decreased with higher pulse rate. Electrode was a wire of



1.8 Effect of machining voltage on material removal rate [3
(work material : glass)

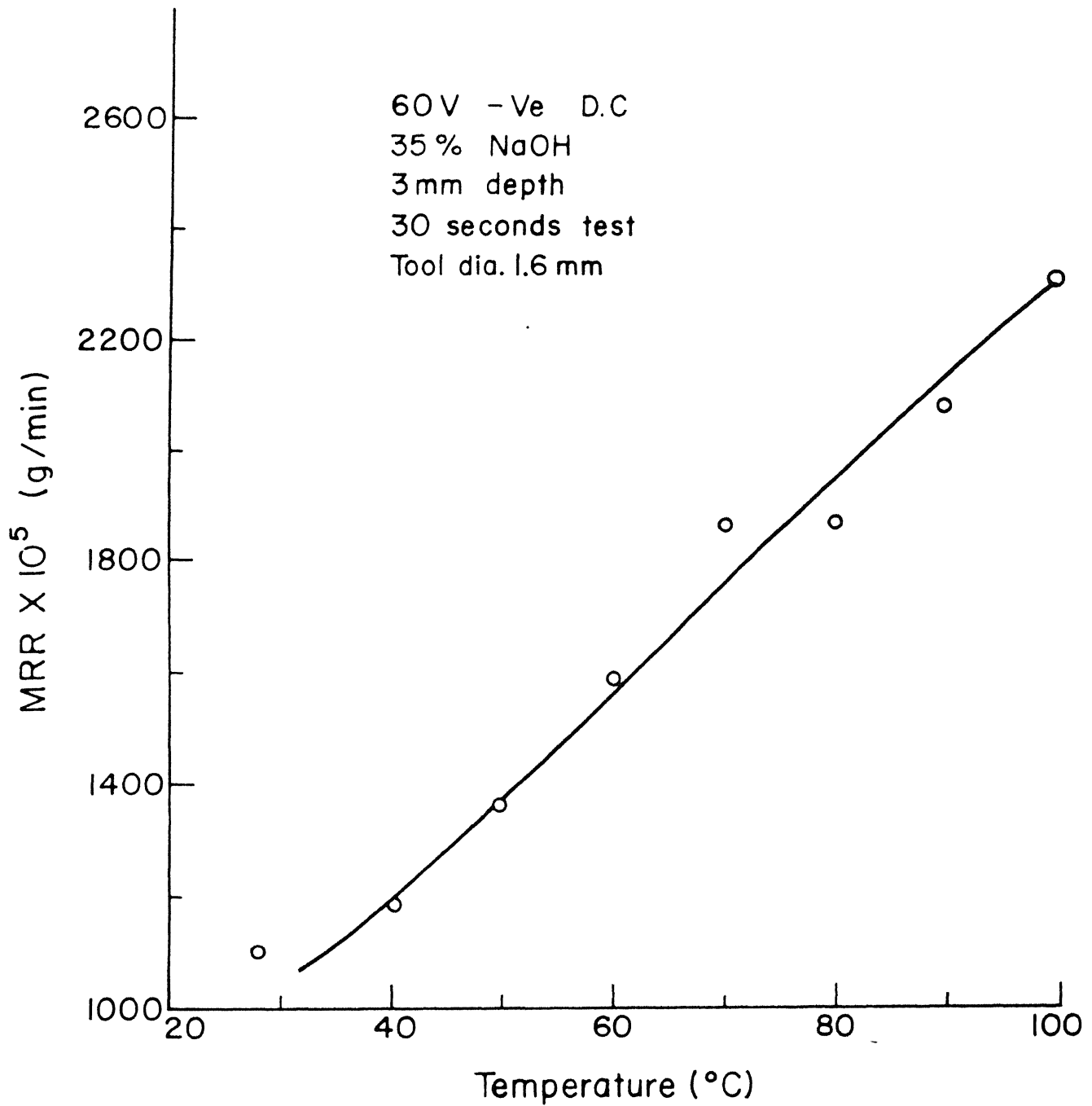


Fig.1.9 Effect of temperature of electrolyte on material removal rate (work material:glass) [3]

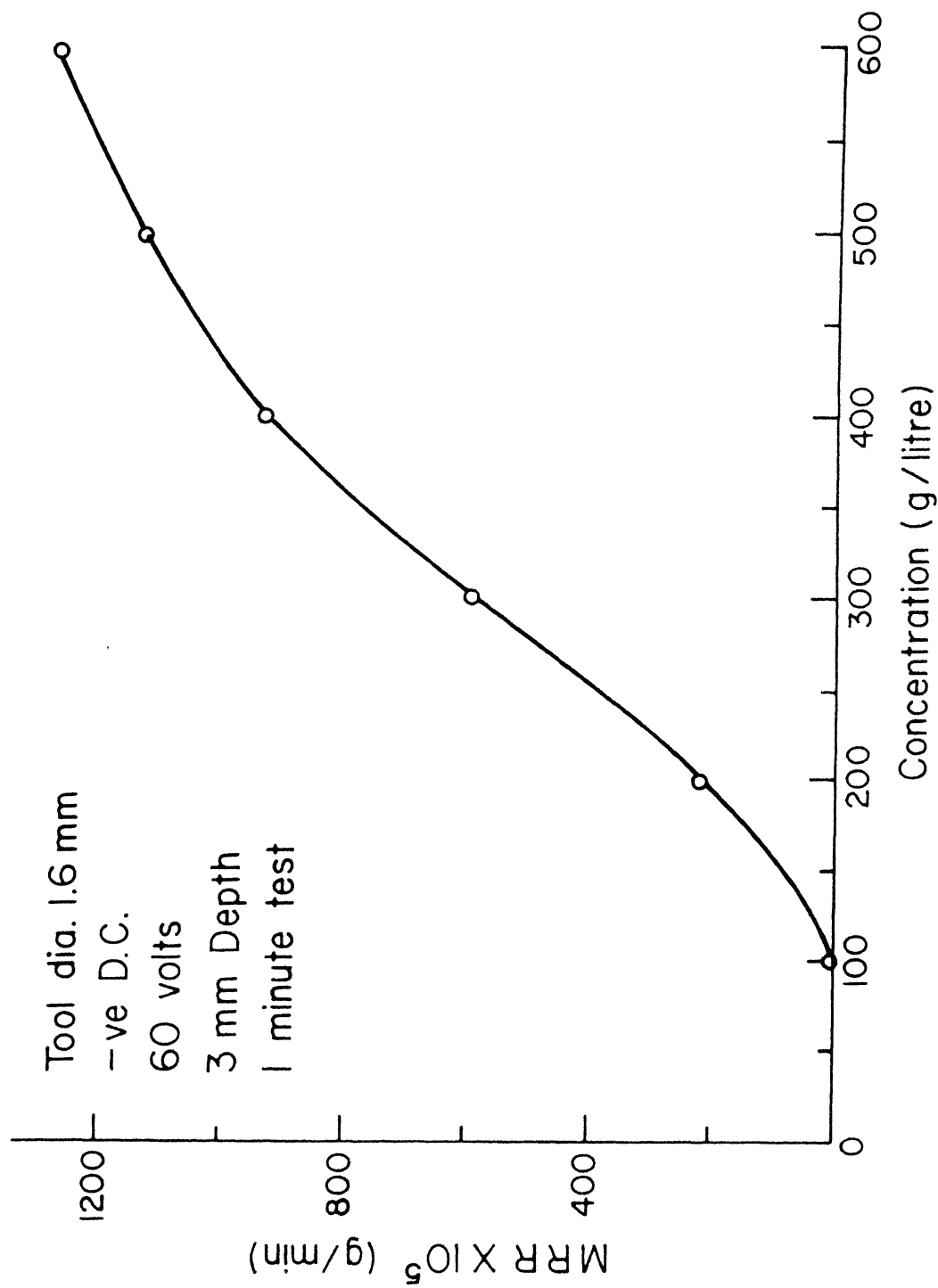


Fig. I.10 Effect of concentration of electrolyte (NaOH) on material removal rate (work material: glass) [3]

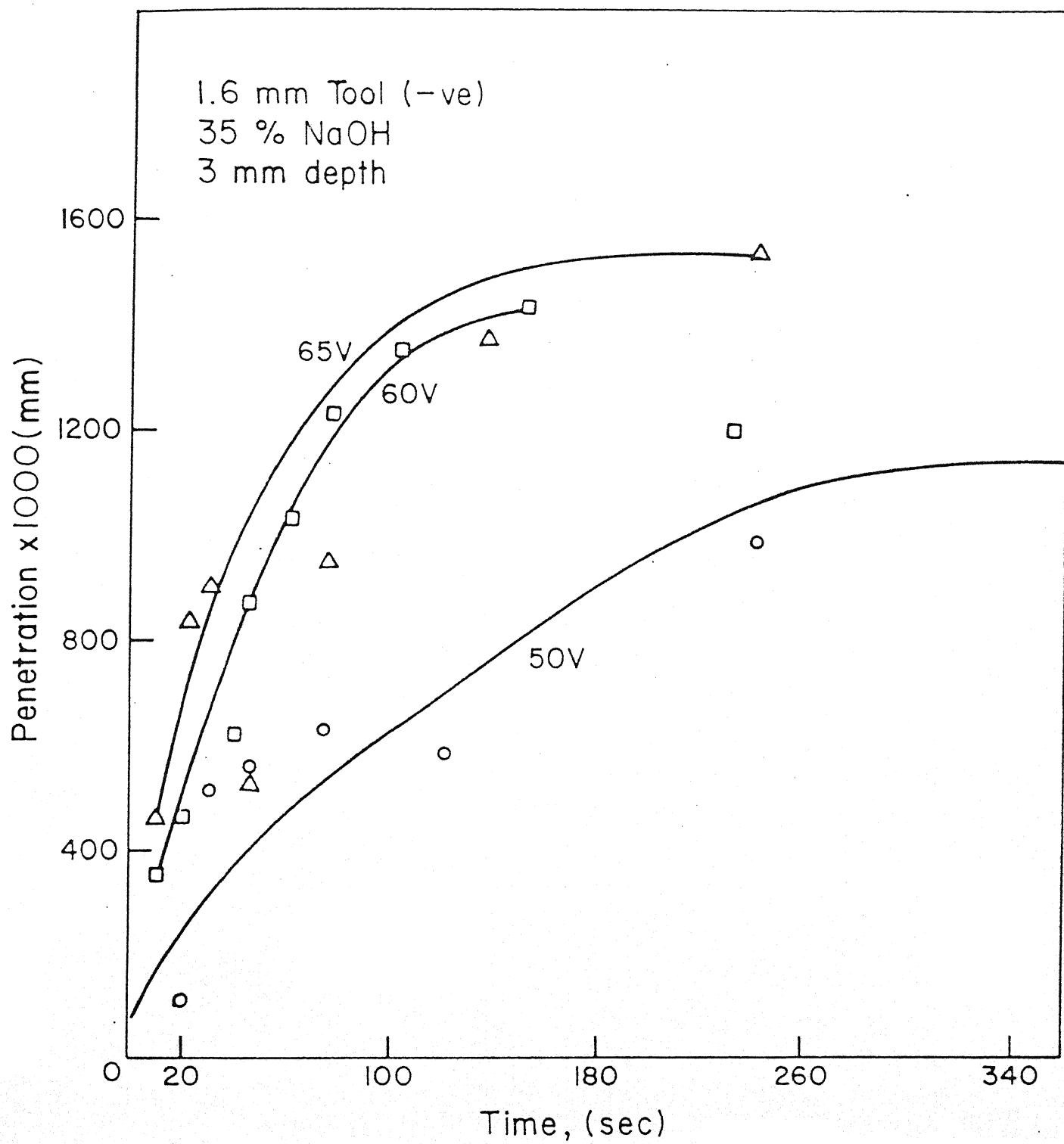


Fig.1.II Limited depth characteristics [3]
(work material: glass)

diameter 0.2 mm and a wire speed of 60 cm/min was used in their experiments. It was observed that machining rate of ceramic was very much low compared to that of glass. They pointed out that the mechanism of material removal was not clear. The process was known as Electrochemical Discharge Machining (ECDM) using wire-EDM technique. Allesu et al [5] made some observations on the phenomena of ECD in machining of non-conducting materials. A glass wafer 0.2 mm thick was cut along the length using a thin blade as tool. Microscopic observations revealed some micro-cracks on the surface of the drilled specimen. The removal mechanisms suggested were thermal heating, cavitation and electrochemical action. The process of machining, was called as Spark Machining of Non-Conducting Materials (SMNCM). Recently some work has been done to use ECD for machining of composites at IIT, Kanpur [6,7].

Researchers have also investigated electrochemical discharge machining of conducting materials and most significant contributions have been made by McGeough and his group [8,9,10,11,12,13,14]. Some of their findings have helped the author in having a better understanding of the process under investigation. They found that the electrical discharges in an electrolyte occurred across localized regions of evolved gas and/or electrolyte vapour. They observed both spark and arc discharges in the electrolyte. According to them the electrolytes can exhibit three different phenomena under an applied voltage pulse between two electrodes. These are

- (1) electrochemical action without any electrical discharges
- (2) electrochemical action followed by discharge between an electrode and electrolyte
- (3) electrochemical action followed by discharge between the electrodes.

1.4 Objective and Scope of Present Work

The broad objectives of the present work are as follows (all related to ECDM of non-conducting materials) :

- (1) To investigate the mechanisms of the process of material removal.
- (2) To find out the reasons for the limiting depth characteristics.
- (3) To study possible means of improving the process and stating areas of application.
- (4) To investigate the process for applications other than machining.

Though the title of the thesis is given as Electrochemical Discharge Phenomena in manufacturing processes, the emphasis is on the studies how the phenomena works in manufacturing process. Some of the works presented in this thesis were not at all thought at the beginning of the work. These has developed during subsequent observations. Enlargement of a hole without tool in glass specimen (Section 3.6.2) and possibility of using the phenomena for microwelding (Section 5.1) are some of the examples.

It was fascinating to observe that material got eroded from the workpiece as the sparking tool touches the work. Electrical discharges produced at the tool can develop a very high temperature in the tool.

Large number of experiments were conducted with diverse approaches covering wide spectrum of materials. The observations indirectly throw some light on the mechanics of material removal. It is interesting to note that the previous researchers thought that the higher mrr obtained in higher concentrations of NaOH electrolyte was because of its higher conductivity; in fact the conductivity of NaOH decreases beyond a certain value of concentration as shown in Figure 1.12. In the course of the present investigation it became necessary to carry out experiments with and without the work specimen in order to investigate any work participation in the machining process. These experiments have helped a lot to understand some salient features of this machining process. Some researchers [2,3] have observed the limiting depth characteristics of the process; the rate of penetration decreases with time of machining and approaches zero. Different experiments were conducted to explain the above character. Experiments with constricted electrolyte passage gave an important insight to the process of material removal. Difference observed in the performance of a negative tool and positive tool were also investigated. The various observations available in the course of experimentation gave ideas to use ECD phenomena for a few non-machining applications also.

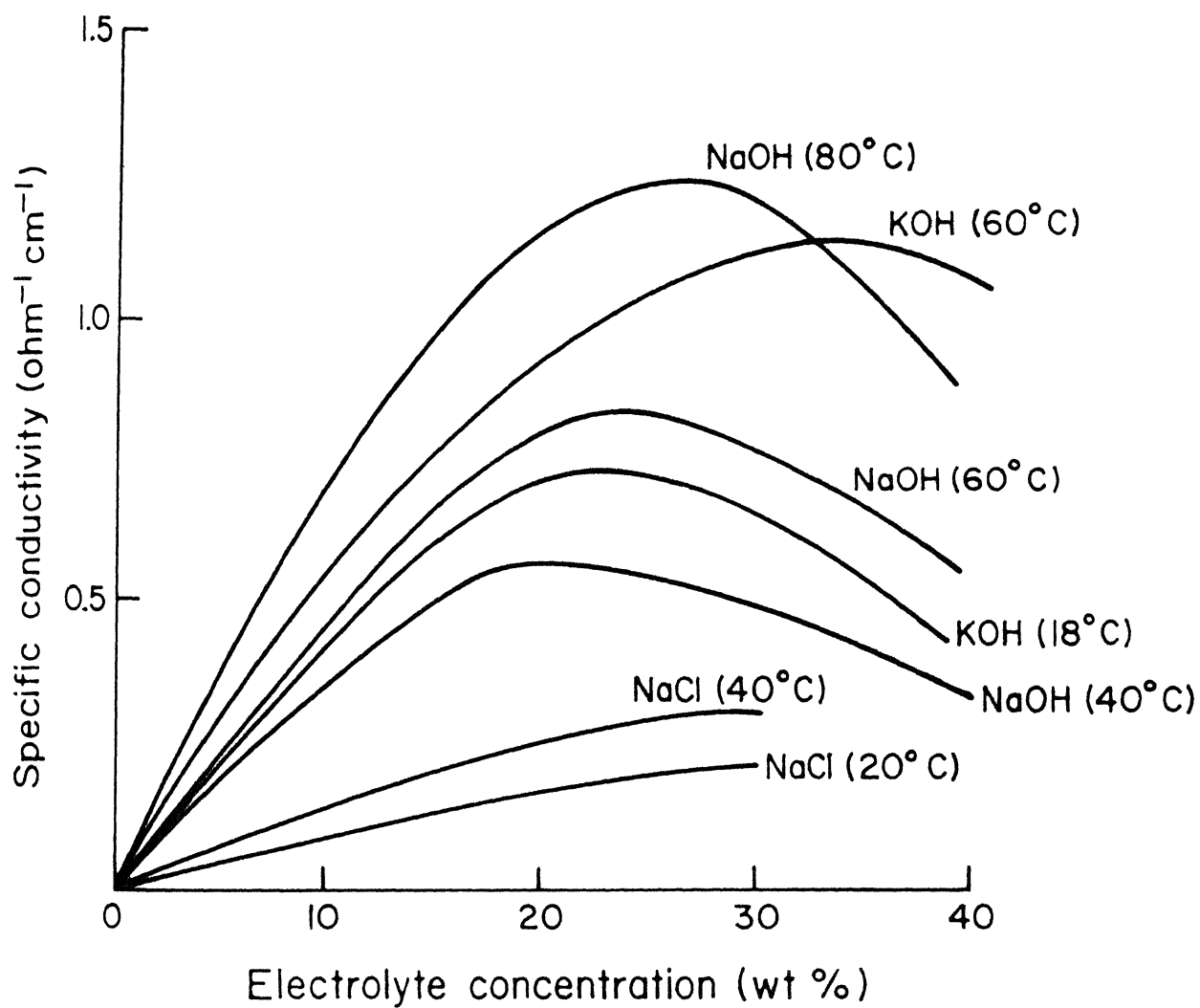


Fig.1.12 Conductivities of electrolytes [23, 31]

The study has the following limitation. This being first attempt in this line, a mathematical model of the process could not be evolved as there are interdependencies of many factors. Author has come to the conclusions that in order to arrive at a reliable mathematical model for the process, extensive experimentation into electrical discharges in electrochemical systems and structure and properties of materials is essential. The major effort was, therefore, given to explore the phenomena basic to the process. Experimental set-ups used were simple. Sophisticated techniques like high speed photography, elaborate chemical analysis etc., have not been resorted to, as the direction of the work was not so obvious within the time framework.

CHAPTER II

ELECTROCHEMICAL DISCHARGE PHENOMENA AND MACHINING OF NON-CONDUCTING MATERIALS

2.1 Discharges in Liquid Dielectrics

EDM normally works with a liquid dielectric. The knowledge of the discharge mechanism in EDM can help to some extent in understanding the discharge phenomena taking place in electrolytes leading to the material removal. The configuration of EDM and the discharge process are schematically shown in Figure 2.1. The tool and the work are the two electrodes separated by a suitable gap known as spark-gap. Generally the tool will be negative and the work will be positive; liquid dielectric such as kerosene fills the spark-gap. The gap varies with machining conditions but generally is $\approx 25 \mu\text{m}$. A suitable voltage (more than the breakdown voltage of the dielectric) is applied in a pulsed manner by specially designed circuits. The breakdown voltage will depend on the shortest gap as well as on the insulating characteristics of the dielectric and the amount of debris present. The pulse frequency can be a few MHz or less than that. High frequency pulses with energy ≈ 0.1 Joule for finish cuts and low frequency pulse with large energies (≈ 0.9 Joule) are common in EDM.

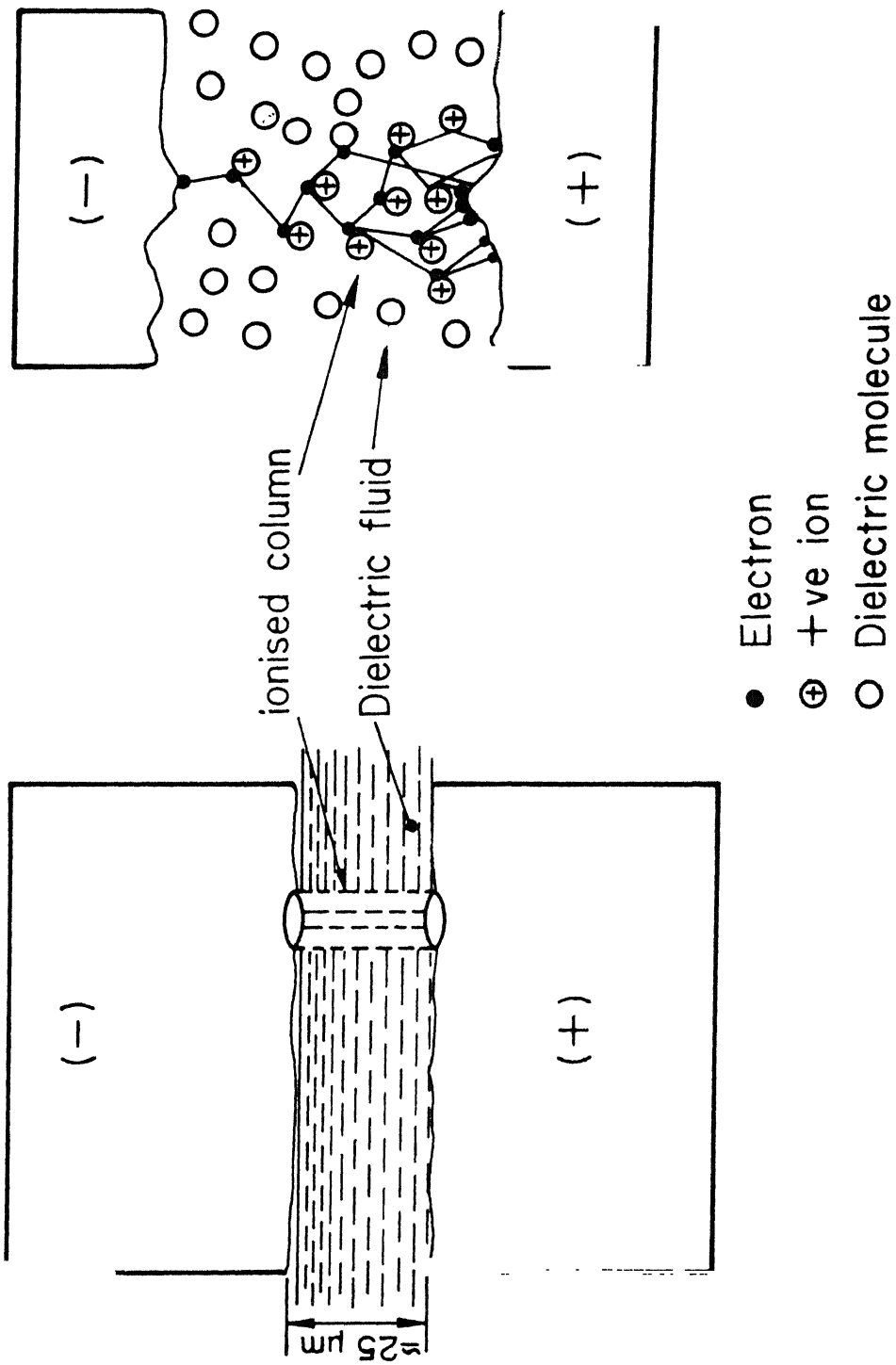


Fig.2.1 Discharge in liquid dielectrics

When voltage pulse is applied between the electrodes, a very high electrostatic field $\approx 10^4$ to 10^5 V/mm is established across the electrodes, causing cold emission of electrons from the cathode surface at a spot, where the distance between the two electrodes is a minimum. These liberated electrons accelerate towards the anode under the field and after gaining sufficient velocity, collide with molecules of the dielectric causing these molecules to break-up into positive ions and electrons. The electrons so produced, also join the already existing electrons on their migration towards anode breaking more dielectric molecules into ions and electrons. The generation of positive ions and electrons continue in this way and may end up in producing a narrow column of ionized dielectric path connecting the two electrodes. Since the conductivity of the ionized column is very large, an avalanche of electrons takes place from cathode to anode producing an electric discharge. The discharges cause instantaneous local temperature of about $10,000^\circ\text{C}$ on both the electrode surfaces at the point where it has struck. During the off-period of the voltage pulse, the ionized column collapses and dielectric fluid tends to attain its original condition (deionizes). The molten metal is scavenged by a mechanical blast produced by the fast rushing-back of the dielectric liquid surrounding the ionized channel at the end of each pulse. This causes eroded craters of few micron size on the surfaces of both the electrodes. Now, since the gap has increased at this discharge spot, next discharge will occur at some other point where

the minimal gap exists. Like this the discharge wanders from point to point in succession covering the whole surface of the work under the tool; finally conforming the shape of the work surface to that of the tool surface. Servo-controlled tool feeding and forced circulation of dielectric are generally used in EDM. Resistance-capacitance relaxation circuit, rotary impulse generator or a controlled pulse circuit can be used as the power supply unit in EDM [15,16,17,18,19].

Heuvelman et al [20] have shown that the emission of electrons obeys the field emission equation of Nordheim and Fowler. The electron released from the cathode by field emission can also cause heating within the liquid dielectric as it moves towards the anode. After a certain period of time, called ignition delay period, the liquid can evaporate locally giving rise to gas bubbles in the dielectric fluid, within which breakdown can also occur by collision ionization. This collision ionization process can reduce the resistance across the gap and, thus, facilitate the formation of a discharge channel between the electrodes [21].

2.2 Discharge Phenomena in Electrolytes

As mentioned in Section 1.2, electrolytes can exhibit three different phenomena under an applied voltage pulse, namely electrochemical action without any electrical discharge, electrochemical action followed by discharge between an electrode and electrolyte and electrochemical action followed by discharge

between the electrodes. Discharges in dielectrics and those in electrolytes differ mainly because of the vast difference in their electrical properties; the former being a non-conductor of electricity and the latter a fairly good conductor of electricity. This means discharges in electrolyte can occur even in cases when the electrodes are far away since electrolyte provides the conducting path between the discharge zone and the electrode.

A general understanding of the discharges in the electrolyte helped the author to analyse the discharge phenomena while machining non-conducting materials.

2.2.1 Electrochemical action (without electrical discharge)

Electrochemical action without electrical discharge, perhaps, can be called as the normal ECM condition. The basic configuration of ECM system consists of two electrodes separated by a gap while an electrolyte is generally forced to flow through the gap. Electrodes receive a DC voltage (8-20 Volts). Unlike in EDM, the polarity of the tool and work is fixed; the tool is always negative and the work is positive, Figure 2.2 shows the schematics of ECM.

The process of metal removal taking place in ECM may be explained as follows. For a sodium chloride electrolyte and iron as work material, the reactions at the anode and at the cathode are



(the anode metal dissolves, leaving two electrons)

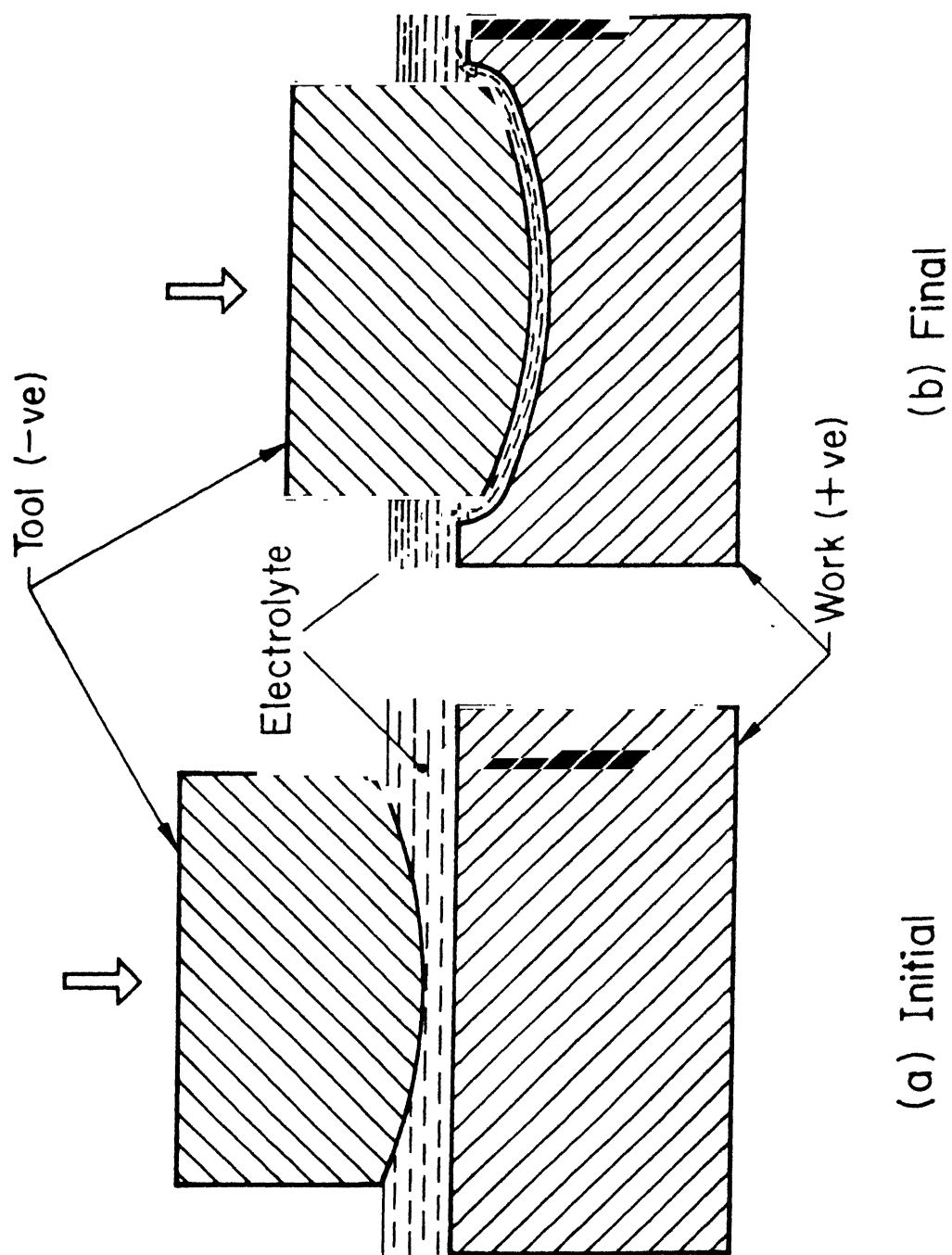
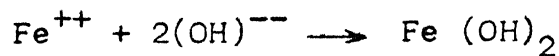


Fig.2.2.2 Schematics of ECM



The water receives two electrons from the cathode and, as a result, the hydrogen gas is evolved and hydroxyl ions are produced. The positive metal ions tend to drift towards the cathode and the negative hydroxyl ions are attracted towards the anode. The metal ions, then combine with the hydroxyl ions to precipitate out as iron hydroxide according to the reaction



Ferrous hydroxide forms an insoluble precipitate. So, the net outcome with this metal - electrolyte combination is the dissolution of anode metal and the generation of hydrogen gas at the cathode while the cathode shape remains intact [15,16,17,22,23]. This is one of the most important feature of ECM which enables it to be used as a powerful process for shaping metal and alloys.

2.2.2 Electrochemical action with electrical discharge between an electrode and electrolyte

This kind of situation arises when a sufficiently high electric field exists across a gas bubble or a non-conducting layer in an electrochemical set-up. In fact, this type of condition is existing in the machining of non-conducting materials (Section 2.3).

McGeough and his co-researchers [13] concluded from their various studies that electrical discharge could arise in normal ECM due to

- (1) electrolytic gas generation at the surface of electrodes,
- (2) growth of layers of low ionic concentration near to the electrodes and formation of partially conducting oxide films on the anode surface,
- (3) local variations in the electrolyte flow pattern caused by flow stagnation and eddies,
- (4) change in the electrolyte composition over prolonged machining time and,
- (5) loose debris of machining and metallic hydroxide.

According to Loutrel and Cook [24] the mechanisms leading to high voltage gradients in the presence of voids in ECM are

- (1) electrolytic gas evolution at electrode surface,
- (2) depletion layers,
- (3) electrode passivation and activation over-voltages,
- (4) local stagnation of flow,
- (5) steam generation and cavitation,
- (6) vapour blanketing of electrode surfaces and
- (7) particles in the electrolyte flow.

It can be seen that the findings of McGeough and his group and that of Loutrel and Cook are almost identical in nature. The high field set across a void, can trigger a discharge probably through ionization within the void [25]. The type of discharge mentioned above (between one electrode and electrolyte) has not been seen to have effect on mrr, but an arc discharge (between tool and work) caused a crater on the workpiece surface while machining conducting materials [10].

2.2.3 Electrochemical action with electrical discharges between electrodes

This is the phenomenon which dominates in the ECD machining of conducting materials (also known as ECAM). In most cases, a discharge between two electrodes (tool and work) is struck in an electrolyte through the phenomenon explained in Section 2.2.2. The discharge originated at an electrode grows in size, bridging the gap between the electrodes. This is possible only if the electrodes are closely spaced ($\approx 100 \mu\text{m}$). Some observers have the opinion that sparking in ECM coincides with the formation of a different type of gas bubbles (irregular in shape) instead of small individual gas bubbles, instantaneously covering the whole surface of one electrode [22]. Situations with narrower equilibrium-gap with greater volume of hydrogen gas as can happen at higher currents also increase the probability of sparking across the electrodes [23]. Larsson and Baxter [26] counted the number of sparks per mm of tool penetration with different tool feed rates and applied voltages while machining mild steel specimens using ECM under high feed rates and high voltage (feed = 5.5 mm/min, $V = 22.5$ Volts). They found that in a sodium nitrate electrolyte, sparking rate (number of sparks per mm penetration) increased with feed rate but decreased with applied voltage. It was also observed that with ageing of nitrate solution the sparking rate has decreased considerably. Ebeid et al [27] found that below a certain threshold feed rate, the sparking in ECM was rare.

They also observed that the frequency of sparking did not increase with the accumulation of sludge in a nitrate solution. A higher back pressure in the machining system decreased the sparking rate which indirectly pointed towards the effect of pressure on gas bubbles present in the machining gap (also known as inter-electrode gap, IED). The pressures they used were $1.4 \pm 0.14 \text{ MN/m}^2$ at inlet and 0.56 MN/m^2 (for high back-pressure experiments) and 0.35 MN/m^2 (for low back-pressure experiments) at the outlet. (In the present investigation also when discharges were studied under pressured condition of electrolyte, the critical voltage for producing discharge did not change much as discussed in section 3.4.5). The sparking rate they observed under high back-pressure, was $\simeq 5$ sparks /mm and $\simeq 8$ sparks /mm under low pressure condition. It was interesting to note how they counted the number of sparks per mm of drilled depth. This is different from the sparking frequency usually mentioned in EDM etc. In EDM it means the number of sparks per second which is quite a high value (usually a few MHz). They counted sparks in their experiments by noting the small 'blip' in the current and voltage traces recorded during the machining. Larsson, Baxter and Ebeid [26,27] studied sparking in ECM mainly to identify the upper limits of feed rate where a catastrophic tool failure would occur. The study helped to extend the use of ECM for high mrr without causing serious damage to the tool. Kubota and Tamura [28] conducted experiments with ECDM of steel

plates. A graphite pipe of 4 mm outside diameter and 1.5 mm inside diameter was used as the tool. A full wave rectified supply (100 Hz) formed the voltage source. They could drill holes in steel plate at a fast rate of ≈ 80 mm/min (penetration rate obtained was ≈ 45 mm/min; the difference in the two rate accounts for tool wear). NaCl or NaNO_3 (20% concentration) electrolyte under a high pressure (≈ 10 kg/cm²) was circulated through the hollow tool. Gap voltage was 20 to 30 volts and intense sparking was observed when high feed rates were used. The apparent current density (current per unit cross-sectional-area of hole) reached a value of 800 amps/cm². At high feeds surface roughness as high as 0.1 mm R_{max} were observed. They concluded that ECDM (conducting materials) is a viable process for high rate removal of metals and alloys, if the surface roughness is not an important factor. The study of McGeough and his co-workers on the ECD of conducting materials [8,9,10,11,12,13,14] has experimentally shown an mrr of as much as five and forty times faster than ECM and EDM, respectively, in such a process. In one such experiments they used a copper tubular tool of 1.88 mm outer diameter and sodium nitrate solution of 20% concentration [11]. The tool size used in another study [8] was copper tube with an outside diameter of 3.175 mm and an inside dia of 1.325 mm. They used a full wave rectified supply of 100 Hz frequency and work was subjected to a vibration of 100 Hz. The machining set-up was in the reverse manner; the

vibrating work at the top and the tool was below the work. The oscillatory nature of the work-tool system and the facility to change the phase angle between the voltage wave form and the oscillation waveform enabled them to analyse the process for maximum mrr. The whole process was viewed by these researchers as a combined action of electrochemical dissolution and electro-discharge erosion (the electrodischarge erosion phase being in the form of arc rather than spark discharge).

Novak et al [29] studied electrochemical drilling under sparking condition of cathode. They used tubular tool of 1.5 mm maximum outside diameter with NaCl, NaNO_3 and NaClO_3 as electrolytes under an applied voltage of 45-55 Volts. The electrolyte was force-flushed and they analysed the situation based on the flow conditions and found that a limiting current density exists for sparking to occur in such situations. In a recent study of ECDM of conducting materials, Ramachandran [30] has pointed out, based on his experimental results, the possibility of mechanisms like contact bridge formed between tool and work and their blowing out, anodic oxidation at kindling temperature etc., other than electrochemical dissolution along with electrodischarge erosion contributing high mrr in this process.

The configurations of ECM and ECDM of conducting materials are one and the same. However, the latter resorts to higher machining voltage and higher tool feed rate. (sparking due to physical metal to metal contact between tool and work do not

need high voltage.) Work of McGeough's group and Kubota and Tamura's work can be considered as extreme ECDM processes, from the point of tool feed rates; the former used feed rate value upto 20 mm/min and **average voltage upto 35 V.** Kubota and Tamura used feed rates upto 80 mm/mm and average voltage upto 35 Volts. Discharges was an integral part (continuously occurring) of the process in their work. Tool diameter was less than 5 mm in both the cases. The work of Larsson and his group can be viewed as a moderate electrochemical discharge process of machining conducting materials. (close to ECM conditions). The discharges were an occassional phenomenon in their work thereby enabled them to count the number of sparks. The maximum feed rate used was 6 mm/min and maximum voltage was 30 Volts. They used a tool of 10.25 mm outside diameter.

2.3 ECD Phenomena and Machining of Non-conducting Materials

The configuration of machining of non-conducting materials is shown in Figure 2.3.. Tool is one electrode and the second electrode is simply kept in the electrolyte at some location. Tool is in contact with the work and the tool feed is provided by the gravity. Power supply can be DC (full wave rectified), DC (smoothed), Pulsed DC or AC and the polarity of the tool can be positive or negative. Electrolyte used are NaOH, NaCl, KOH etc. Any conducting materials can be used for making electrodes.

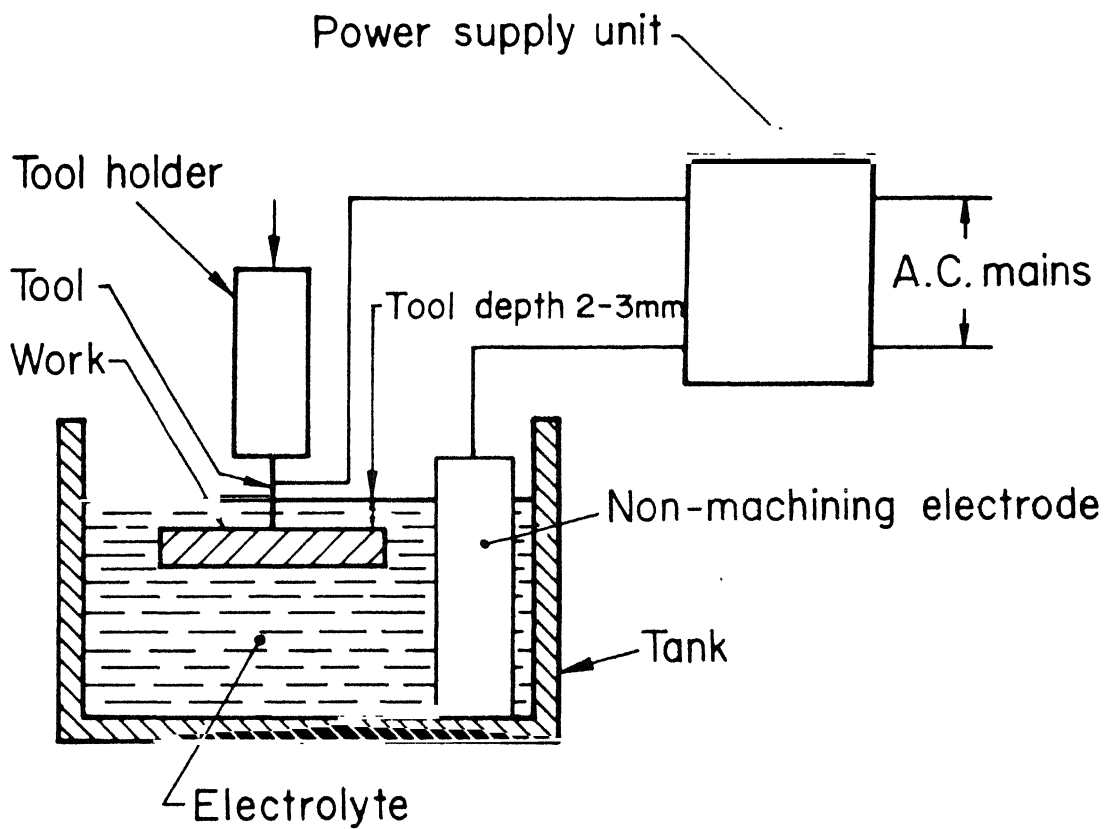


Fig.2.3 Configuration of non-conductor work machining using ECD.

When a voltage of say, 60 Volts is applied; discharges are produced at the tool and the material from the non-conducting work gets eroded. There is no discharge at the non-machining electrode. The area of contact of the tool with the electrolyte is much less compared to the contact area of non-machining electrode with the electrolyte. A variety of materials like glass, stone, ceramics etc., can be machined by this process. The mrr depends mainly on 1) applied voltage, 2) electrolyte type, 3) temperature and concentration of electrolyte, 4) tool polarity, 5) type of supply, and 6) work material.

As mentioned in Section 2.2.2 this machining configuration can be viewed as an electrochemical system in which the discharges are produced between an electrode and electrolyte. The stagnant electrolyte, high applied voltages (30-120 Volts) and small contact area of the tool with electrolyte leads to the conditions required for the production of a discharge between one electrode and the electrolyte as mentioned in Section 2.2.2. Since the electrodes are far away, condition mentioned in Section 2.2.3 (discharge between electrodes) would never occur.

It has been pointed out in Sections 1.3 and 1.4 that production of bubble at the tool and the discharges through them are believed to be causing high temperature in the work leading to melting and vaporization of work material. The findings in the present study are discussed in Chapters 3 and 4.

CHAPTER III

EXPERIMENTAL OBSERVATIONS AND DISCUSSIONS

3.1 Introduction

A close look at the machining of non-conducting materials using ECD phenomena raises many questions and doubts which need to be explained. The already available limited results of the previous investigators [1,2,3,4,5] formed the starting point and guidelines for the experimentation in the present work. For instance all the previous researchers believed that the erosion of the material was due to the electrical discharge through the bubbles and possibly assisted by chemical or electrochemical action (Section 1.3). However, the present investigations revealed that the surface phenomena taking place in the work plays the major role in the removal mechanism (Chapter IV).

Sections 3.3 through 3.8 present the various experiments which have been conducted to examine and clarify some of the questions arising out of the previous research works. These experiments can be grouped in the following manner. (Obviously some of the experiments are only off-shoots of the major experiments).

(a) Preliminary experiments

These experiments are based on the recommendations of a previous researcher [3] and the objectives has been to enhance the depth of drilling. Details of these experiments are presented in Section 3.3.

(b) Study of the basic configuration of ECD used for machining non-conducting materials.

The objective of this group of experiments has been to investigate the voltage-current characteristics in free electrolyte (without the presence of work). These are presented in Section 3.4.1 through 3.4.12.

(c) Shifting of discharge zone from tool tip and associated experiments :

Experiments presented in this category are to study the aspects relating to shifting of discharge from tool tip under confined configurations. Sections 3.5.1 to 3.5.3 gives the details.

(d) Experiments devoted to investigate current density effects :

Experiments in Sections 3.6.1 and 3.6.2 gives details of these experiments.

e,f) Experiments related to surface conduction and Interfacial Phenomena of Glass and other Non-Conducting Materials.

These experiments are based on the consequence of observation in the shift of current waveform (case d above). Sections 3.7 and 3.8 explain these experiments.

3.2 Experimental Set-ups

Experimental set-up and arrangements varied from test to test. However, most of the experiments were done with the arrangement shown in Figure 3.1 which gives the schematics of this set-up. It consists of a power supply unit, tool feed arrangement, heater for heating electrolyte and various

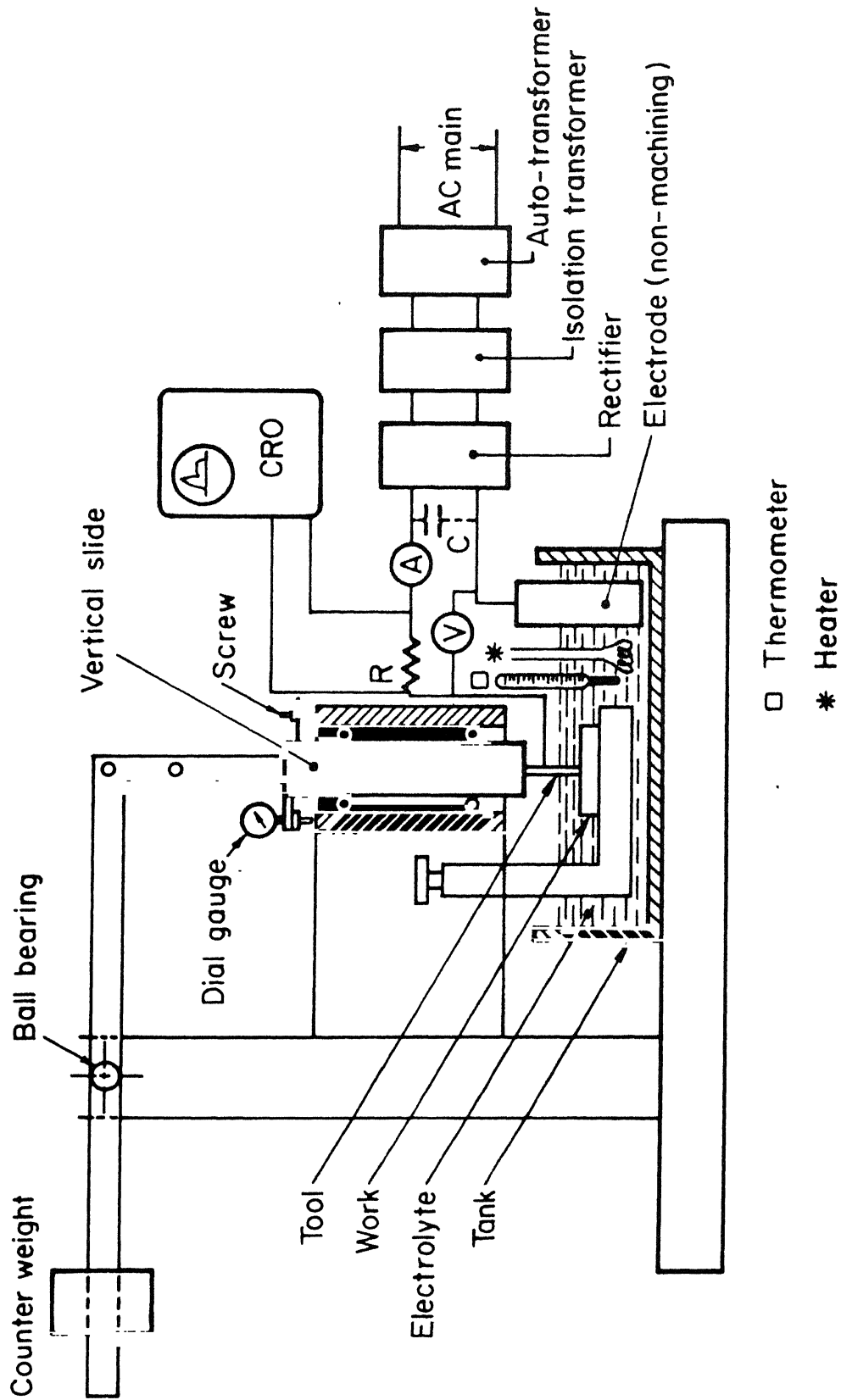


Fig.3.1 Schematics of experimental set-up

measuring instruments. The power was taken from AC mains through an autotransformer, isolation transformer, and bridge rectifier. A resistance of 0.1 Ohm (shown as 'R' in Figure 3.1) was connected in series and the voltage drop across this resistance was measured by an oscilloscope to observe the current waveform. Voltage wave forms were also observed with the help of the oscilloscope. When experiments were to be conducted with DC (smoothed), an electrolytic capacitor of 1000 μ F, 350 VDC was connected across the supply (shown as 'C' in Figure 3.1). The tool feed arrangement was based on gravity as used in USM since the tool has been always touching the work. The tool was attached to a vertical tool-slide having linear bearing (of balls) to reduce friction. The horizontal lever with the counter weight was hinged through a ball-bearing in the main frame. The counter weight could be adjusted for tool force of few grams to few tens of grams. A dial gauge fitted on the tool slide, measured the penetration of tool into work. A screw fitted on the frame helped to set the tool at correct electrolyte depth for the calculation of current density at the tool tip. Different type and size of electrolyte tanks were used depending on the need of experimentation. A voltmeter and an ammeter have been used to note the average value of voltage and current. An electrical heater and a thermometer were used to control the temperature of the bath. In all experiments conducted, the non-machining electrode was a graphite block of ≈ 15 mm diameter and

40 mm length positioned \approx 30 mm away from tool. The work was held on a platform with facility for vertical adjustment of work height.

3.3 Preliminary Experiments

The experiment described in Sections 3.3.1 and 3.3.2 were essentially those recommended by the previous researcher [3] to enhance the drilled depth in machining of glass. (glass refers to soda-lime glass purchased from the local market with thickness ranging from 0.2 mm to 5 mm).

3.3.1 Machining of glass with coated tools

Earlier workers have used a tool depth of 3 mm in the electrolyte. As the drilling progresses, this depth would increase (since the level of electrolyte is constant; as the drilling proceeds more depth of tool comes in contact with the electrolyte). It was thought that the increased contact area of the tool with electrolyte would decrease the efficiency of spark since the sparking now occurs on a larger area of tool. It was suggested by Umesh Kumar [3] that a coating on the tool except the tip could possibly concentrate the discharge at the tip of the tool. (This is similar to the coating of tools used in ECM). The procedure in brief, adopted for coating the tool for experiments with coated tools, was as follows. 50 ml of warm water was taken in which 30 g sodium silicate (binder) was mixed thoroughly to form a consistent slurry. Alumina

(Al_2O_3) in fine powder form was added to the already prepared slurry and stirred to obtain uniform mixing. The tool of 1.6 mm diameter made of stainless steel was dipped in the slurry to develop a uniform coating a fraction of a millimeter thick. The tool was then air dried for 24 hrs and was sintered at $\approx 800^\circ\text{C}$. Experiments were performed and the drilled depths were compared with coated and uncoated tools under similar conditions. (NaOH (35%) was used as electrolyte). The coated tool did not show any improvement in penetration, moreover the coating also peeled-off at some spots on the tool during the operation. So a better material for coating has been searched and Vikram Sarabai Space Centre, Trivandrum has recommended a coating material as a possible solution. Anabond Pvt. Ltd., Madras supplied the coating material called silibond for this purpose. Though this coating survived the machining process, it also did not improve the machined depth. Experiments presented in Section 3.5.2 will show, how the limitation on the drilled depth arises due to the voltage drop taking place in the side gap of the drilled hole because of the high bubble void fraction condition.

3.3.2 External supply of bubbles to the machining zone

Umesh Kumar [3] had suggested that the presence of large number of microbubbles near the tool would initiate discharge and possibly lead to improvement in the drilling depth. This was based on the logic that sparking is essentially due to

discharge across the gas bubbles generated in the process. In such a situation the size of the gas bubble also would be an important parameter deciding the energy per spark and hence the mrr. An attempt was, therefore, made to measure the diameter of gas bubbles generated in the process. Such an arrangement is shown in Appendix . This experiment did not, however, become a part of the work in any major way but is included in the work for reference only. The following method was adopted for the experiments with injected gas bubbles. Holes of 0.4 mm diameter were drilled along the circumference of the tool (copper tube, \varnothing 3.125 mm) near the machining end. The hollow end of the tube was plugged with several wires of \approx 0.3 mm \varnothing to create a perforated end. Machining tests were conducted using this tool with air supplied at 1.5 atm pressure. The machined works with air injection and without air injection were compared and these has not shown any observable difference in performance. In fact the bubbles coming out of the 0.4 mm \varnothing hole were quite big, 1 to 3 mm in size and it has been felt that discharge could not be induced across such large bubbles. So various methods were tried to produce bubbles of micron size. It was interesting to note that even an injection needle of \approx 0.2 mm bore produces bubbles of 1 to 2 mm \varnothing or more. In the literature [32] a method has been given to produce very small diameter bubbles. The method basically uses a capillary tube made out of micro pipette (made of glass) drawn to a very large taper. A given nozzle could produce a constant diameter bubble.

In the present investigation, a simple method conceived by the author was able to produce bubbles of very small diameters. The arrangement is shown in Figure 3.2. A copper tubing of 3.125 mm \varnothing had been pressed against a rubber sheet with the help of 3 screws. A micro air-opening was made available between the tube and the rubber sheet at (location 'A' in Figure 3.2) by adjusting the screws. The arrangement enabled to produce different diameter bubbles by varying the size of the micro opening. It was found that bubbles which could only be seen by magnifying glass (10X magnification) were produced by this arrangement. However, this system could not be tested for air injection machining because of the difficulty in supplying these bubbles to the machining zone of the tool. Thus, the role of microbubble in machining process remains uninvestigated. However, as will be seen in the subsequent sections their role may not be of great significance.

3.4 Study of the ECD Configuration used for Machining Non-conducting Materials

3.4.1 Basic features of the ECD configuration

Since the preliminary experiments as suggested by the previous researcher [3] have not shown any positive result, it was considered useful to investigate the basic features of the ECD configuration used for machining non-conducting materials. As already mentioned in Section 2.3, the configuration has the

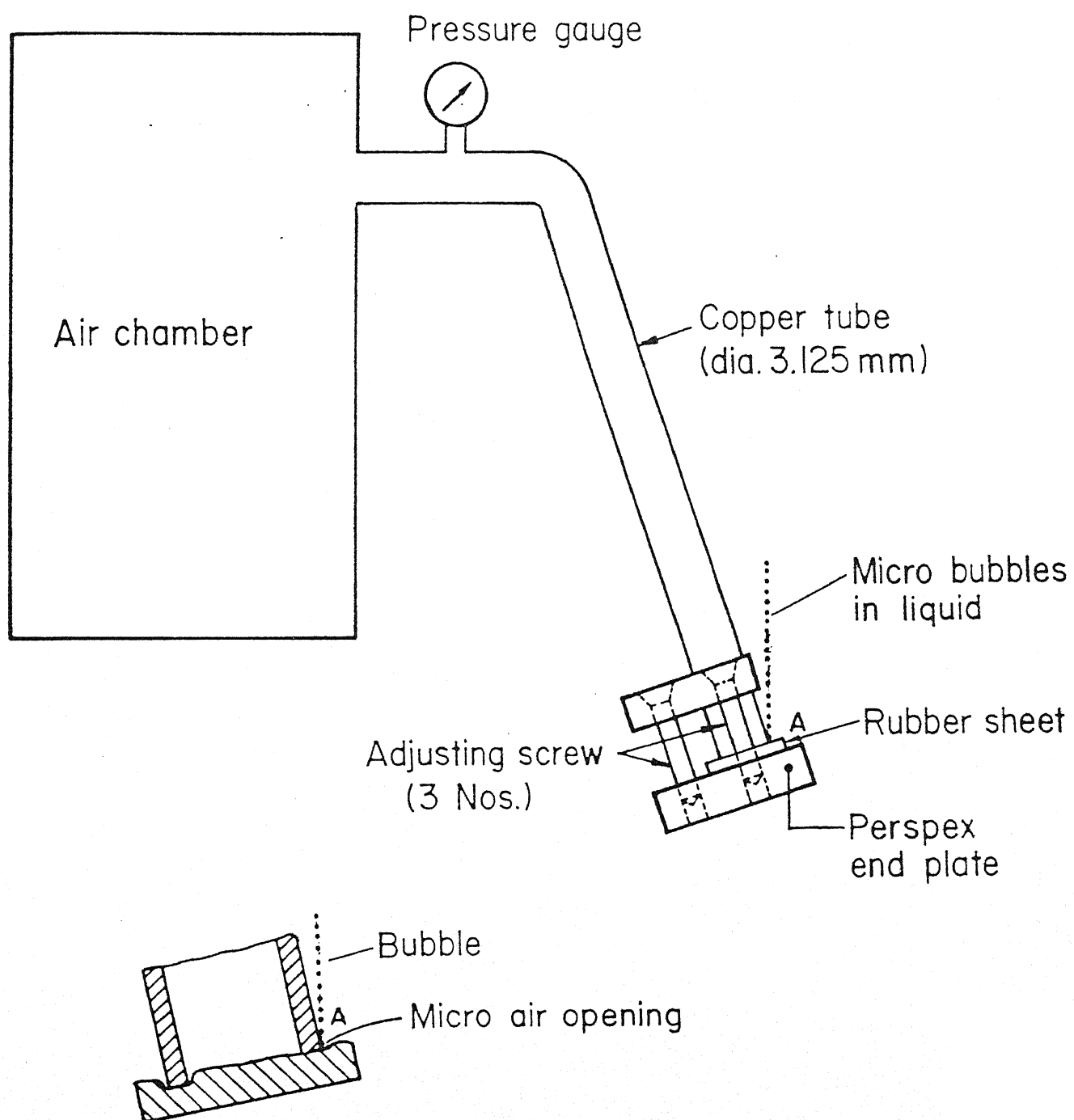
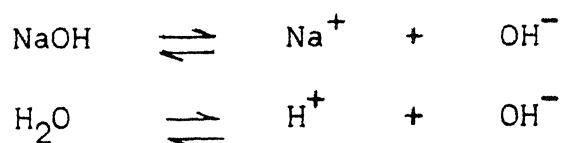


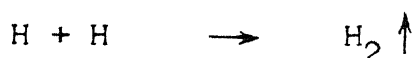
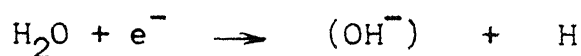
Fig.3.2 Schemetics of μ bubble generation

speciality in that the two electrode-electrolyte interface areas are unequal. The tool has a very little contact area with the electrolyte compared to that of non-machining electrode. In fact this is the only factor that selects the sparking electrode. If the two electrodes have equal contact area with the electrolyte, the discharge would start on cathode and after some time would shift to anode as the anode is dissolved electrochemically reducing anodes contact area with the electrolyte. The experiments, detailed in the following section, lead to better understanding of the process. These experiments were conducted in the absence of workpiece and are referred to as free-electrolyte experiments. The motivation behind these experiments was to study the system characteristics (voltage-current relation) of the configuration under various conditions. These system characteristics provide some useful information regarding the mechanism along with the material removal rate behaviour. NaOH (35%) electrolyte was used in all these experiments because detailed results on mrr are available with this electrolyte only [2,3]. So, for the purpose of comparison, 35% NaOH was chosen as the electrolyte. It is established that following chemical reaction takes place in NaOH electrolyte.

The ionization reactions are :

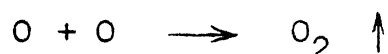
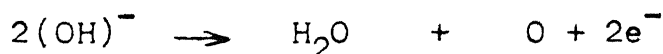


The reactions at cathode are :



i.e., electrolysis of water takes place at cathode. Water molecule receives one electron from the cathode and form one hydrogen atom and one hydroxyl ion, (OH^-) . So, hydrogen gas is produced at cathode and (OH^-) drifts towards the positive electrode. In the present experimentation as the voltage levels used are very high, other types of reactions may also occur.

The reactions at anode are :



The hydroxyl ion, (OH^-) surrenders its electrons to the anode forming water vapour and oxygen.

With graphite anode it has been observed that gradual disintegration of anode takes place; while gradual dissolution reaction occur with metallic anodes. Subsequent sections give experimental insight into the system behaviour of the configuration mentioned above.

3.4.2a Behaviour of bubbles and voltage-current characteristics in the electrolyte bath without workpiece (negative tool).

As discussed in Sections 2.2.2 and 2.2.3 the discharges in

electrolyte are produced by the formation of voids with high voltage gradients. If the tool is negative, hydrogen gas bubbles are generated and if the tool is positive, oxygen gas bubbles are generated at the tool-electrolyte interface. In the present work the gas bubbles generated at the tool were observed using a magnifying glass. The bubbles at the tool have very high population density since only limited area of the tool is in contact with the electrolyte (bubbles at the non-machining electrode have a very low population density and do not produce any effect at the anode).

When DC (full wave rectified) or AC was used, the observation of bubbles did not provide much useful information as the voltage value changed from zero to maximum in every pulse. The bubble generation rate in such a supply also followed similar variations leading to transients in the system. So a DC (smoothed supply) was used in this experiment. This was obtained by connecting a capacitor across the supply as shown in Figure 3.1. Larger diameter tools caused capacitance discharge because of the higher current drawn through the circuit and thereby caused high ripples in the smoothed DC. So, a very small tool having diameter 0.13 mm was selected; with this choice ripples in the supply were almost negligible. A tool depth of 2 mm was used. The voltage was increased gradually and the current and the bubbles were closely watched. At lower voltages, the bubbles were rising upward in the bath due to

buoyancy force. As the voltage reached a critical value (V^* in Figure 3.3) the bubbles started shooting radially from the tool and the current came down to a considerably low value as shown in Figure 3.3.

The rate at which hydrogen gas generates at the cathode is given by [17],

$$C' = \frac{M_H R' T I}{n P F}$$

where C' = rate of hydrogen generated, cm^3/sec .

M_H = atomic weight of hydrogen, g

R' = gas constant = 420.3×10^2 g.cm/g $^{\circ}\text{K}$

T = temperature, $^{\circ}\text{K}$

n = valency of hydrogen

P = pressure, g/cm^2

F = Faraday's, constant

I = current, amps.

Therefore, under a given condition, the volume of hydrogen generated is proportional to the current flowing through the circuit. At the critical voltage, V^* , since the average current density, i_a was at peak value, the gas generation rate also reached the peak, causing a kind of insulation between the tool and the electrolyte. However, with the voltage beyond V^* , the average current density, i_a decreased considerably (the instantaneous values of current might be high depending on discharge condition) and under this condition, the system should have

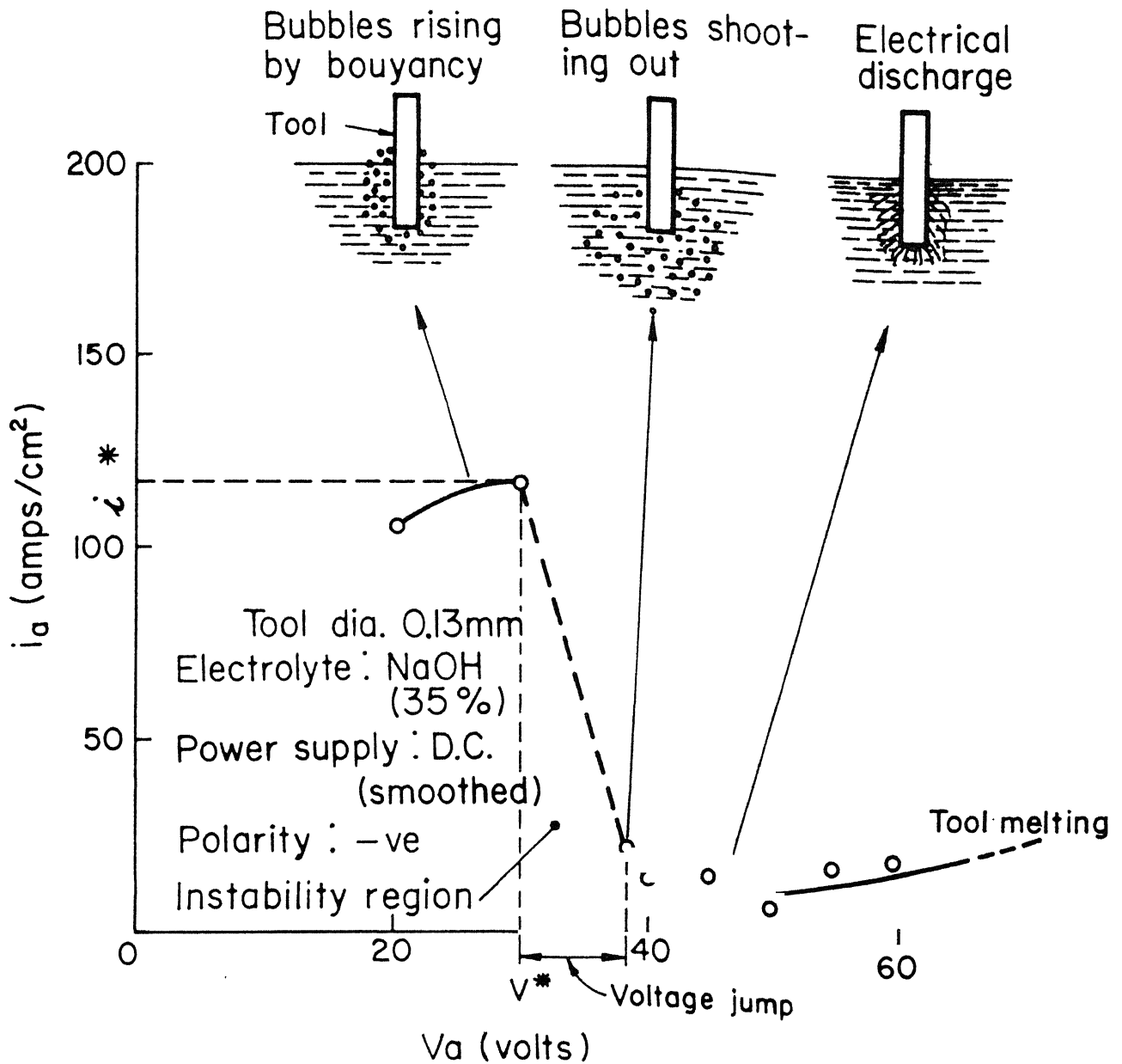
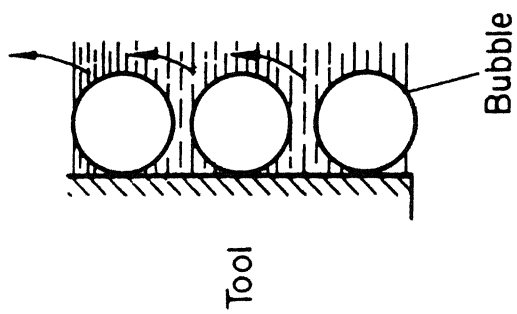


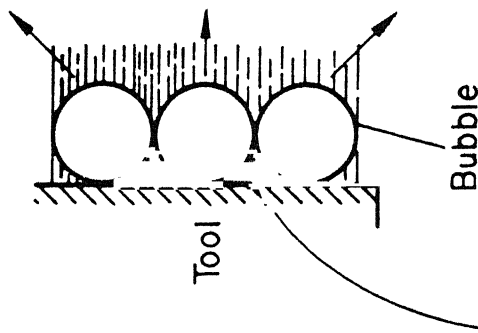
Fig.3.3 Behaviour of bubbles at various voltages

gone back to the original critical current density, i^* . Therefore, it is logical to assume that some interesting phenomena has happened which prevented the tool-electrolyte interface to deliver high current. The author postulates that the most probable reason could be the instantaneous boiling of the local narrow electrolyte-bridges between the bubbles due to the high local current density causing a vapour phase in the interface as explained below (other reasons explained in Section 2.2.2 could also be taking place).

Bubbles immediately after their generation are schematically shown in Figure 3.4 under both no boiling and boiling conditions. The bubble shooting from the tool could be considered as a result of the instantaneous boiling of the local electrolyte. The local boiling and vaporisation of electrolyte results in quick expansion of gas forcing the nearby bubbles to shoot out. The average voltage and average current density curve shown in Figure 3.3 indicate an instability region in which a state can not be located. The voltage makes a jump from V^* to a value which is close to the open circuit value of the voltage as the average current flowing through the circuit has come down to a lower value. Discharge now takes place at tool-electrolyte interface along with bubble shooting. The discharge became more vigorous as the voltage was further increased, eventually melting the tool. It was observed that melting of the tool always started from the corner points of the tool. The non-machining graphite electrode (positive in



(a) Bubble rising up



Local boiling of electrolyte bridge

(b) Bubble shooting

Fig. 3.4 Schematics of bubble shooting

this case) showed small amount of disintegration of particles from its surface.

Moreover, an instability loop exists at the instability region. When the voltage was reduced, the discharge phenomena could be sustained even with a voltage 2 to 4 Volts less than the jumped voltage value. The above experimental observations suggest the following :

- i) The average current density, i_a decreases beyond the critical voltage, V^* ,
- ii) local boiling of the narrow bridge of electrolyte between the bubbles is taking place, probably due to high current density, and
- iii) the tool melts at high voltages;
the melting of negative tool probably occur due to the thermionic emission of electrons from the red hot cathode and thereby causing intense discharge (arcing) at the tool.

Further investigation with regard to voltage-current characteristics with a positive tool are presented in the next section (Section 3.4.2b).

3.4.2b Voltage-current characteristics in the electrolyte bath without workpiece (positive tool)

The experimental conditions were same as that of the experiments described in Section 3.4.2a. The only difference being that the tool was connected to the positive polarity.

Because of the dissolution of the tool, the bubble behaviour was not observable clearly. The i_a - V_a characteristics of a positive tool is shown in Figure 3.5. The major difference in the performance of a positive tool was that it never underwent melting. Since the average current density, i_a was very low at higher voltages, the dissolution of tool was also low (NaOH electrolyte). It has been reported [33] that the mrr obtained in stainless steel in ECM using NaOH as electrolyte was negligible. The present observation correlates with the results obtained [33] in ECM using NaOH electrolyte. The probable reason could be the formation of some insulating interface such as metal hydroxides on the surface of the anode (in the present case tool) preventing it from dissolution.

The main conclusion which can be drawn from these experiments is that the response of a negative tool and a positive tool differ considerably in an ECD bath of NaOH. A negative tool melts at high voltages, while a positive tool never melts but shows limited dissolution at high voltage even under discharge condition.

3.4.3 Potential drop across the tool and the non-machining electrode

Earlier researchers [2,3] have always positioned the non-machining electrode at a distance of 30-50 cm under the work and the axis of tool, work and non-machining electrode formed

a vertical plane. This arrangement gave an impression as if a continuous conducting path between the electrodes through the non-conducting work was essential for the machining to take place. So the effect of disposition of non-machining electrode was tested by measuring the voltage drop across the tool and the non-machining electrode along the electrolyte bath. Figure 3.6 illustrates the voltage drop along the bath. The potential drop has been measured by a multimeter. The tool was 0.13 mm ϕ cu wire and DC (smoothed) supply was used. Under various applied voltages between the electrodes, the voltage drops were measured (i) between the tool and the immediate electrolyte volume, (ii) along the electrolyte path between electrodes and (iii) between the non-machining electrode and the immediate electrolyte volume. The potential drops with applied voltages of 20, 25 and 45 Volts are shown in Figure 3.6. With non-sparking condition, a voltage drop of 3 to 4 Volts has been observed along the 30 mm electrolyte path. But at sparking condition (45 Volts) the voltage drop was negligible along the electrolyte path. Figure 3.6 also illustrates that the voltage drop at the non-machining electrode-electrolyte interface remains almost constant irrespective of the applied voltage and is about 2 Volts. The voltage drop at the tool-electrolyte interface is very high, probably, the whole voltage drop is taking place at this interface. This situation arise from the unequal area of contact of the electrodes with the electrolyte.

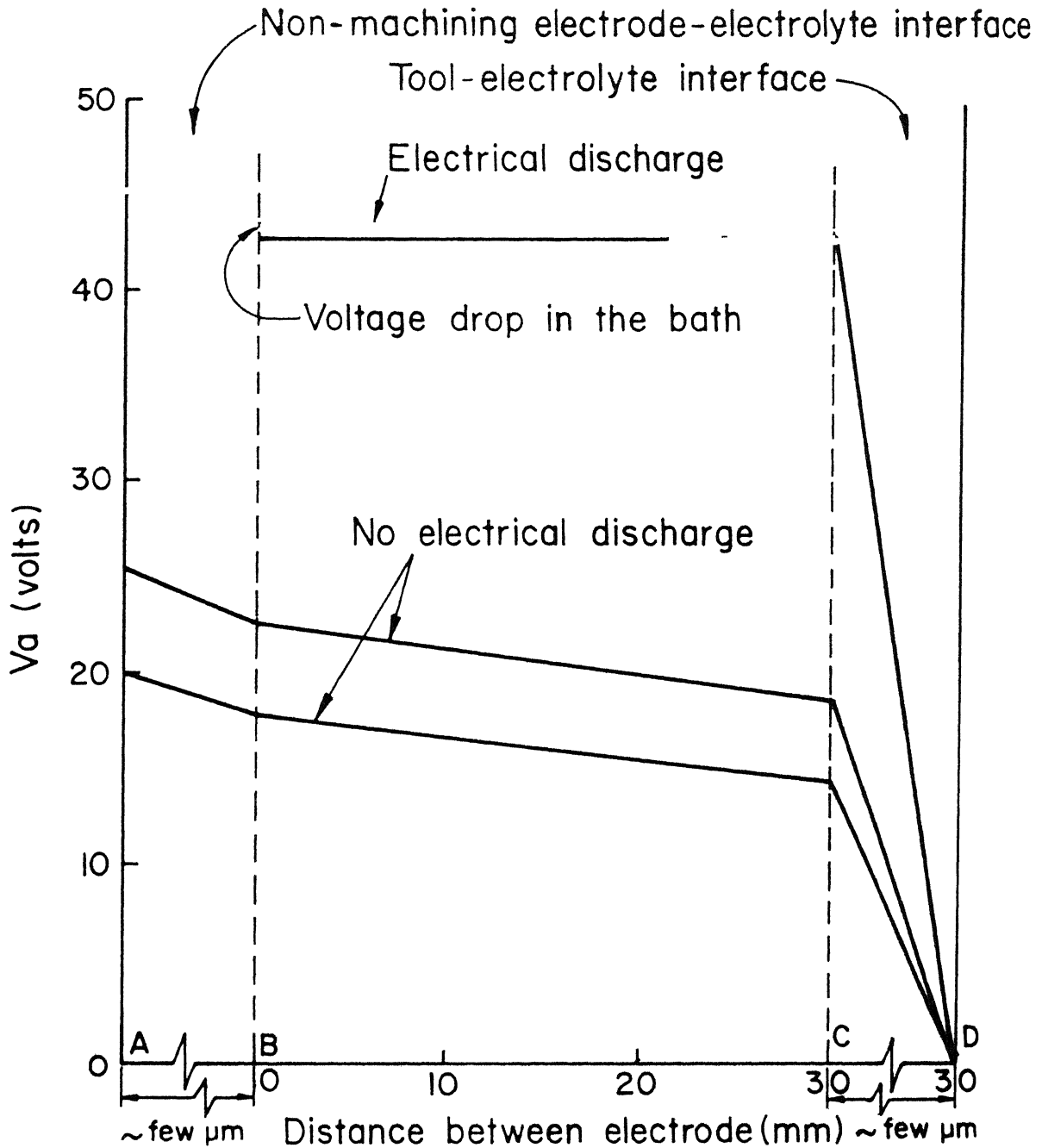


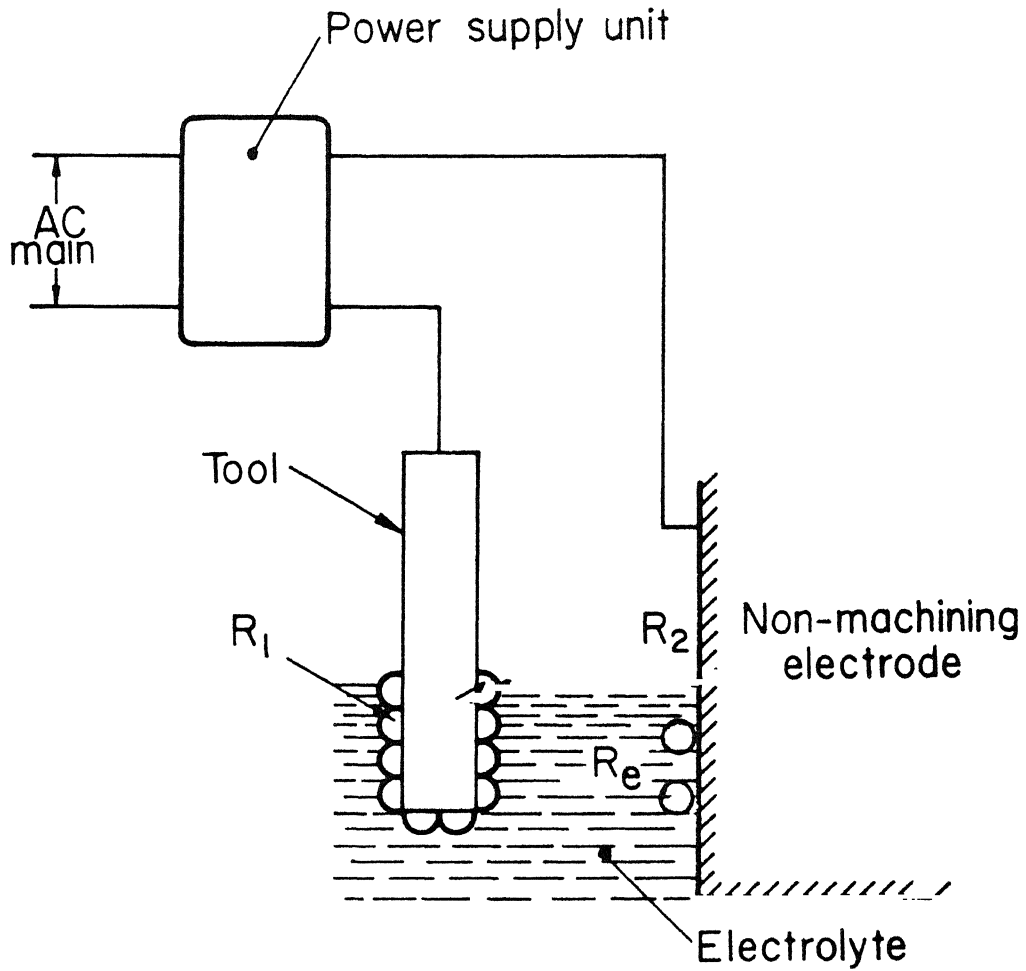
Fig. 3.6 Distribution of voltage drop in an ECM bath
 [Electrolyte : NaOH (35%); Tool polarity : -ve;
 Power supply : D.C. (smoothed)]

The high gas bubble population density (multiple bubble layer) at the tool forms a high resistance for the current to flow. This feature is schematically shown in Figure 3.7. The tool electrolyte interface resistance will, as a fact, vary instantaneously depending on the discharge conditions. The location of the non-machining electrode, whether it is below the work or at the side of the work does not matter since the resistance in the whole circuit other than tool-electrolyte interface is very low. However, the voltage drop in the electrolyte path would vary a few volts depending on the distance between the electrodes and the current flowing through the circuit. So, for consistent results, a fixed distance between the tool and the non-machining electrode is to be maintained. With a DC (full wave rectified) supply, the conditions shown in Figure 3.6 for different DC (smoothed) voltages will repeat in every pulse.

3.4.4 Effect of electrolyte temperature on voltage-current characteristics

The sudden drop in average current at the critical voltage has been discussed in Section 3.4.2a based on local boiling of the electrolyte bridge current carriers due to high local current density. Heat required H , to raise mass of the electrolyte from the initial temperature, T_i to the boiling point, T_b is given by

$$H = m_e c_e (T_b - T_i)$$



R_e = Electrolyte path resistance

R_1 = Tool - Electrolyte interface resistance

R_2 = Non-machining electrode - electrolyte interface resistance

R_1 Fluctuates depending on voltage

Fig.3.7 Resistance in ECD (non-conductor machining) configuration

where,

H = heat required to raise m_e mass of electrolyte from temperature T_i to T_b , cal

m_e = mass of electrolyte forming the narrow current carrying bridge between the bubbles, g

c_e = specific heat of electrolyte, cal/g/ $^{\circ}\text{K}$

T_b = boiling point of electrolyte, $^{\circ}\text{K}$

T_i = initial temperature of electrolyte, $^{\circ}\text{K}$

The heat produced by the current flow is given by

$$\text{Heat produced} = I^2 R_e$$

where,

I = current flowing through the narrow bridge

R_e = resistance of electrolyte under consideration

Thus when the electrolyte is heated, its conductivity increases (Figure 1.12) and the heat produced also will increase for a given applied voltage. At the same time the heat required to boil the electrolyte should decrease, thereby, a lowering of the critical voltage needed at higher temperature of the electrolyte is expected. However, as shown in Figure 3.8, the critical voltage does not decrease with increase in temperature. Moreover, at 100°C , the critical voltage slightly increased too. The possible explanation for the above phenomena is as follows. Since the critical voltage depends on bubble population and local boiling of the electrolyte bridges at the tool-electrolyte interface, any change in the removal rate of

Electrolyte : NaOH (35 %)

Supply : D.C. (smoothed)

Tool dia. 0.5 mm (-ve)

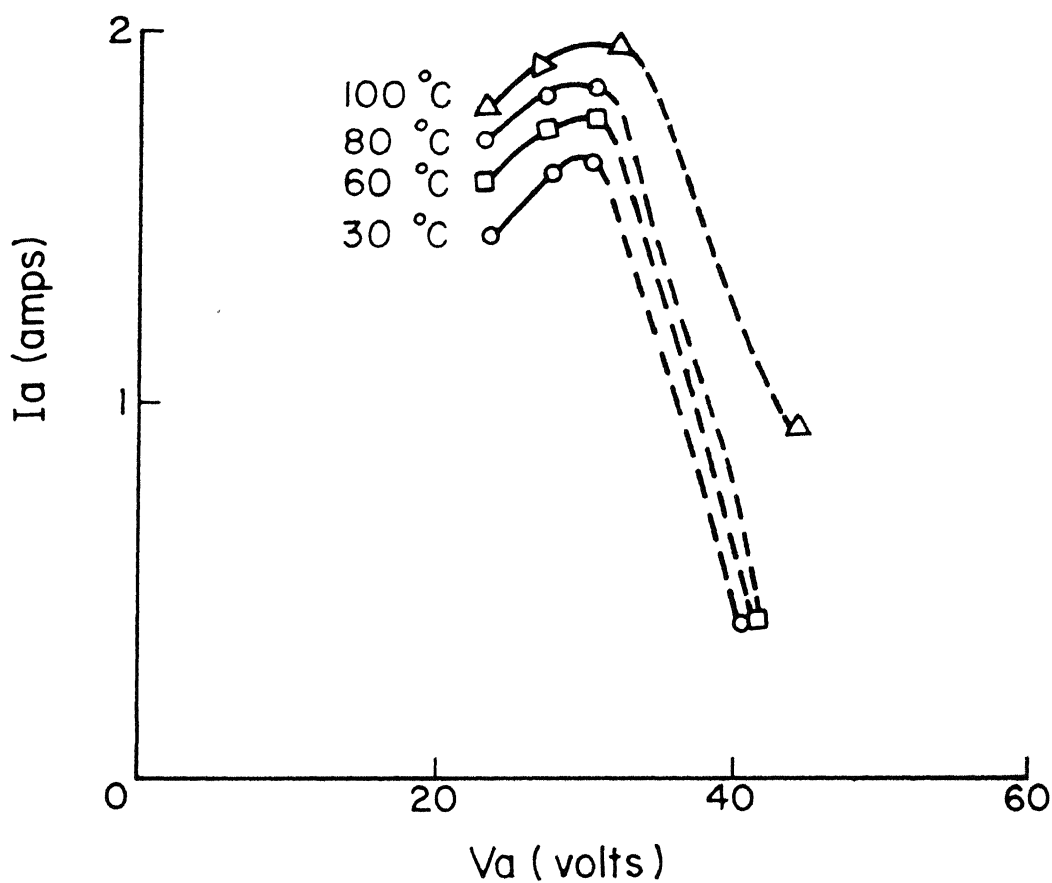


Fig.3.8 Effect of bath temperature on $I_a - V_a$

bubbles and movement of electrolyte molecules at the tool will also affect the critical voltage. The viscosity of electrolyte decrease with increase in temperature and the velocity with which the bubbles rise in the electrolyte due to buoyancy is inversely proportional to the viscosity of the solution. So, at higher temperature of the electrolyte, the bubbles are expected to move fast. The mobility of electrolyte molecules also increases with increase in electrolyte temperature. The net effect arising out of these factors may be negligible resulting in almost a constant critical voltage. Figure 1.12 actually represents the conductivities of electrolyte under bubble free condition. The values of conductivity given in Figure 1.12 hold good for a parallel plate electrode configuration usually encountered in ECM. Figure 1.12 shows an increase of about 100% in the conductivity value of NaOH (35%) for a temperature change from $\approx 30^{\circ}\text{C}$ to $\approx 100^{\circ}\text{C}$. But in the ECD configuration of non-conductor machining the increase in peak current, I^* is only 20% for a change in temperature from 30°C to 100°C . Also, the average current during discharge condition remains almost constant for different electrolyte temperatures except the boiling condition of electrolyte. This is logical only since the current during discharge is mainly controlled by the ionization taking place in the voids present at the tool-electrolyte interface.

Experiments conducted up to this stage has not provided any valuable information to pin-point what causes the material removal. So it was thought necessary to conduct further experiments described in the next section.

3.4.5 Effect of pressure on critical voltage

A pressure chamber, shown in Figure 3.9, was fabricated for this experiment. The body of the chamber was made of perspex tube of 44 mm \varnothing having a 2.5 mm wall thickness. This transparent material was chosen so as to enable viewing of the discharge from outside. A reinforcement ring (not given in Figure 3.9) was also provided at the middle height of the chamber. The large electrode (graphite) was kept at the bottom of the chamber and the tool holder had the provision for fixing tools with different diameters. The chamber has been provided with a pressure gauge, a safety valve and a gas filling valve. A 0.5 mm \varnothing cu wire was used as the tool (negative polarity). While conducting experiments, care was taken not to allow the chamber to fill with the reaction gases (H_2 and O_2) in large volumes. If the duration of the experiment is large, pressure may build-up by the generation of hydrogen and oxygen and at the event of sparking it could lead to explosion as hydrogen and oxygen react explosively under the heat of the spark forming water vapour. Higher voltages were also not attempted to avoid explosion. As shown in Figure 3.10, the average current increased with the increase in pressure of the electrolyte. The

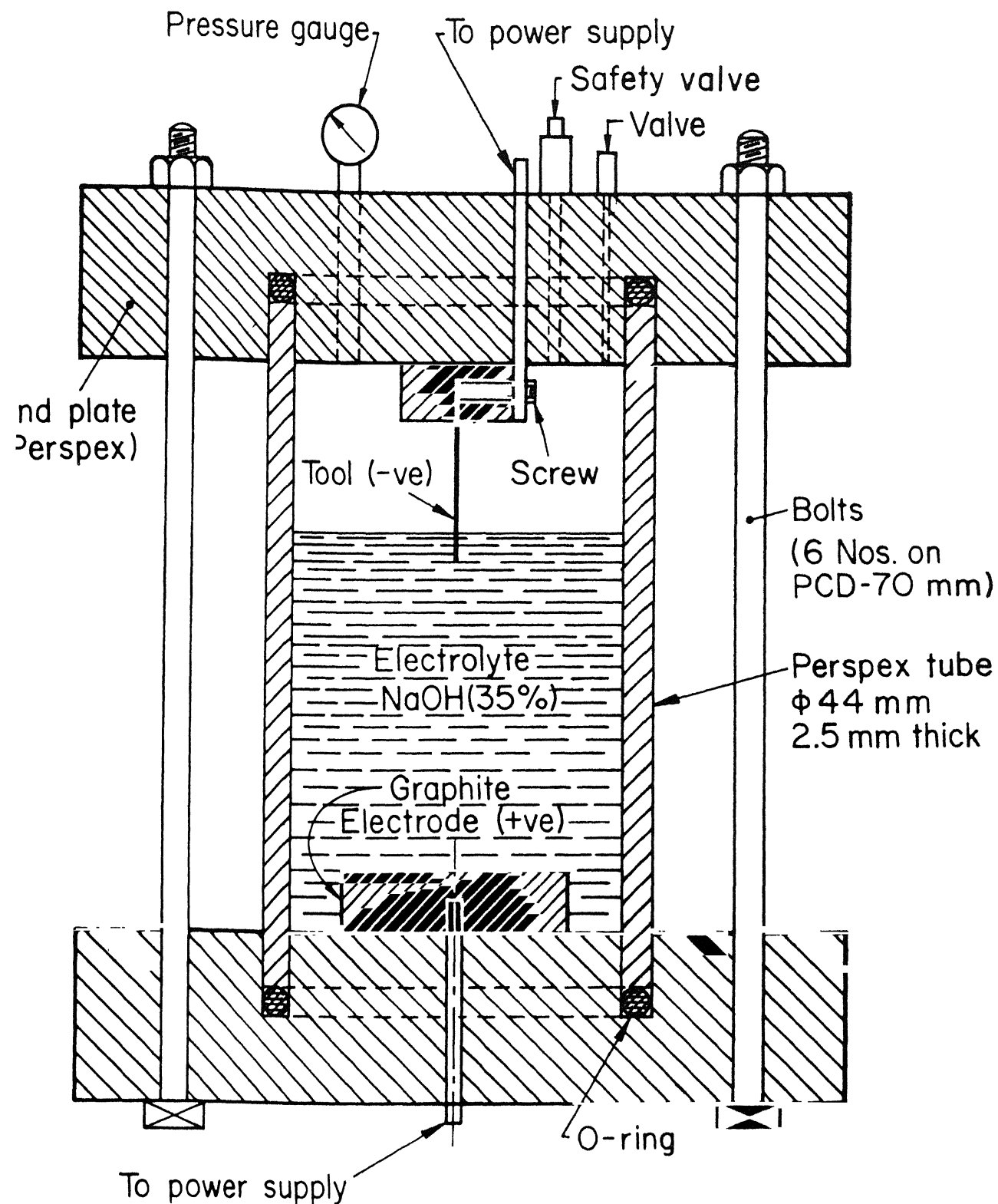


Fig.3.9 Schematics of set-up for studying discharge under pressure

Electrolyte : NaOH (35 %)

Supply : D.C. (smoothed)

Tool dia. 0.5 mm (-ve)

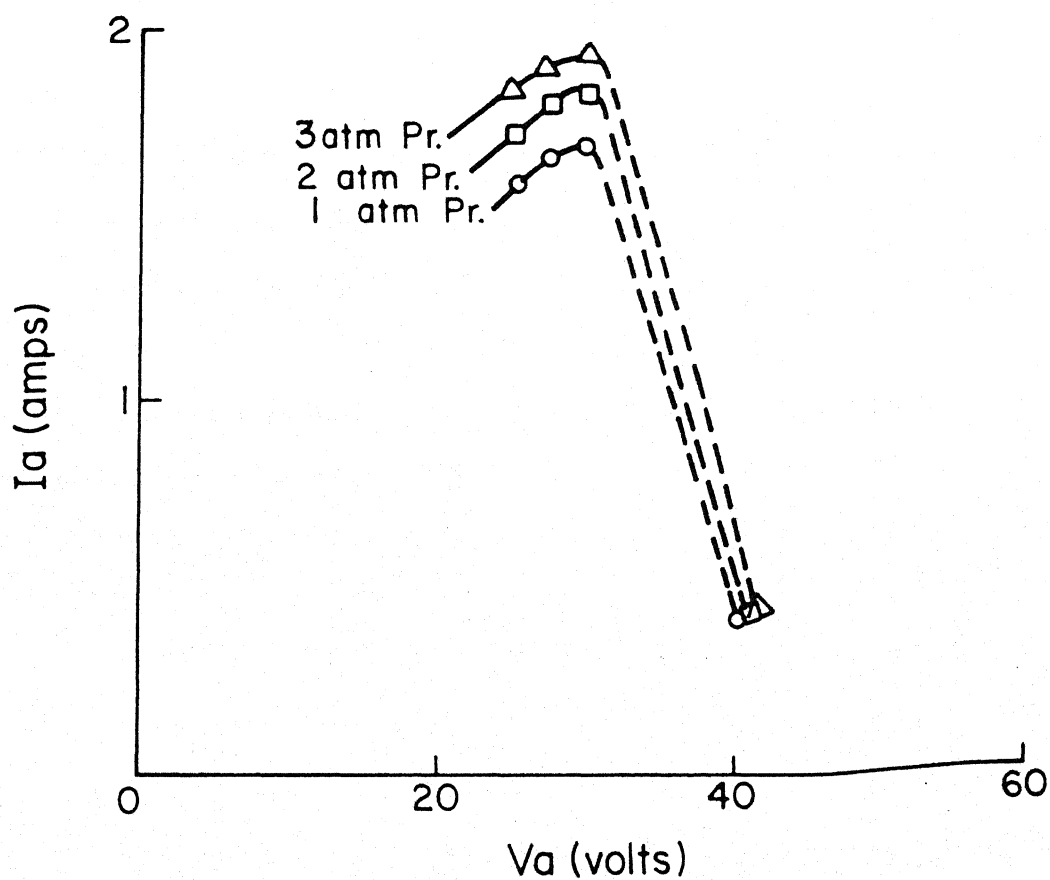


Fig. 3.10 Effect of pressure on I_a - V_a

possible explanation to this could be the compressive effect of pressure on the gas bubbles. When the bubbles get compressed, the volume occupied by the bubbles reduce and more electrolyte can come in contact with the tool. The critical voltage, however, did not vary with the pressure range (3 atm) used in this experiment. It has been reported [34] that the breakdown voltage of a gas is not a function of the distance between the electrodes alone; but is a function of the product of the distance between the electrodes and the pressure of the gas. So, if a gas is compressed and the electrodes are brought closer proportionately the breakdown voltage remains constant. In the experiments described above, a similar situation could be responsible for the observed trends. These results also do not provide much due to the mechanism of material removal except that the conductivity of the electrolyte in an ECD bath increases with increasing pressure. So more experiments were thought off. The next section presents the results of experiments conducted in flowing electrolyte condition.

3.4.6 Effect of electrolyte flow on critical voltage

This experiment was conducted to study the effect of flowing electrolyte on the critical voltage and to confirm whether the stagnant condition of electrolyte in the machining bath is needed or not. It is a fact that in ECM, the electrolyte is always made to flow between the tool and the work to avoid passivation and for getting higher mrr. The set-up used in the present study of

the electrolyte under circulation consisted of a circulating pump, a valve for controlling the flow and a plastic tube for holding the tool and non-machining electrodes. The arrangement is shown in Figure 3.11. The non-machining electrode was a copper tube of 3.18 mm diameter. NaCl solution was used in this experiment. The flow velocity was calculated by measuring the flow rate and the cross-sectional area of the tube at the tool location. These experiments showed that the critical voltage increased considerably with the flow velocity. This indicates that the presence of bubbles at the tool-electrolyte interface is an essential condition for producing the discharges. Under flowing electrolyte condition, the main influence would be to carry away the bubbles by the electrolyte.

3.4.7 Voltage and current profiles with DC (smoothed) supply

Since only the average current and the average voltage were noted in the experiments described so far, the results have not given any idea of what was happening with the passage of time in the tool-electrolyte interface. These experiments have been conducted with a 0.5 mm diameter tool. The voltage drop across the resistance shown as 'R' in Figure 1.1 has been used to get the current profiles using an oscilloscope. The voltage profiles were also noted. As shown in Figure 3.12 the voltage and the current profiles (negative tool), showed almost a straight line pattern with small ripples of low frequency

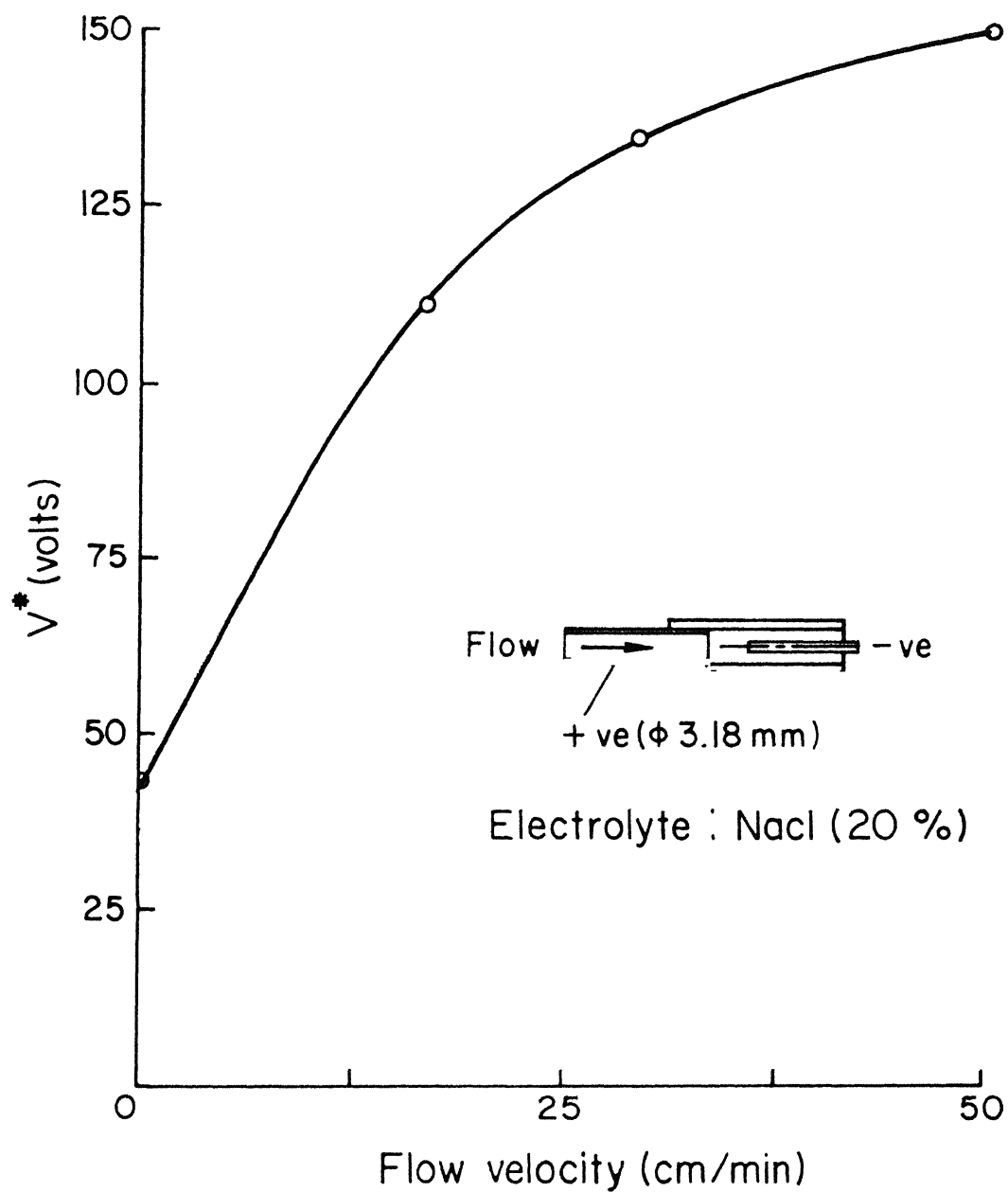


Fig.3.II Effect of flow on V^*

which indicates nothing but the characteristics of a smoothed supply produced by a capacitor (at an applied voltage of less than 20 Volts). The average current level was about 1 amps. But as the voltage was increased further, the discharge phenomena occurred and the profiles of the voltage and the current are shown in Figure 3.12 (at an average voltage of 40 Volts). The profiles indicate that high frequency discharge is taking place at the tool-electrolyte interface at this voltage. The average value of the current was, however, low during the discharge condition. The peak to the valley height of the voltage and the current profiles has increased at higher applied voltages as shown in Figure 3.12. At still higher voltages, the discharge became vigorous eventually melting the tool. With a positive tool, the conditions remained same except that the tool did not melt at high voltages. The peak to the valley height of the voltage and the current profiles were also less, at higher voltages with a positive tool; indicating the formation of some non-conducting phase in the tool-electrolyte interface.

In the subsequent section, the voltage and the current waveforms with a DC (full wave rectified) supply were investigated since the machining of non-conducting materials are usually done with a DC (full wave rectified) supply.

3.4.8a Waveform of current with DC (full wave rectified) supply (negative tool)

In this experiment a DC (full wave supply) was used for

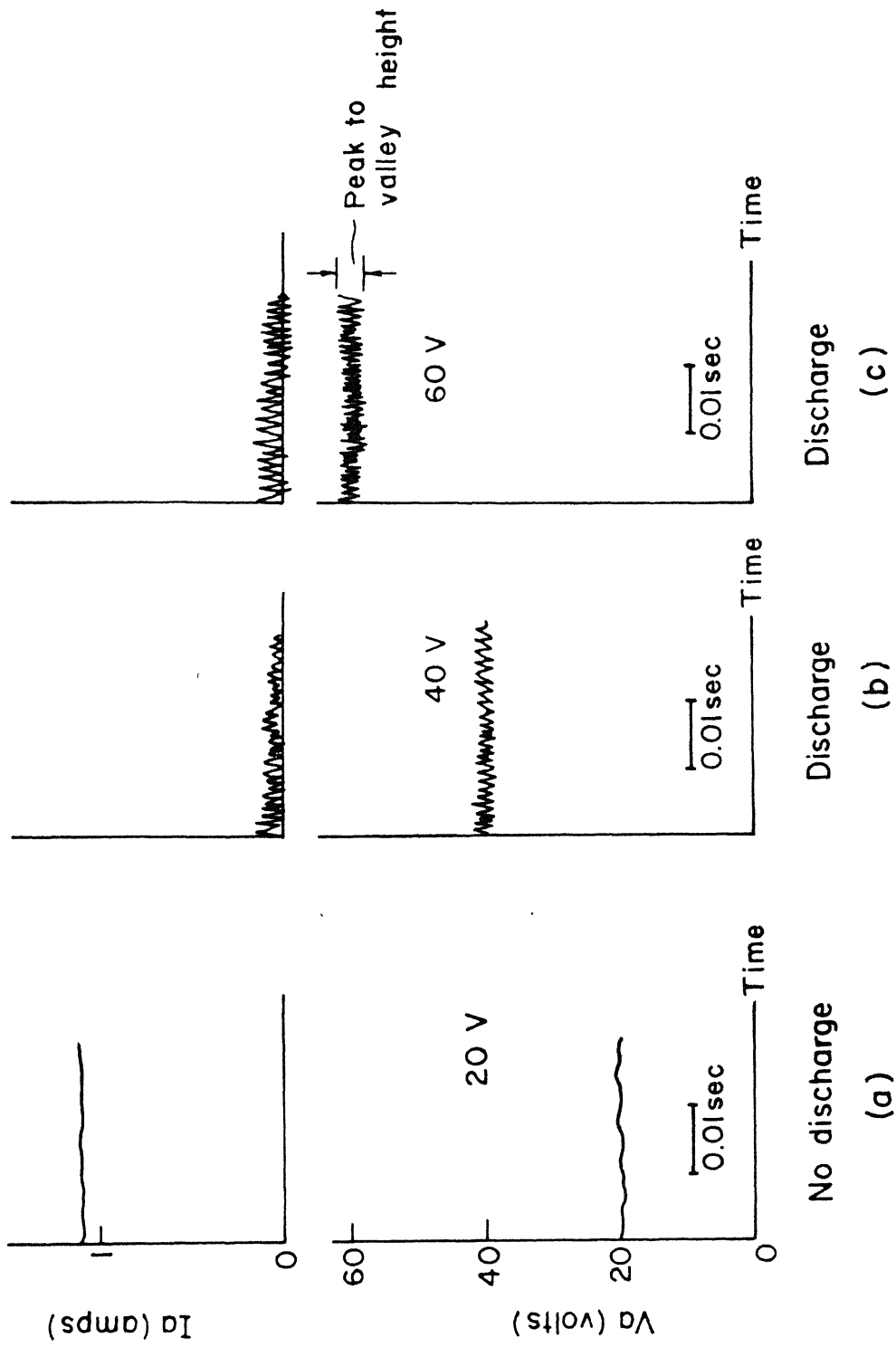


Fig.3.12 V and I profiles (DC smoothed supply) at various voltages

Studying the voltage and the current waveforms. (The name waveform has been used in this case since the applied voltage follow a pulse pattern with frequency value double that of the AC Frequency used). Since the voltage and the current form a complimentary pattern, emphasis was given to observe the current waveform. Tool was of 0.5 mm diameter in this experiment. Figure 3.13 shows the voltage-current characteristics curve along with the current waveforms at different regions of the curve. At low voltages, less than the critical voltage, the waveform was a part of sine wave, shown at 'A' in Figure 3.13. Perfect electro-chemical conduction can be considered to have been taking place at these voltages. But as the voltage was increased, the waveform of the current bent downwards (shown at 'B' in Figure 3.13) and the voltmeter and ammeter readings started fluctuating. A hissing sound was also started coming from the system. The average current passing through the circuit decreased beyond this critical voltage, V_a^* . (The critical voltage in a DC (full wave rectified) supply is taken in the present work as the average voltage beyond which current will start decreasing. The value of the critical voltage in a DC (full wave rectified) supply will be always lesser than the critical voltage value of a DC (smoothed) supply; $V_a^* \simeq \frac{2}{\pi} V^*$. These values are considered only to compare the system character under different conditions.) As the voltage was further increased, the bend in-the-wave had come closer to the bas

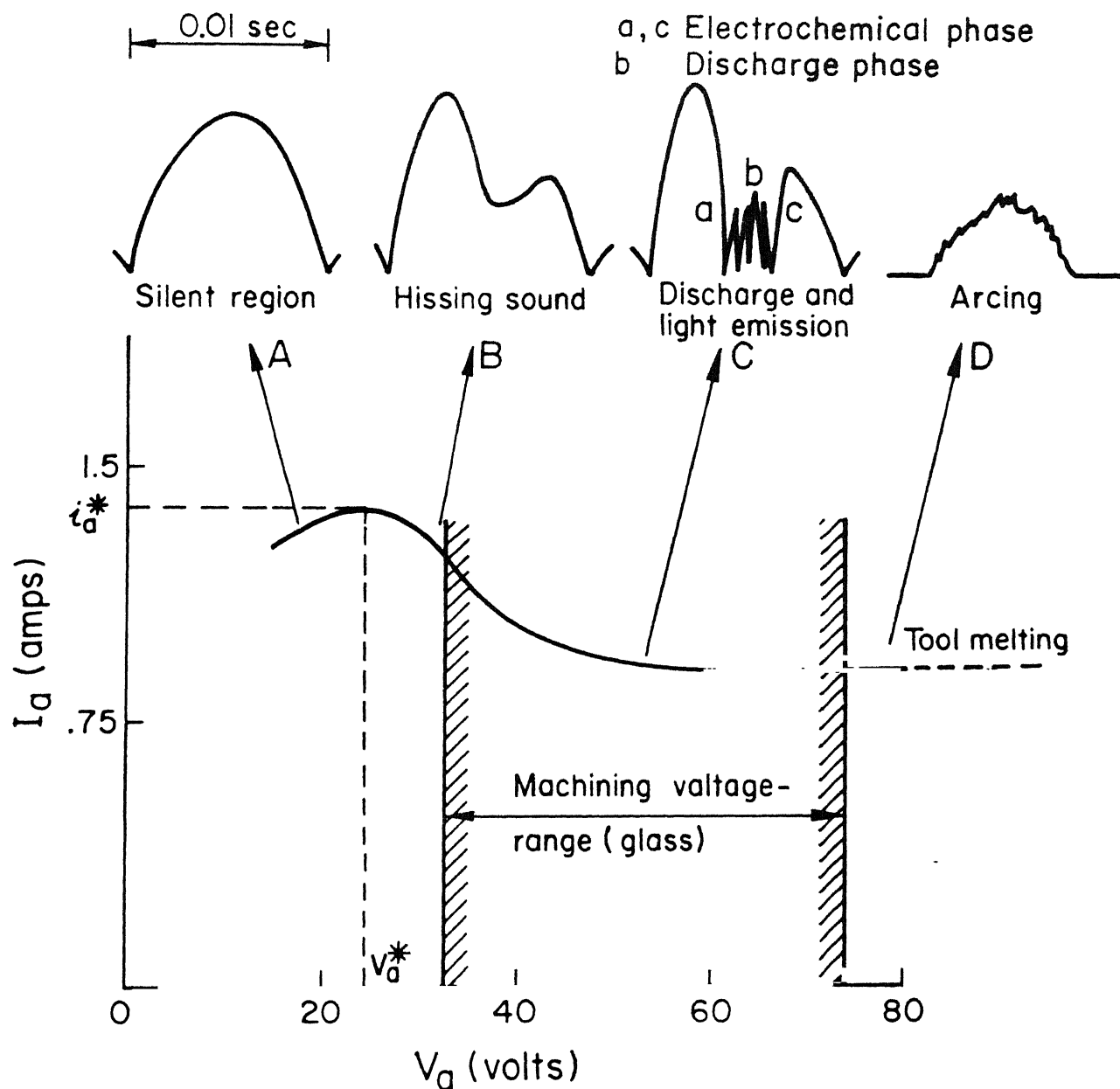


Fig. 3.13 Observed wave forms of current with free electrolyte
 [Tool polarity : -ve ; Power supply : D.C. (full wave rectified)]

of the graph and started fluctuating at high frequency and electrical discharge were seen in the system. The waveform shown at 'C' in Figure 3.13 represents the condition at a voltage about 50 Volts. When the voltage was further increased a waveform shown at D in Figure 3.13 was obtained and the phenomena eventually ended with the melting of the tool. The critical voltage value was about 22 Volts and the discharge was able to observe at about 34 Volts in this experiment. The machining voltage range usually used in the machining of glass with a negative tool is also shown in Figure 3.13 for the purpose of comparison.

A look at the current waveforms reveal some interesting features of the phenomena. At low voltages, the waveform obtained indicates that only electrochemical mode of conduction is taking place in the configuration. But at higher voltages, the configuration is subjected to some kind of blockade in current in the circuit; the blockade being a reversible one. A further increase in the voltage results in electrical discharge and under this condition the current fluctuate at high frequency. The waveform at this voltage range can be considered to have a electrochemical phase and a discharge phase. The discharge phase is occurring at the peak values of voltage in every pulse. The duration of discharge phase in a single pulse increase with increase in the applied voltage. (This feature is not shown in Figure 3.13). The melting of the tool is taking

place with a current waveform in which the electrochemical phase is absent and the discharge phase is occurring somewhat in an arc mode. The disappearance of the electrochemical phase and the arc type discharge at high voltages can be logically linked with the red hot condition of the tool. A red hot cathode (tool in this case) liberates electrons by thermionic emission and this can lead to an arc type discharge phenomenon. The electrochemical conduction phase seen in the waveform can be due to the bulk electrolytic conduction taking place between the tool and the electrolyte. When the tool becomes red hot, this mode of conduction may not be possible, thereby the electrochemical phase disappears from the waveform. It can also be seen from waveform at 'C' in Figure 3.13 that the voltage needed to sustain an electrical discharge is less than the voltage needed to initiate a discharge. In the next section, similar experiment with a positive tool are described.

3.4.8b Waveform of current with DC (full wave rectified) supply (positive tool)

This experiment was conducted to study the waveforms of the current and the voltage with a positive tool. The experimental conditions remain the same as those described in Section 3.4.8 except, for the tool polarity. The results are shown in Figure 3.14. There is no observable change in the performance of a positive tool and a negative tool in the

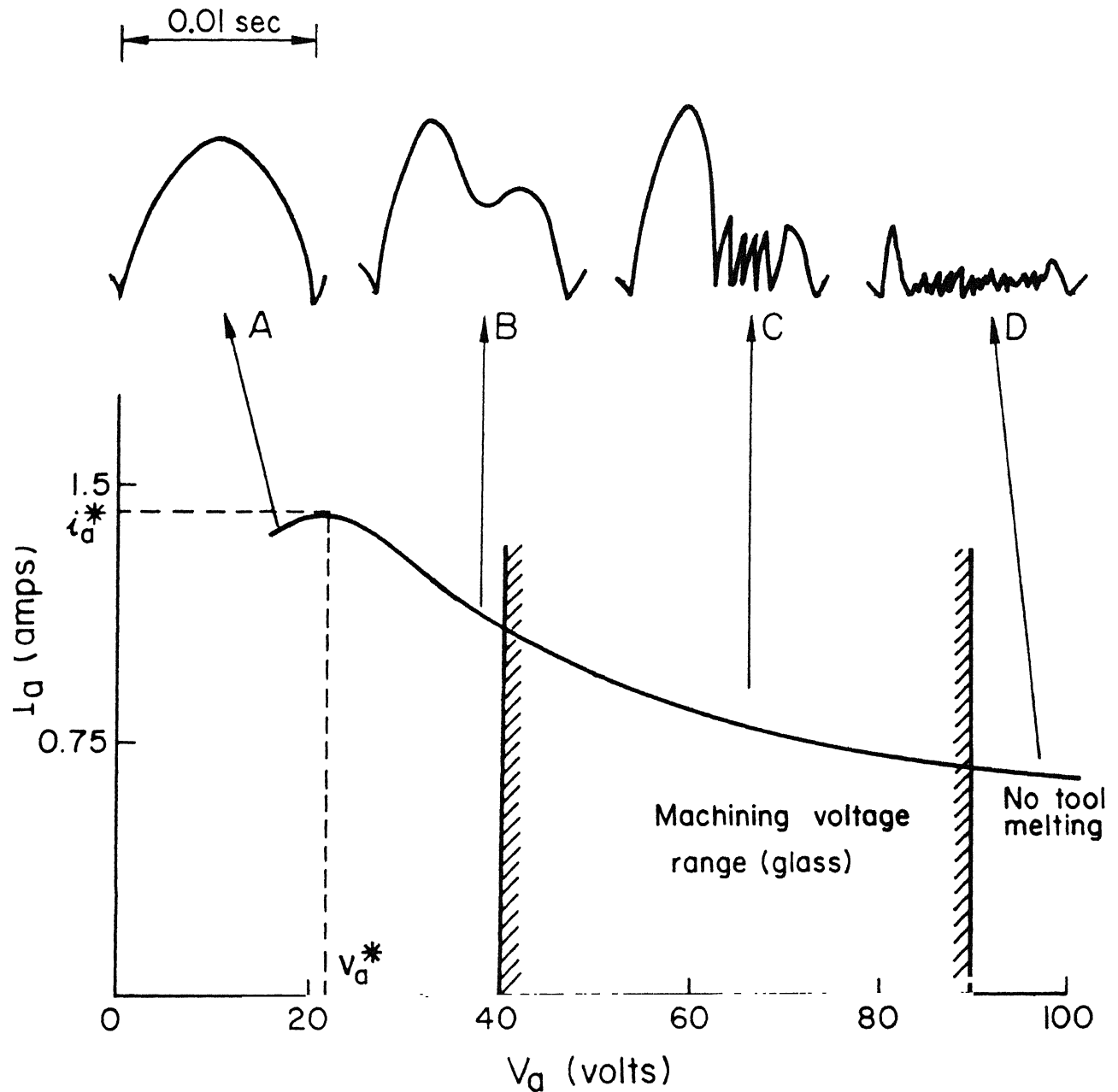


Fig.3.14 Observed wave forms of current with free electrolyte
 [Tool polarity : + ve ; Power supply : D.C. (full wave rectified)]

lower voltage ranges, say, upto a voltage of about 60 Volts. At higher voltages, however, the discharge pattern (peak to valley of the current waveform) has become less vigorous as shown at 'C' in the Figure indicating the initiation of some other phenomenon, similar to passivation. The tool did not melt in any of these tests but showed gradual dissolution. In fact, the dissolution rate was lesser at higher voltages. The average current was also less at higher voltages. In the next section, the effect of electrolyte concentration and electrolyte temperature on discharge phenomena is discussed. These experiments have become essential as mrr was found to increase with increase in the concentration as well as temperature of the electrolyte. Since one of the primary objective of any machining experimentation would be to enhance mrr, these experiments were considered important.

3.4.9a Effect of electrolyte concentration on the nature of discharge phenomena

It has been observed by the previous investigators [2,3,4, 5] that mrr increases with increase in concentration of the electrolyte. Figures 1.6 and 1.10 shows this trend. Seeing the trend in mrr, it was expected that there will be good amount of change on the nature of discharge-critical voltage, frequency, pattern of discharge, the peak to valley variation as well average value of the current during discharge. However, the discharge pattern has not shown any observable change at

the higher concentration range. But in lower concentration range, the voltage needed to produce the phenomena has gone up. The variation of the critical voltage and the critical current density with electrolyte concentration is shown in Figure 3.15. Author thinks that the following discussion is relevant in this regard. Discharge behaviour can be classified into two regions based on the concentration and conductivity of electrolyte (conductivities of electrolytes is given in Figure 1.12), (i) the concentration range where the conductivity depends on the ionic mobility and (ii) the concentration range where the conductivity depends on the ionic concentration. The latter condition exists at lower concentrations of the electrolyte. Since the test was conducted at room temperature (about 30 °C); the conductivities of NaOH electrolyte at 30 °C with concentration is discussed here. The conductivity is low at low concentration as well as at high concentration; the maximum being at about 20% concentration. In Section 3.4.4 it was pointed out that the effect of change in conductivity of electrolyte with change in temperature had only limited effect with respect to voltage-current characteristics in the ECDM configuration for non-conducting material. The reason for this type of response was explained in Section 3.4.4 and is based on the local effect at the tool-electrolyte interface. It was also observed that the voltage drop was mainly taking place at the tool-electrolyte interface as shown in Figure 3.6. This can also mean that the discharge phenomena is mainly controlled

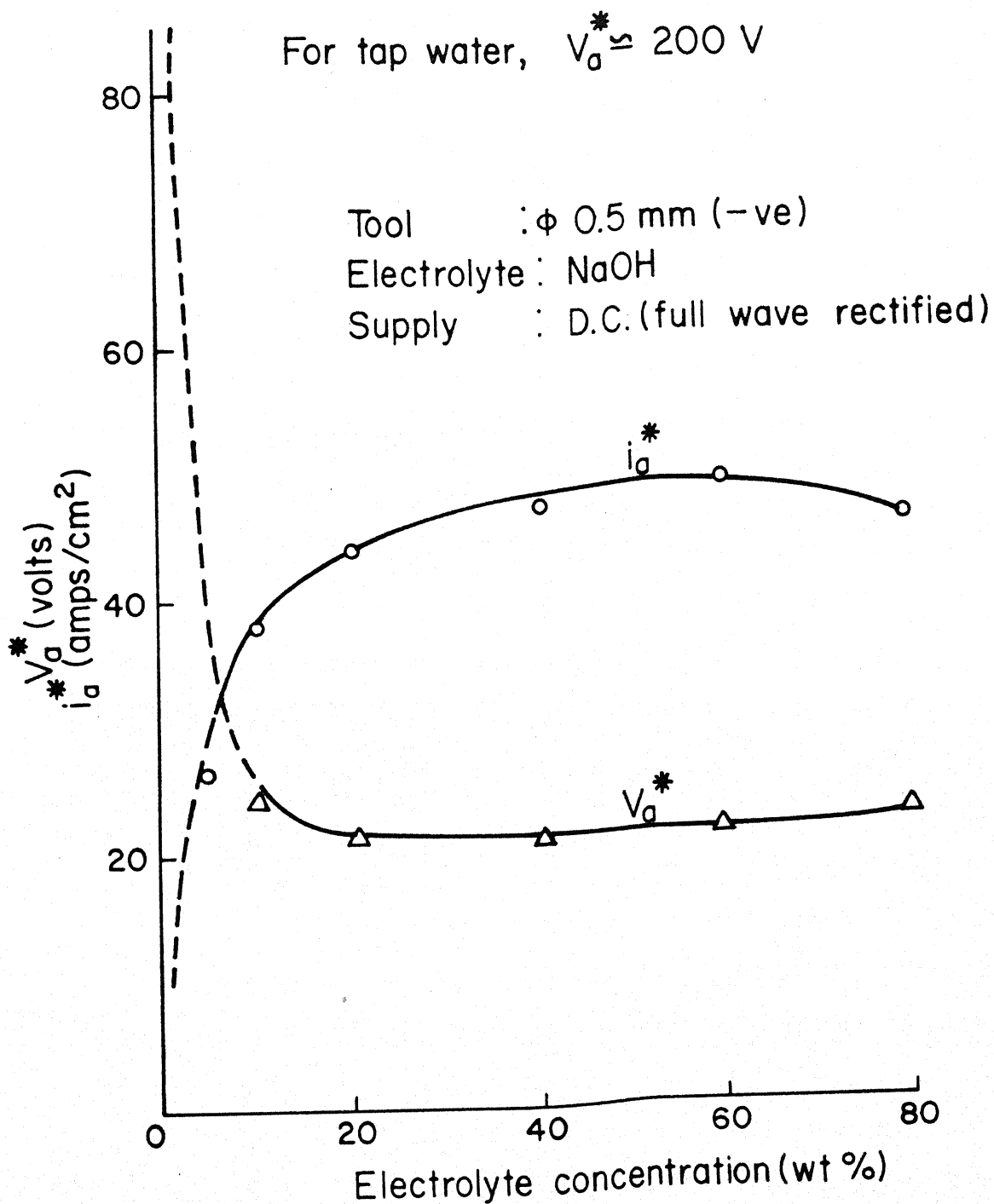


Fig. 3.15 Effect of electrolyte concentration on i_a^* , V_a^*

by the conditions of the bubbles and the properties of electrolyte at the tool-electrolyte interface. (The power expended at any section of the circuit can be taken as the product of voltage drop and current.) Since the voltage drop is maximum at the tool-electrolyte, the heating is also maximum in this section. The remaining portion of the circuit, i.e., the bulk electrolyte and the non-machining electrode-electrolyte interface is not much affected by the current flow.

Consider an electrolyte concentration of, say 60% ; its conductivity is low as obtained by extrapolation of the curve given in Figure 1.12. When the voltage is applied, the heating mainly takes place at the tool electrode interface. The conductivity of the electrolyte at this section can go high as shown schematically in Figure 3.16, since the conductivity of an electrolyte (60%) is very high at high temperatures (Figure 1.12). So, the lowering of the conductivity at higher concentration of the electrolyte does not produce any observable change on the discharge phenomena in a EDC configuration of non-conducting material machining. But the behaviour of an electrolyte, say 2% concentration is different from that of a 60% concentration, though the specific conductivity values are almost same in both the concentrations. A 2% concentration electrolyte would need about 70 Volts to reach the critical voltage as shown in Figure 3.15. This feature could be arising from the fact that an increase in the temperature due

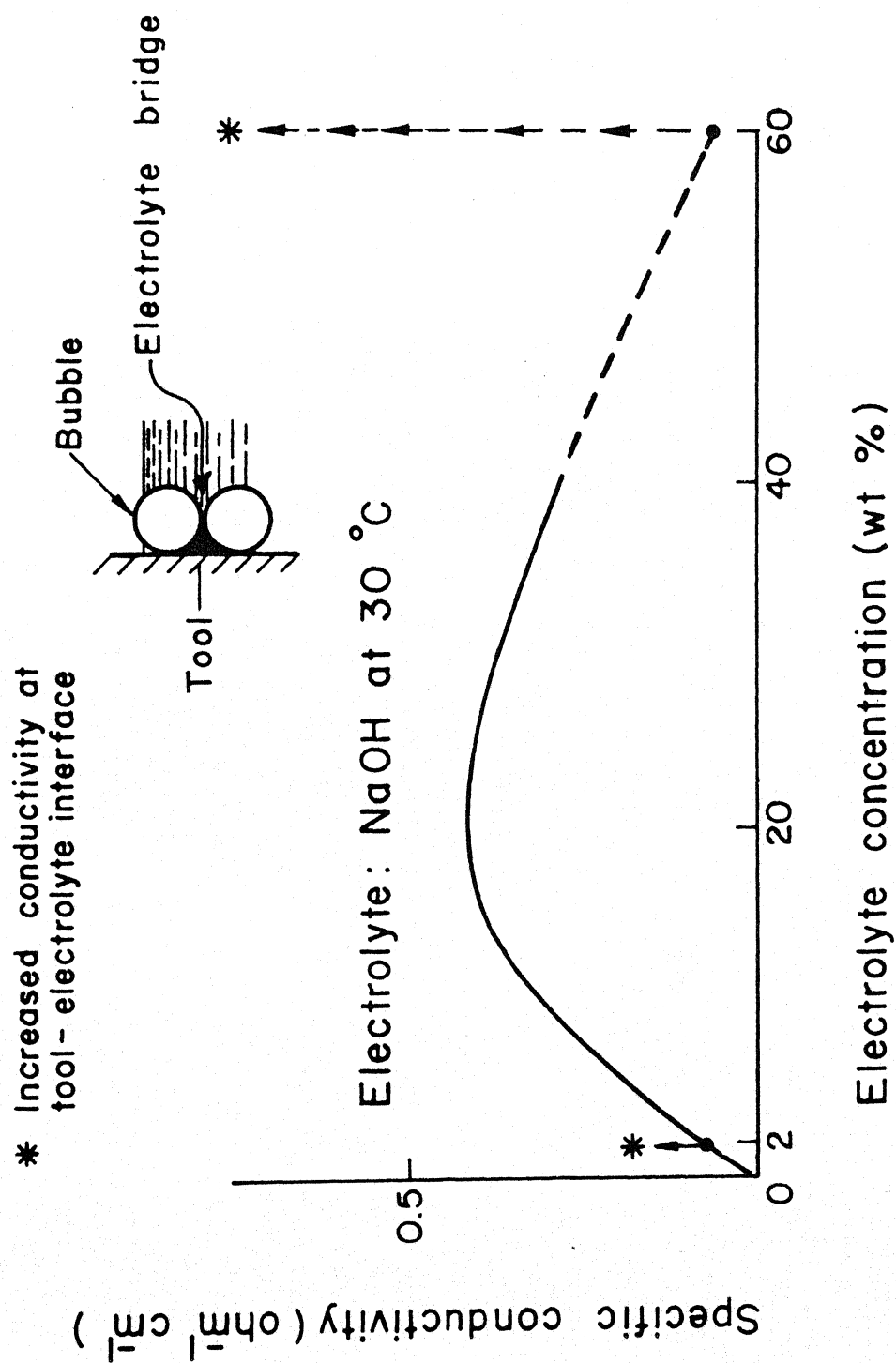


Fig.3.16 Increase in conductivity of electrolyte bridge due to heating. (Schematic)

to the current flow at the tool-electrolyte interface increases the conductivity of the electrolyte bridge only a little (Figure 1.12) and thereby needs higher and higher voltage to boil the bridge and producing the phenomena. This discussion regarding electrolyte bridging and boiling at different concentrations in the production of discharge phenomena is essentially a transient instantaneous phenomena and an accumulation (long time effect) is not envisaged.

From the observations it can be concluded that the ECD configuration of non-conductor machining, the local effect at tool-electrolyte interface is the main factor which controls the phenomena. Section 3.4.9b describes the effect of electrolyte temperature on the nature of discharge phenomena.

3.4.9b Effect of electrolyte temperature on the nature of discharge phenomena

The variation of average voltage and average current with change in temperature of electrolyte has been already presented under Section 3.4.4. In the present test where waveforms were observed, the system has not shown any observable change in terms of discharge pattern (frequency, peak to valley variations of current, voltage etc.) with different electrolyte temperatures. However, some variation was seen in terms of average current when the electrolyte was boiling probably due to the turbulence caused due to the bulk boiling of the electrolyte at the tool-electrolyte interface.

3.4.10 Effect of tool diameter on voltage-current characteristics

This experiment became necessary as it was observed that tools with larger diameters formed crater only at the corners whereas the smaller diameter tools drilled into the work [2,3]. So, it was felt necessary to study the effect of tool diameter on the voltage and current characteristics. The effect of tool diameter on the critical voltage and critical current density is shown in Figure 3.17. It was observed that large variation of critical current density occur with different tool diameter in this type of configuration. However, the variation of critical voltage was less with tool diameter. The results of this experiment indicate that the configuration exhibits a kind of size effect. It is a well established fact that sharp points always produces high field concentrations. The bubble ionization can take place easily due to field concentrations with a smaller diameter tool and this might be the probable reason for the lowering of critical voltage when small diameter tools were used. Also an electron flowing through the tool will find it easier for an exchange of electron with an ion of the electrolyte when the tool diameter is small. So a higher current density can be expected with smaller tools. In a further study (Figure 3.18) it was also observed that the ionization and discharge initiate first at the sharp points on a tool where the field concentration effect is more. The copper-foil tool shown in the figure has no tip as such but sharp points on sides are present.

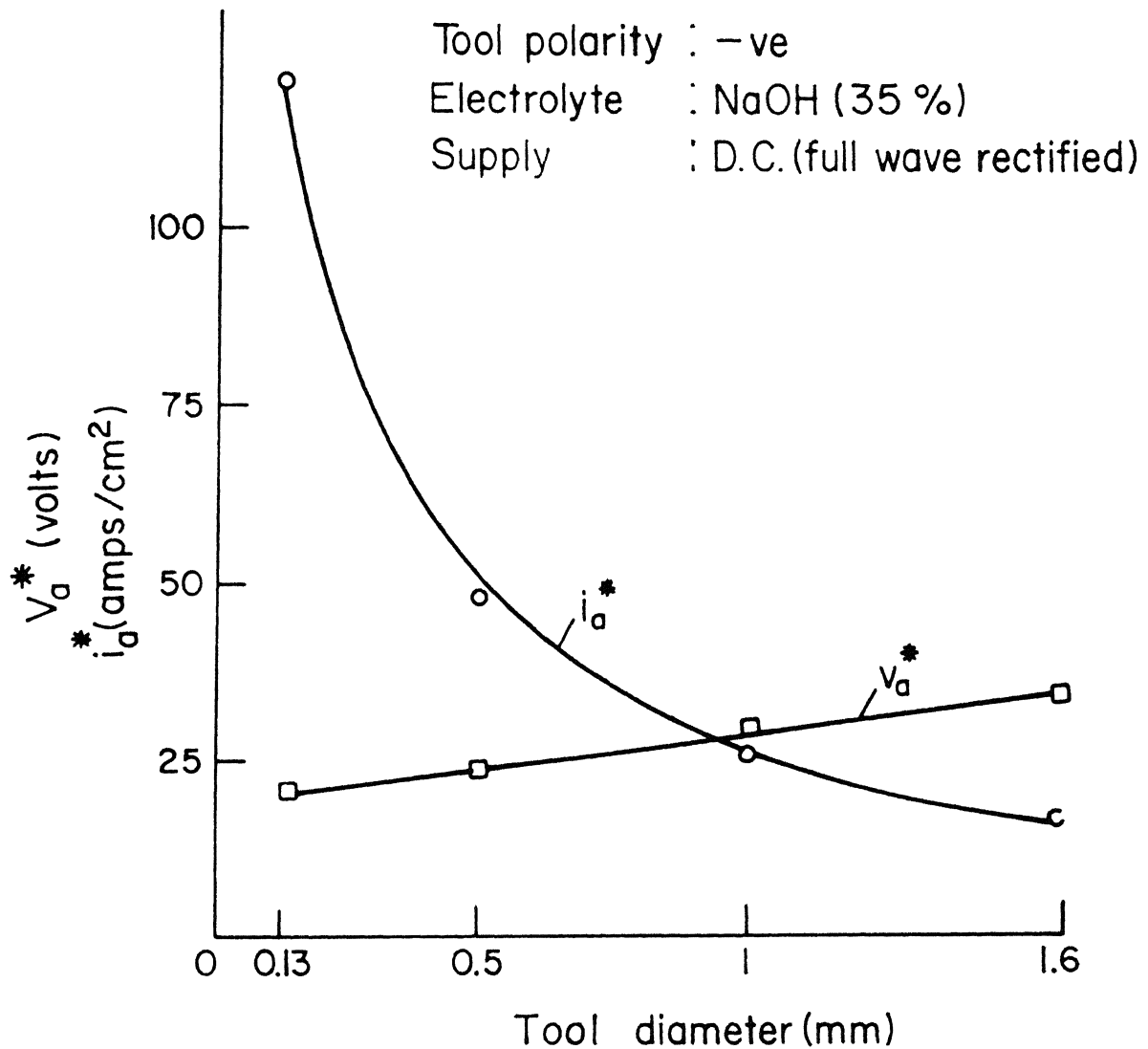


Fig. 3.17 Variation of critical current-density, i_a^* and critical voltage, V_a^* with tool diameter

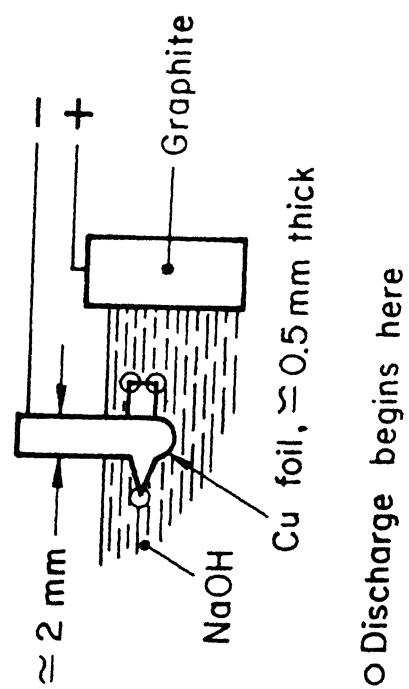


Fig. 3.18 Initiation points of discharge

3.4.11 Test for examining the bulk conductivity of glass

This test was conducted to clear up some prevailing doubts regarding the conduction of glass through its body during machining conditions. Since no real breakthrough in the process has taken place, author considered it worth while to test this aspect. The arrangement for this test is shown in Figure 3.19. The glass test tube was filled with NaOH. The thickness of the glass tube was 1 mm which is less than the usual 2 mm glass plates used as workpiece in all machining experiments conducted hitherto.

The set-up used ensured that if the system showed some current flow, it must have been passing through the bulk of the glass tube. The levels of voltage, electrolyte concentration and the bath temperature used by researchers [1,2,3,4,5] were covered in this test. It was observed that no current flowed though the circuit, indicating that there was no conduction through the work, (from the bottom of the work to the tool tip) in the machining process.

3.4.12 Voltage and current characteristics with NaCl and KOH electrolytes

These experiments were conducted in a way similar to those conducted with NaOH electrolyte. The voltage-current density plot of NaCl (25%) is shown in Figure 3.20. With NaCl electrolyte the critical voltage value for a negative tool is higher than that of NaOH (35%). In consequence of this, the discharge also occurs only at higher voltages in a

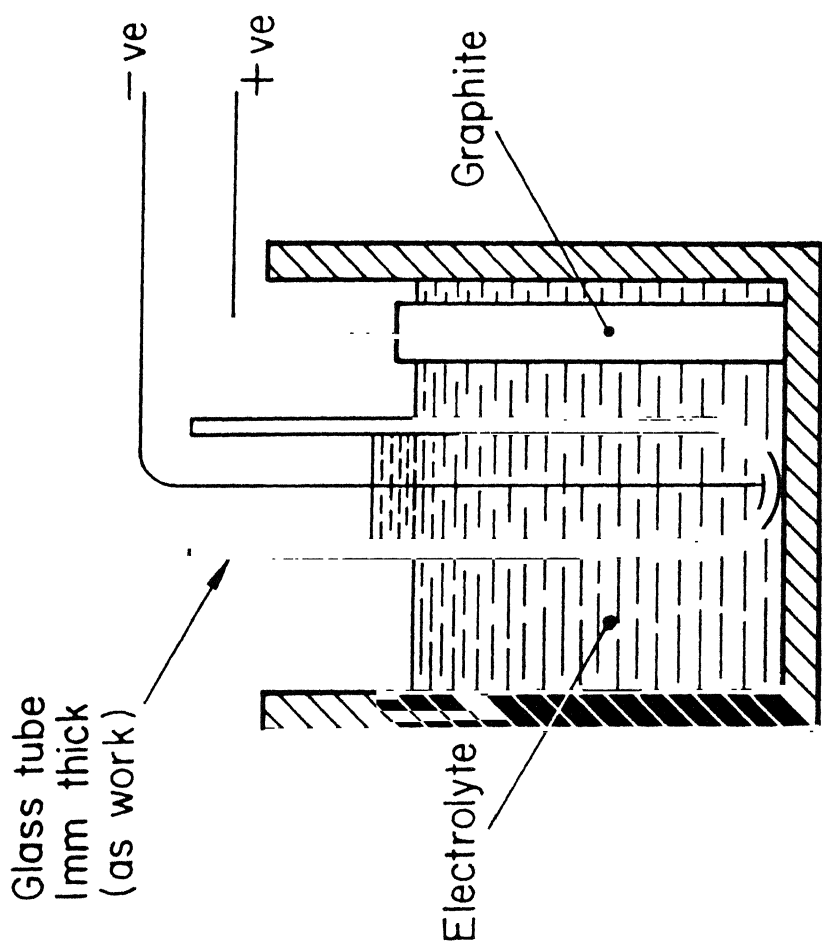


Fig.3.19 Schematics of volume conductivity test (for glass)

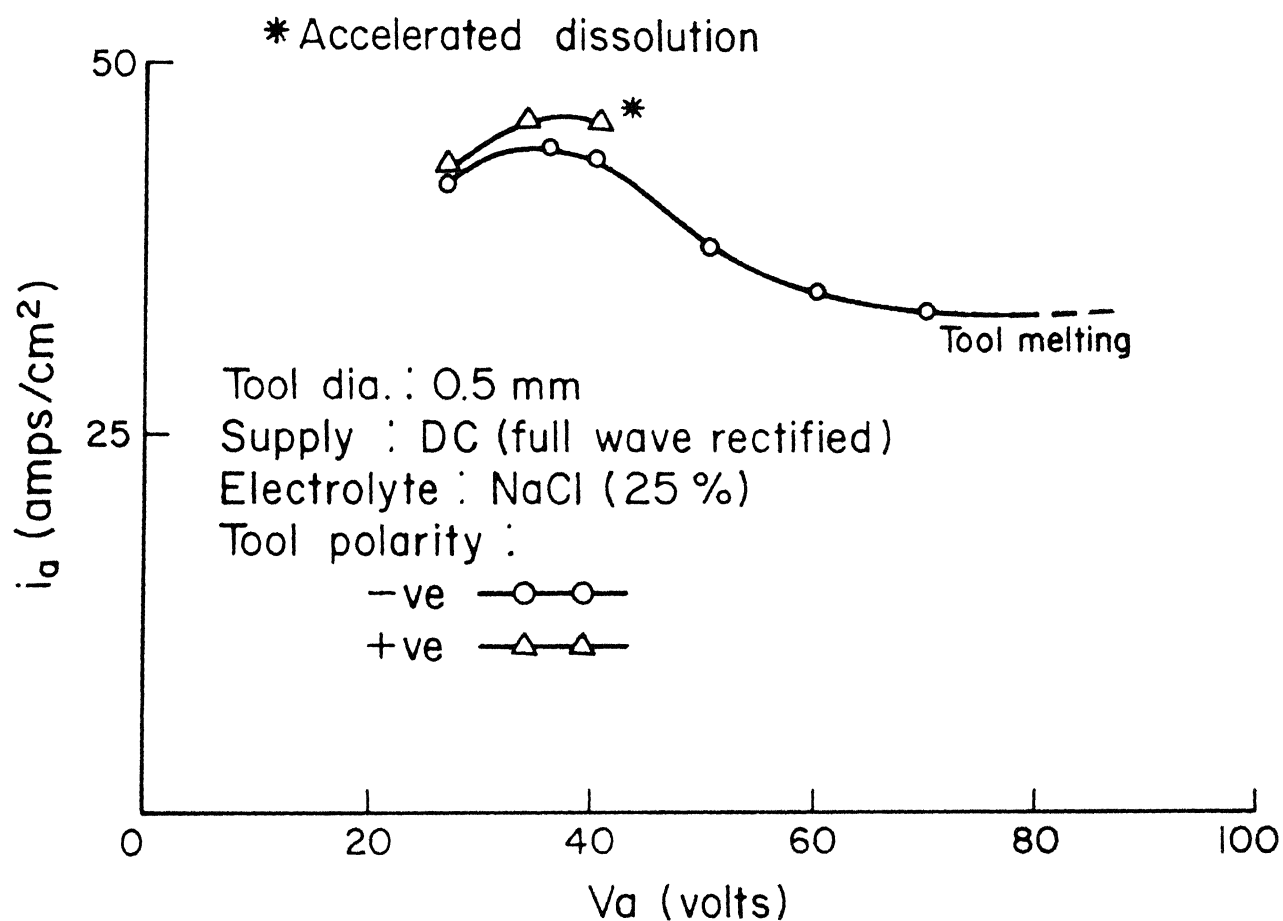


Fig.3.20 V_a - i_a characteristics (NaCl)

NaCl compared to that of a NaOH electrolyte. The most probable reason for this would be the lower conductivity of NaCl. The melting of the negative tool takes place at 75-90 voltage range which is also higher than that of a NaOH solution. The positive tool on the other hand exhibits an entirely different phenomenon in NaCl bath. At high voltages discharge appears on a positive tool in an NaCl electrolyte also, but the current through the circuit never came down as was observed in NaOH electrolyte (Section 3.4.8). Moreover, the anode dissolved at a very fast rate. The whole portion of the tool in contact with the electrolyte, has been consumed within a few seconds (0.5 mm diameter tool). In the present work this property of NaCl has been used for shaping of micro tips in the tools used for drilling of non-conducting materials. This experiment also indicated that drilling in non-conducting materials is difficult to accomplish with a positive tool in a NaCl electrolyte.

The voltage-current characteristics of a KOH electrolyte is almost like that of NaOH. Figure 3.21 shows the average voltage-average current plot in a KOH electrolyte. Experiments were also conducted with NaNO_3 electrolyte. A graphite anode (non-machining) disintegrate considerably in NaNO_3 electrolyte. A positive tool showed high random behaviour and therefore the results are not presented here.

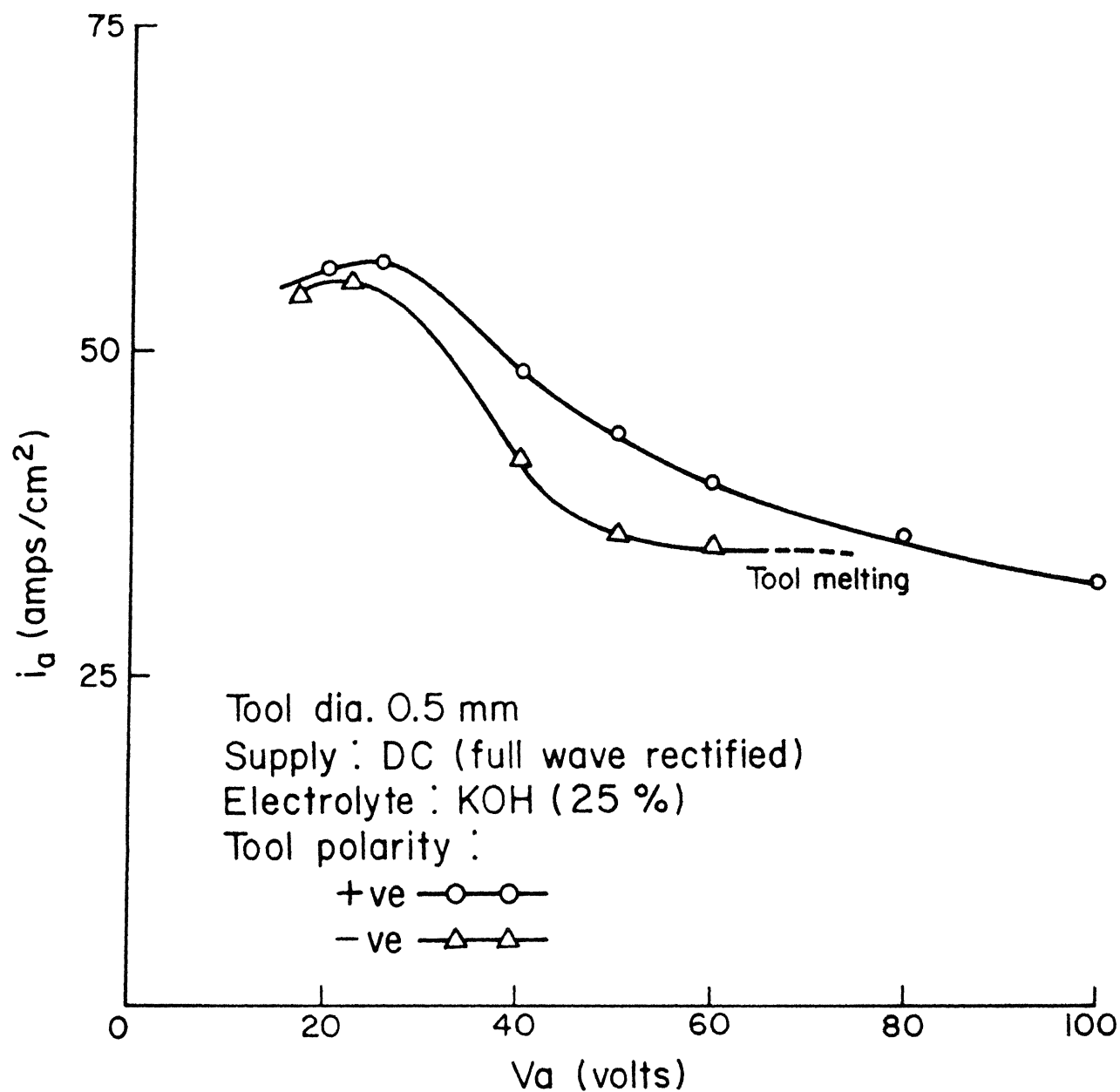


Fig.3.21 V_a - i_a characteristics (KOH)

3.5 Shifting of Discharge Zone from Tool Tip

3.5.1 Visual observation of shifting of discharge zone from tool tip

This experiment, conceived by the author to observe the tool under confined configuration, has yielded very useful information to explain the depth limiting factor observed by the researchers [2,3,5], while drilling glass using ECD phenomena. A transparent plastic tube of inside diameter 1.5 mm with one end sealed by a perspex disc was used as the confined configuration (simulating a drilled hole) for observing the discharge on the tool. A tool of 0.5 mm diameter and NaOH as electrolyte (35%) was used in the experiment. As already mentioned in Section 3.4 in free electrolyte test with a voltage of more than 30 Volts, discharge was observed along the entire surface of the tool in contact with the electrolyte. But in the present configuration, when the tool was introduced into the tube, with the same voltage condition, it was interesting to observe that the discharge moved up, leaving the tip of the tool devoid of any discharge phenomenon as shown in Figure 3.22. It was also observed that the discharge was sometimes shifting to the tool tip inside the hole and instantaneously retracting its path. Tools of various diameters showed more or less similar behaviour. This characteristic of discharge was observed at all voltages in the range 40-65 Volts. A negative tool polarity was used only for the sake of clarity of observation as a positive

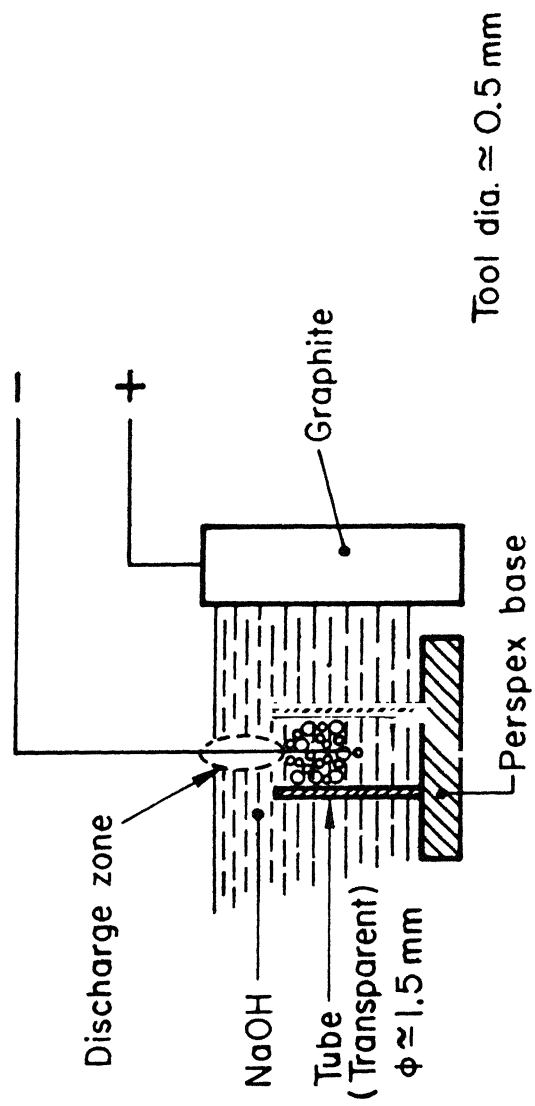


Fig. 3.22 Shifting of discharge zone

tool would lead to reaction products because of anodic dissolution. Smoothed DC as well as full wave rectified supply showed similar effect. During these experiments bubbles were seen generated on the portion of the tool which was inside the tube and the author intuitively felt that the configuration may be influencing the potential available at the tool tip. To examine this aspect further a specific test was conducted as outlined in the next section.

3.5.2 Potential along the hole depth and under the tool

Figure 3.23 shows the arrangement used for the measurement of potential along the hole depth. A perspex block with a hole of 2 mm diameter and 5 mm depth having electrical connections from the inside surface was used in the experiment. The electrical connections were arranged at 1 mm interval, one connection being at the top of the perspex block. The electrical leads had contact with electrolyte only at their tips (ends). The lead number 1 gave the potential at zero depth and other leads 2,3,4 and 5 indicated potentials at 1,2,3 and 4 mm depths, respectively. The potentials were measured between the tool and the different electrical leads with an applied voltage of 52 Volts. The tool was maintained at a constant depth of 4 mm inside the hole for all these tests. Figure 3.24 shows the potential available at different depths. The potential available decreases with increase in the depth and the reduction in potential being more with a larger diameter tool.

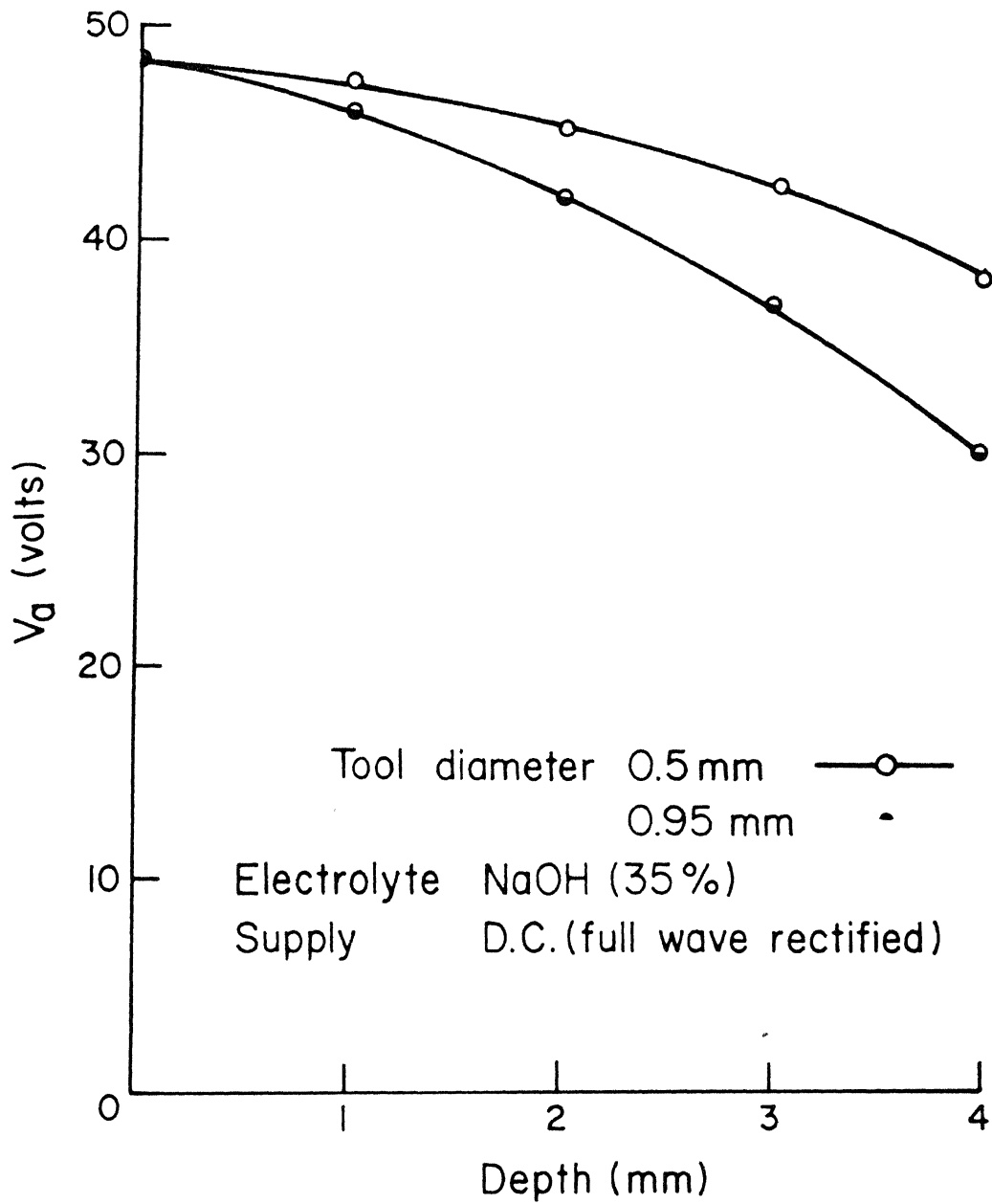


Fig.3.24 Potential variation along the hole

Since electrochemical action is taking place at all conditions, gas bubbles are generated on the tool. The bubbles generated on the tool portion, which remains inside the hole, find their way out through the side clearance between the tool and the hole. The discharge heat produces further vapour phase in this gap. Since the tool is of metal (cu) its surface can be considered as an equipotential one. The potential between the tool and the immediate (free) electrolyte can be taken as equal to applied voltage less the voltage drop at (non-machining) electrode - electrolyte interface and other drops in the electrolyte bath. Lead number 1 represents this free electrolyte potential with respect to tool whereas when lead 2 is considered, it gets the potential from the free electrolyte only. So the circuit of lead 2, encounters an additional 1 mm path which contains bubbles as well as electrolyte under confined condition (two phase mixture). The conductivity of such a two-phase mixture is always less than the conductivity of bubble-free electrolyte. And lead 3 encounters additional 1 mm path and hence additional drop, and so on. Therefore, the potential available between the tool and the electrolyte decreases with increase in depth.

Figure 3.25 shows another set-up for the measurement of potential between tool and electrolyte inside a hole in glass plate with different tool positions. The hole in the 2 mm thick glass plate was drilled by a 0.95 mm diameter tool using

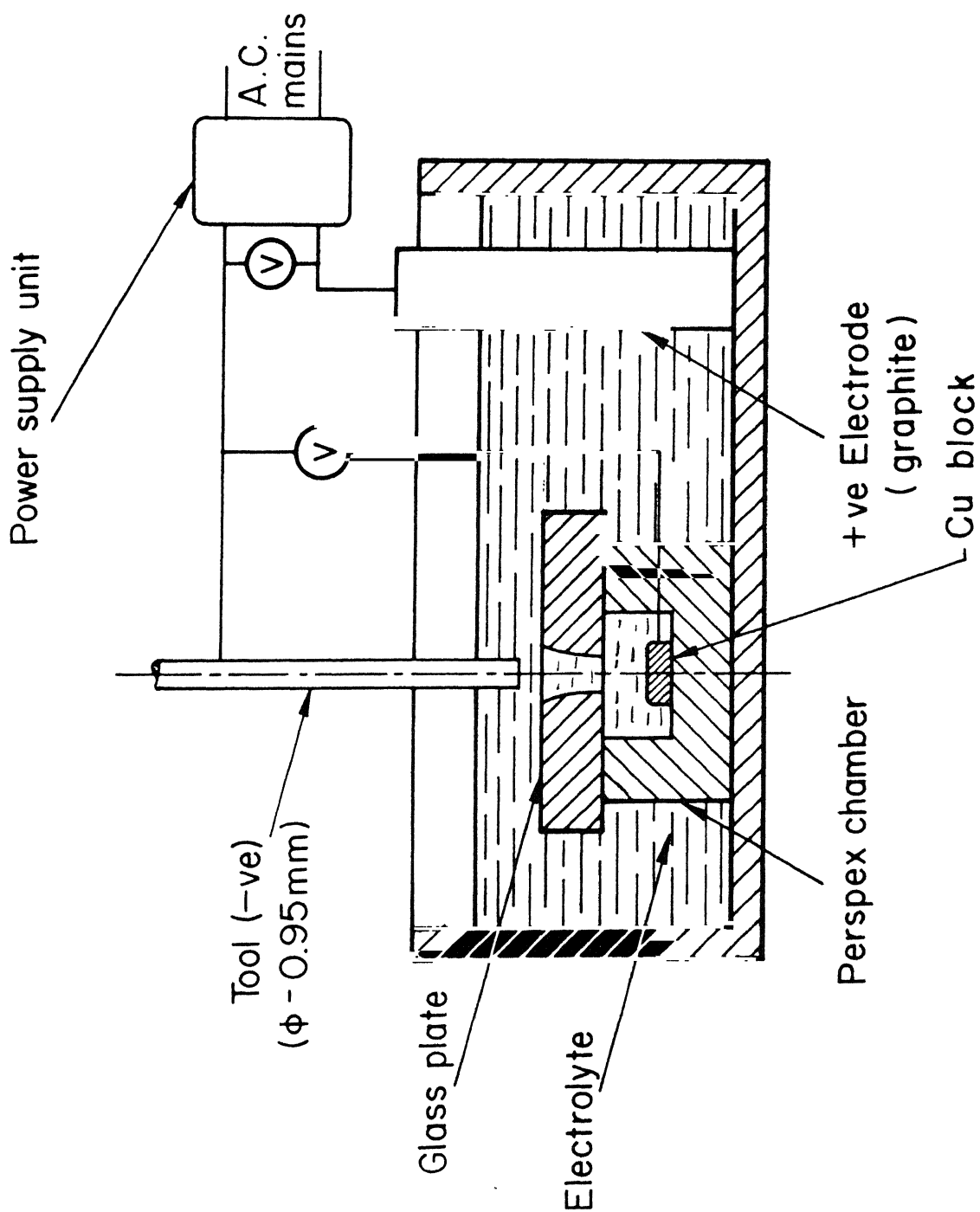


Fig. 3.25 Schematics of set-up for measuring potential below the tool

ECD phenomena. This arrangement was used to get a closer approximation of real ECD drilling condition. The copper block, kept inside the perspex chamber, can develop potential through the electrolyte, only via the hole. The experimental values of potential available between the tool and the copper block at various tool depths is shown in Figure 3.26. It can be seen that as the tool moved inside the hole, the potential available between the tool and the copper plate decreased. Obviously the circuit has encountered more length of two-phase (gas bubble and electrolyte) region. It is to be noted that the actual situation of drilling is different in many ways. For instance in a drilling operation, the hole is progressively generated and the tool is always in contact with the work, whereas in the present experiment hole already exists and the tool does not touch the work. Hence, the measurements presented here only gives an approximate idea of the potential drop in the clearance gap as the drilling proceeds to larger depths.

The side (clearance) gap (Fig. 3.27) can be considered to be composed of bubbles and electrolyte. In normal ECM also the side cutting is a function of the amount of hydrogen gas present in the clearance space [35]. The conductivity of a heterogeneous medium depends on the conductivity of the dispersed and the continuous phases. The conductivity K_m of a bubble-electrolyte mixture can be expressed as [36,37].

$$K_m = K_e (1 - \alpha)^{1.5}$$

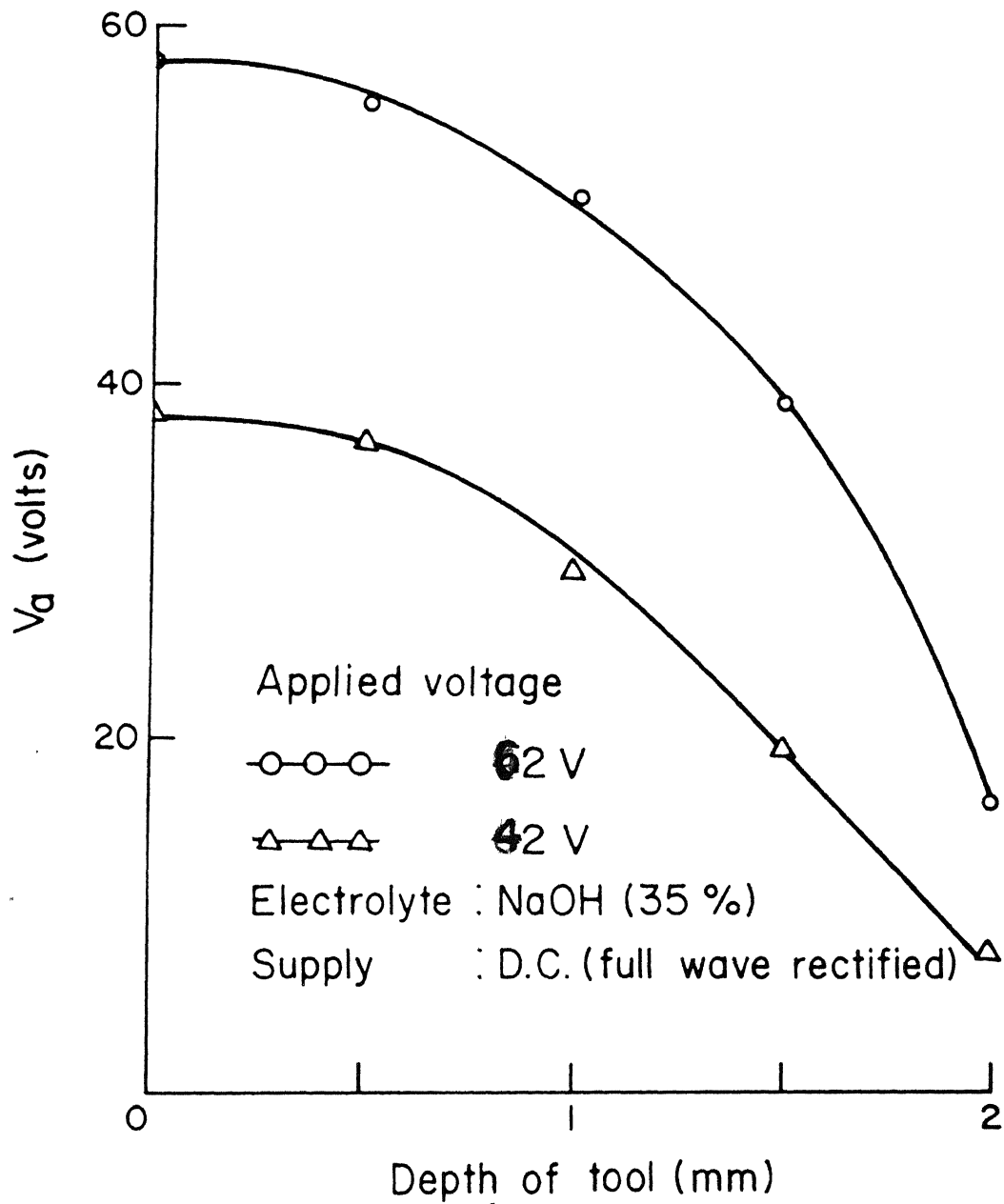


Fig.3.26 Potential between electrode and electrolyte with depth of tool

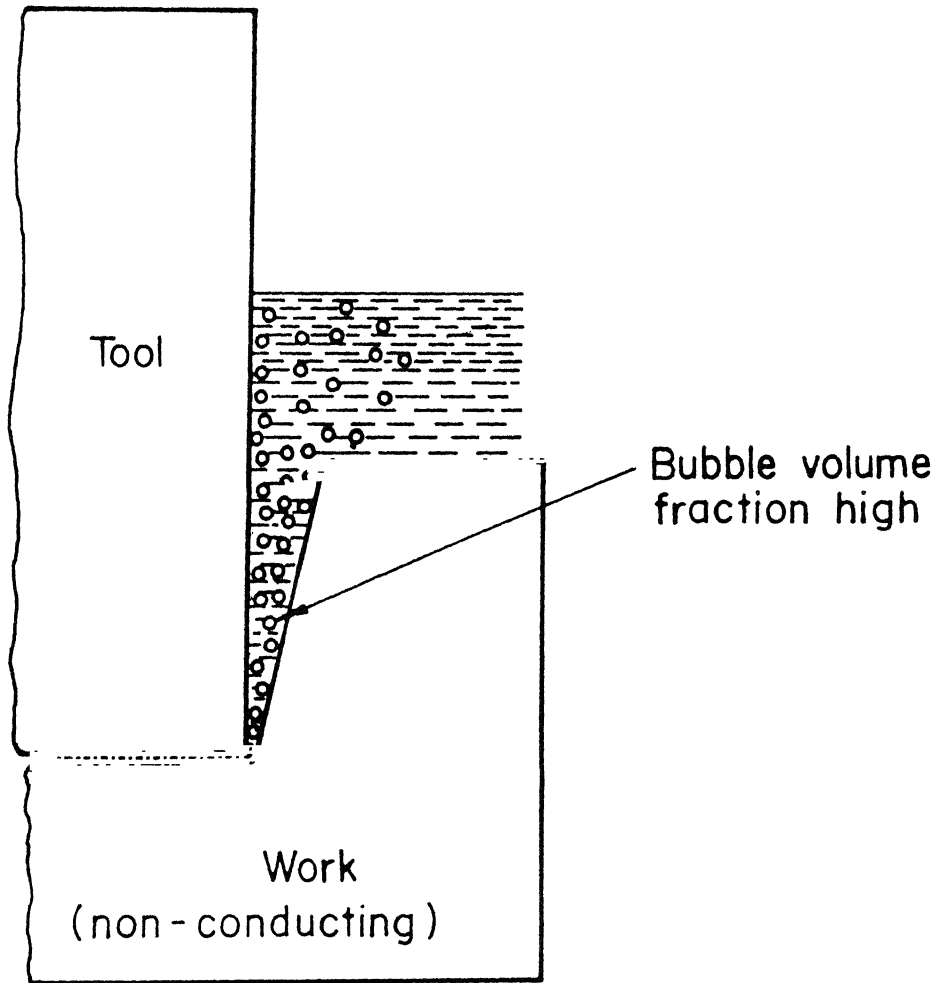


Fig.3.27 Schematics of side clearance gap

where

K_m = conductivity of the mixture

K_e = conductivity of electrolyte

α = void fraction .

Under a close packing condition of spheres (spherical bubbles) in electrolyte space

$$\alpha = 0.7405$$

and the conductivity of the mixture reduces to about 15% of that of the bubble free electrolyte. Therefore, depending upon the bubble volume fraction with side gap, the potential drops considerably at this confined space of electrolyte. In addition, to such gross presence of bubble, additional complicated phenomena such as, bubble coalescence and growths and bubble adherence to the surface of the hole may also influence the process. All these would affect the potential drop adversely. It was mentioned in Section 2.2.2 that to produce discharge in electrolyte a sufficient voltage gradient should be available across a void. Now, while drilling proceeds and the potential drops with the depth, the electrolyte near the tool tip starts lacking in sufficient voltage-gradient to produce a discharge. The reduction in penetration rate with time, observed by various researchers, could be due to this potential drop characteristics. However, the next section shows how a constant rate machining is possible if the configuration restriction is absent.

3.5.3 Constant rate machining

This experiment was conducted to verify whether continuous machining can be achieved if the configuration restriction is removed. The schematics of the experimental configuration and the penetration achieved with time are shown in Figure 3.28. A 3 mm glass rod and a 3 mm copper tube formed the work and the tool, respectively. The tool depth in the electrolyte was maintained around 2-3 mm by draining electrolyte from the bath as the machining proceeded. Continuous machining for a long time was possible with this arrangement, thus supporting the hypothesis forwarded by the author in Section 3.5.2.

3.6 Experiments Related to Current Density Effects

3.6.1 Voltage-current characteristics and waveform of current in a constricted electrolyte passage (plastic partitions)

The experiments in Sections 3.6.1 and 3.6.2, intuitively visualised by the author, revealed an important aspect of the machining of non-conducting materials using ECD, namely work participation. In Sections 3.4.3 and 3.4.9, it has been noted that local boiling of the electrolyte bridges is one of the reasons for the ECD phenomena. Then why not produce local boiling by deliberately constricting the electrolyte at a section. Under this condition, the whole current has to pass through a small sectional volume of electrolyte and can result in the boiling of electrolyte at that section. The experimental

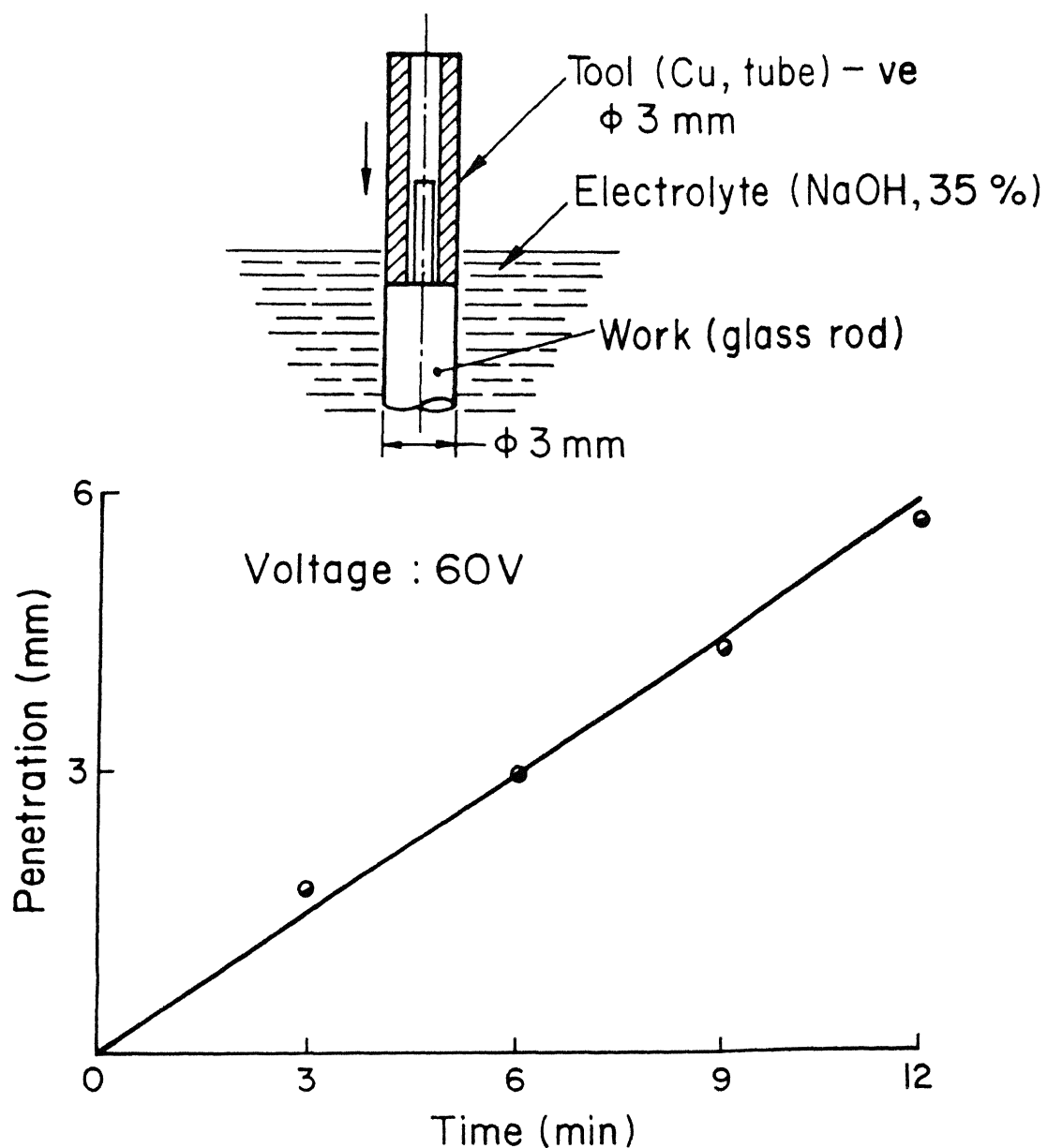


Fig. 3.28 Constant rate machining

set-up used is shown in Figure 3.29. In this configuration the electrolytic conduction between the electrodes can take place only through the small hole (1.5 mm diameter) in the plastic partition of thickness 1 mm as indicated. Both the electrodes in this experiment were of larger size like the non-machining electrodes of the previous experiments, since the prime idea was to produce a high current-density section only at the constriction. On application of voltage, the current was found to increase with increase in voltage but at higher voltages the average current decreased and showed interesting behaviours. Decrease in average current was found to be drastically different in the two cases - (i) when the electrolyte was stirred (Curve 1 and (ii) when the electrolyte was in static state (Curve 2) as shown in Figure 3.29. In the stirred condition, violent rushing of electrolyte (probably due to boiling) through the hole was seen and in the unstirred condition, a bubble was always found to block the hole preventing any visible movement of the electrolyte. It was observed that the bubble emitted dim light at higher voltages say, 60 Volts. The waveform of current with DC - full wave rectified and DC - smoothed supply are shown in Figure 3.30(a) and (b). Fig. 3.30(c) shows the current waveform under blocked conditions of the hole, irrespective of the type of supply. It was also observed that a smooth DC supply showed more tendency for bubble blockade. In condition 1 the plastic got burn scars at the hole surface and the diameter also increased; within a few minutes of starting the experiment 1.5 mm hole increased to 2 to 2.5 mm diameter.

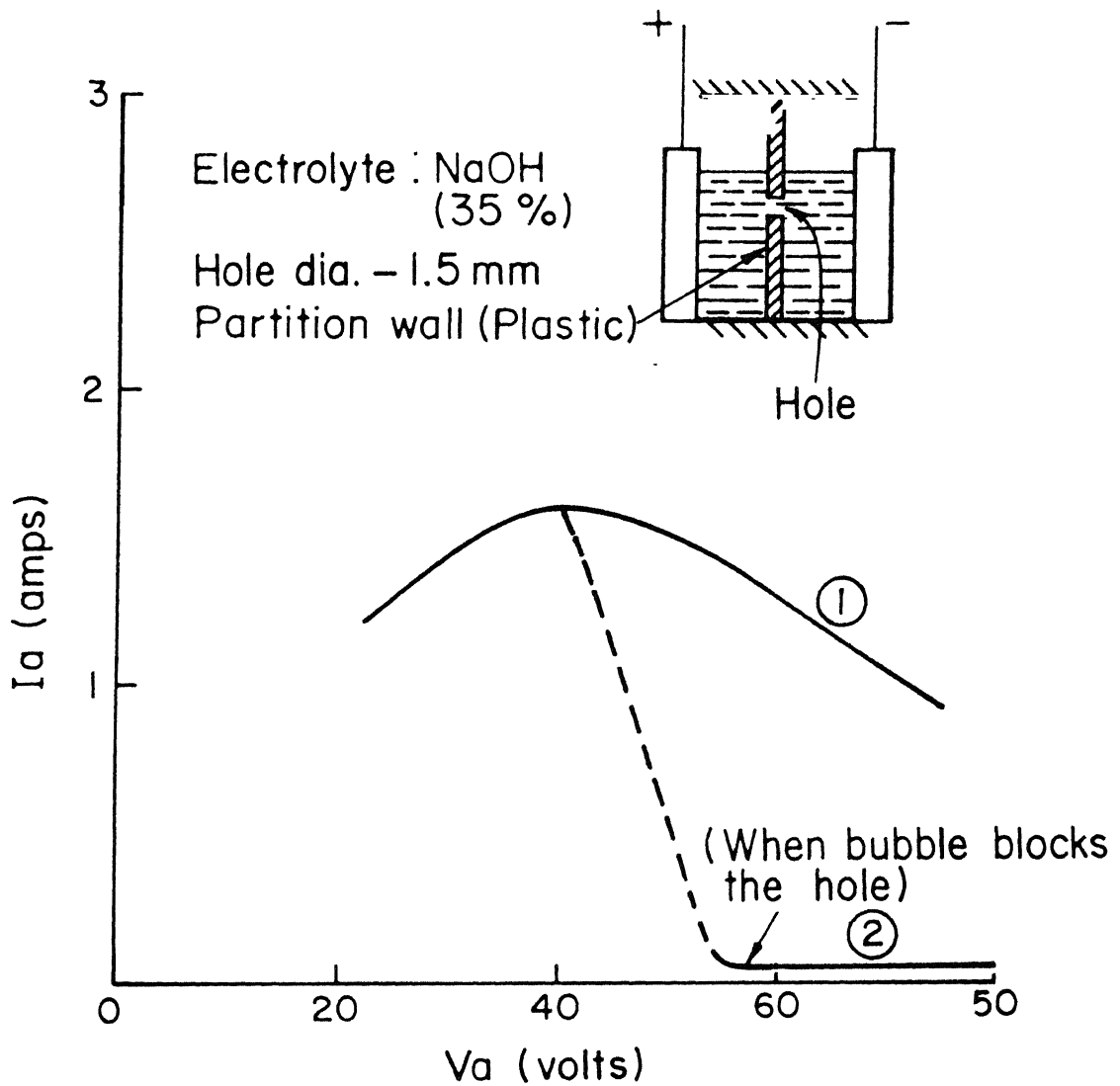
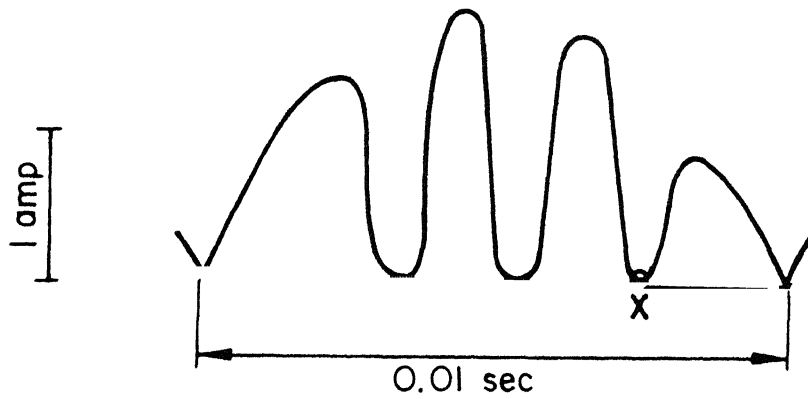
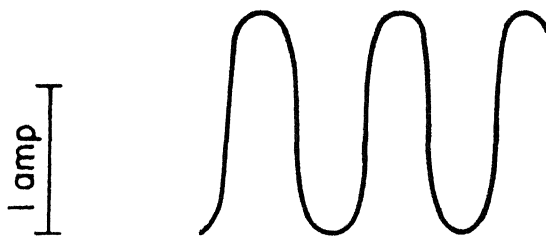


Fig.3.29 V_a - I_a of a constricted passage (electrolyte)



(a) Full wave rectified supply



(b) Smoothed D.C.

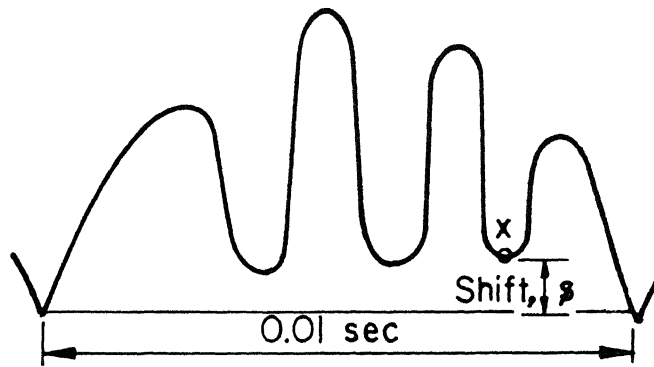


(c) Blocked condition of hole

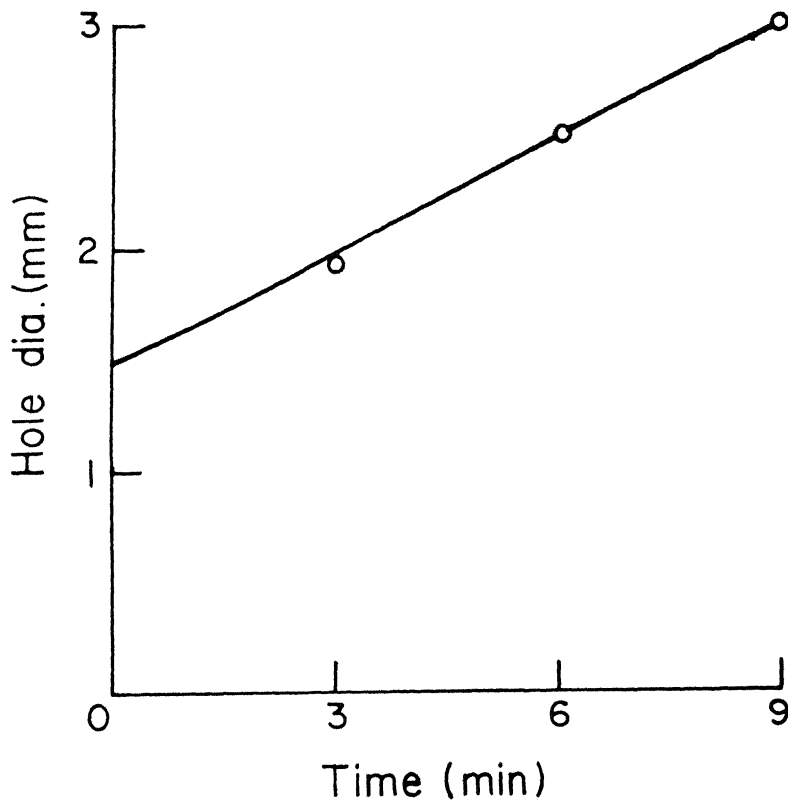
Fig. 3.30 Wave forms of current (Partition: plastic)

3.6.2 Voltage-current characteristics and waveform of current in a constricted electrolyte passage (glass partitions)

The experimental conditions for this experiment were similar to those described in Section 3.6.1 except that the partitioning wall was of glass plate. It was very interesting to observe that the hole in the glass plate never experienced a blockade by a gas bubble. This made the author to surmise that the response of a glass constriction is quite different from that of a plastic one. The voltage-current characteristics is similar to condition 1 of Figure 3.29 with average values of current more than that of a plastic constriction. But the prominent difference is depicted in the waveform of the current, the current waveform never touched the base line whenever a voltage was existing in this case. The hole was also found to be enlarged. The waveform and the hole enlargement is shown in Figure 3.31. The waveform of the figure showed a shift from the base line. Figure 3.30(a) and 3.31(a) also indicate that the waveform has shifted from baseline (point 'X') in the case of glass, by an amount shown as 's' in the figure. This interesting result can be interpreted as follows. When the partition is made of glass, the hole is providing a current path while the similar hole in the plastic partition does not allow it. Photographs of the storage oscilloscopic signals are shown in Figures 3.32(a) and (b).

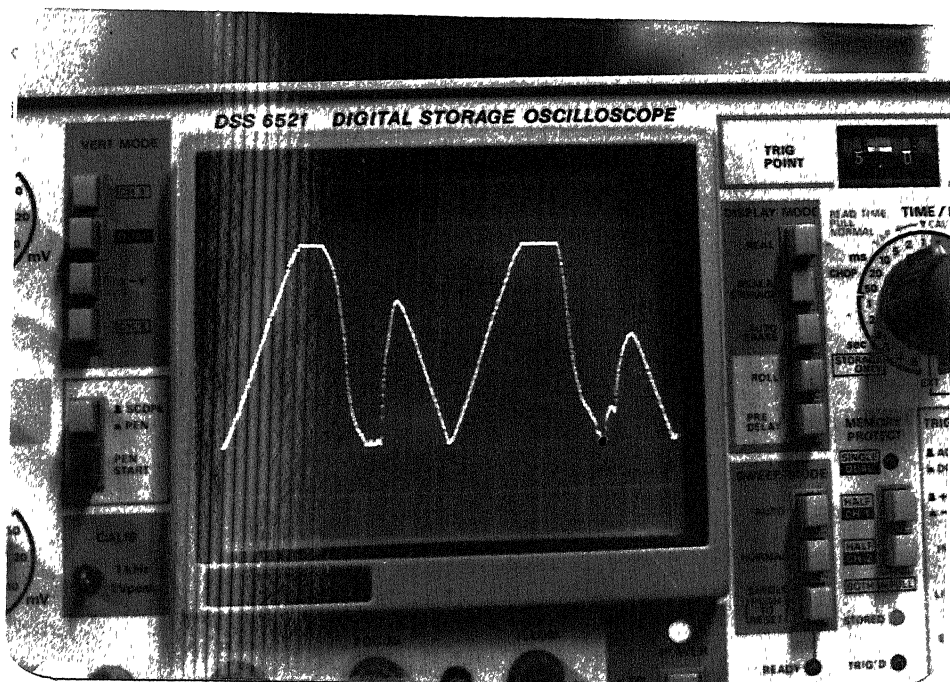


(a) Current wave form

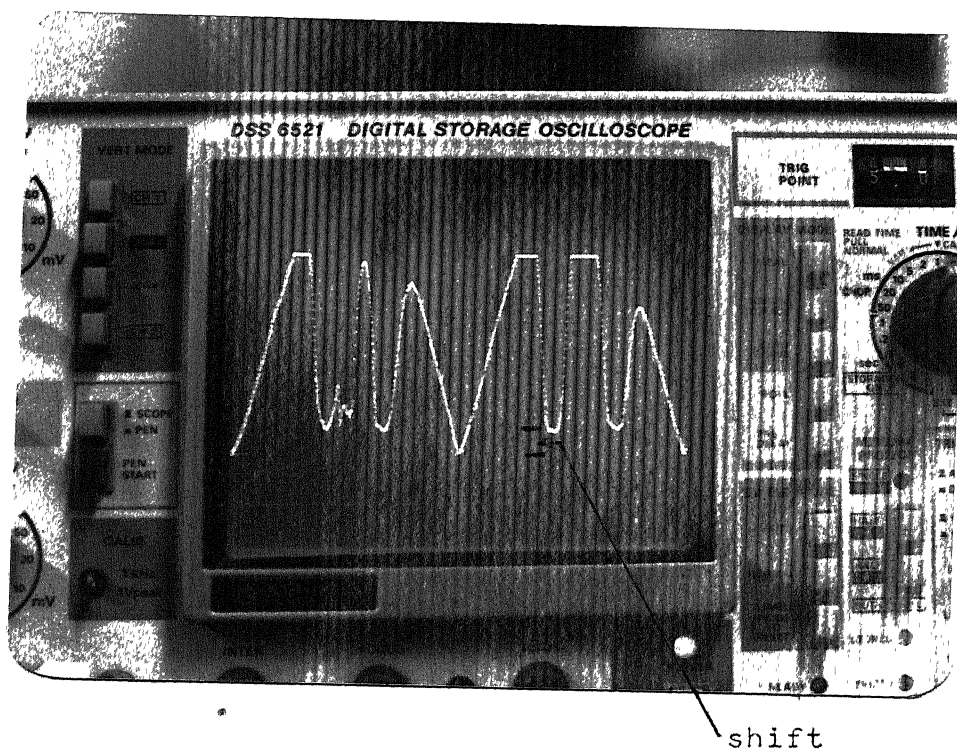


(b) hole enlargement

Fig. 3.31 Wave form of current and hole enlargement (partition: glass)



(a) Plastic partition (no shift in the waveform)



(b) Glass partition (shift in the waveform)

Fig. 3.32 Current waveforms (plastic and glass partitions)
($V_a \approx 60$ Volts)

The enlargement of hole in plastic partition in the boiling electrolyte could be expected but the enlargement of hole in glass which has a high melting temperature was an unexpected phenomenon. Since boiling of electrolyte-bridges under the influence of an impressed voltage took place in this experiment it is logical to think that a similar mechanism operates in actual machining of glass also. The enlargement of hole and shift in current waveform indicate the possibility of thermal, electrical and chemical activities on the surface of the hole, even without a tool. To investigate this aspect further, a specific experiment on surface conduction was conceived by the author. Next section illustrates this experiment in some detail.

3.7 Experiments Related to Surface Conduction and Interfacial Phenomena of Glass and Other Non-conducting Materials

In this experiments two electrodes were clamped on to the surface of the work (Figure 3.33) which was either a glass slide or a plastic sheet. With clean glass slide (75x25x2 mm) and an electrode separation of about 3 mm, no current flow between the electrodes was observed even with a voltage of more than 100 Volts. But, when drops of electrolyte (NaOH 35%) were introduced in the space between the electrodes, interesting phenomena were observed at different applied voltages. These were (i) when the applied voltage was below 15 Volts the current flowed through the circuit for few minutes as shown by curve 1 in Figure 3.33 and (ii) when the applied voltage was more than 40 Volts, violent boiling of

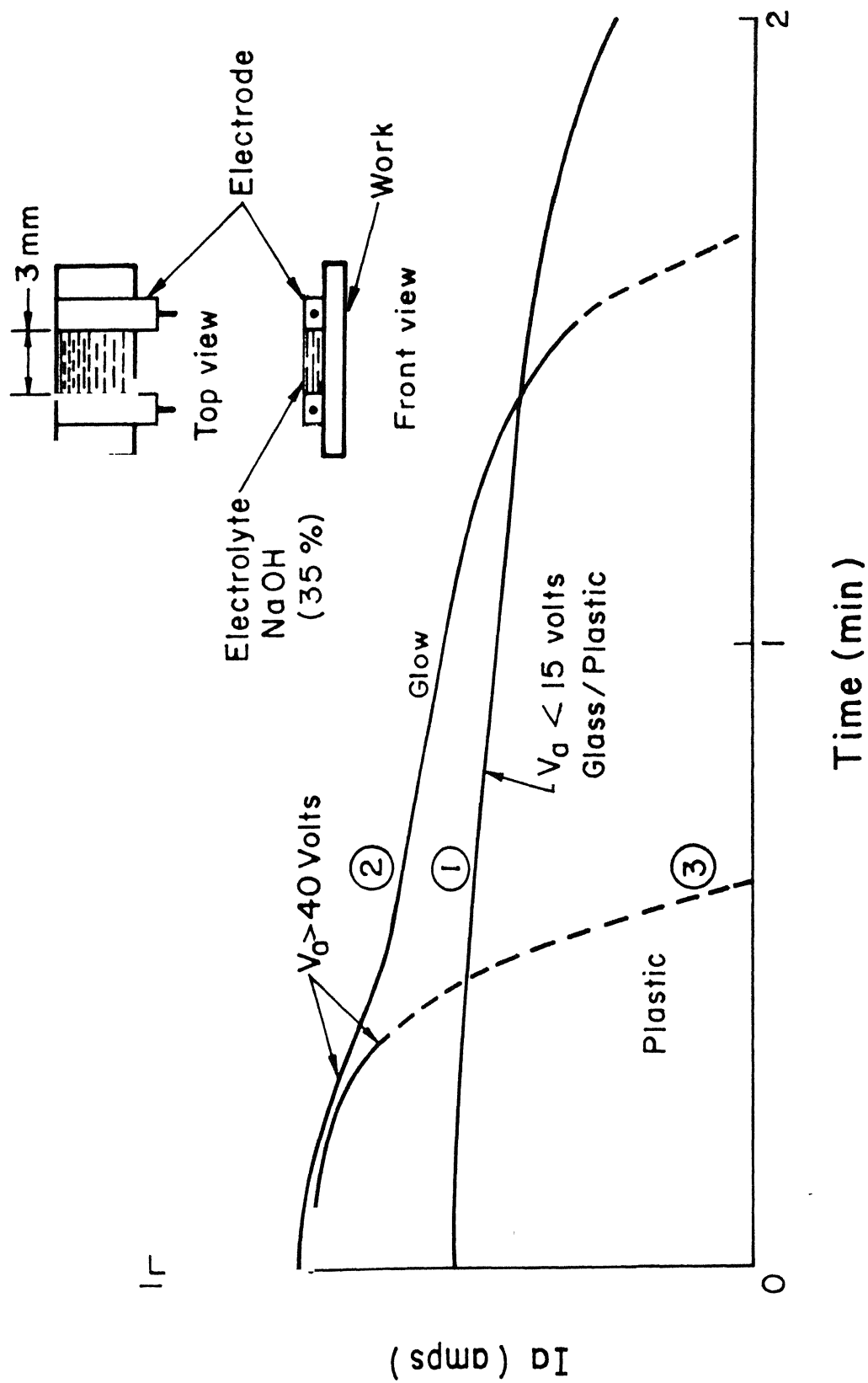


Fig3.33 Conduction through interfacial electrolyte .

electrolyte was observed on the glass surface; and within few seconds the surface of the glass became orange-red in colour. Current continued for some more time as shown by curve 2 in the figure and glass slide eventually broke into pieces. In each of these experiments fresh areas of glass were selected for each investigation, to avoid any possible adsorbed layer of electrolyte and its effect. These experiments were also repeated with plastic sheets. In presence of electrolyte and voltage of less than 15 Volts, plastic behaved like glass. Similar observations were available. But, with voltages more than 40 Volts, the electrolyte boiled off and current decreased very steeply as shown by curve 3 in the figure. No glow, like that **seen** in glass was observed on the plastic surface. The results of these experiments bring out an important aspect of these two materials. A glass surface continued to carry current even after boiling of electrolyte under an applied voltage, and the surface also emitted a glow. Plastic, however, did not display any such characteristics. The author intuitively thinks that conditions similar to this also exist during machining of glass using ECD phenomena.

It is difficult to correlate the above observed phenomena of glass and plastic with their electrical resistivities as one would normally believe it to be. Resistivities of both glass and plastic are very high as seen in Table 3.1. Even with the increased conductivity of soda-lime glass with temperature as given in Figure 3.34, the observed phenomena of

Ceramic MaterialsResistivity (20°C)
(Ohm - cm)

Soda - lime glass	10^{11}
Pyrex glass	10^{12}
Fused silica	10^{15}
Mica	10^9
Porcelain	$10^9 - 10^{15}$

Polymeric Materials

Polyethylene	$10^{11} - 10^{14}$
Polystyrene	10^{14}
Polyvinyl chloride	10^{12}
Phenol - formaldehyde	10^8

Table 3.1 Resistivity of electrical insulators [38]

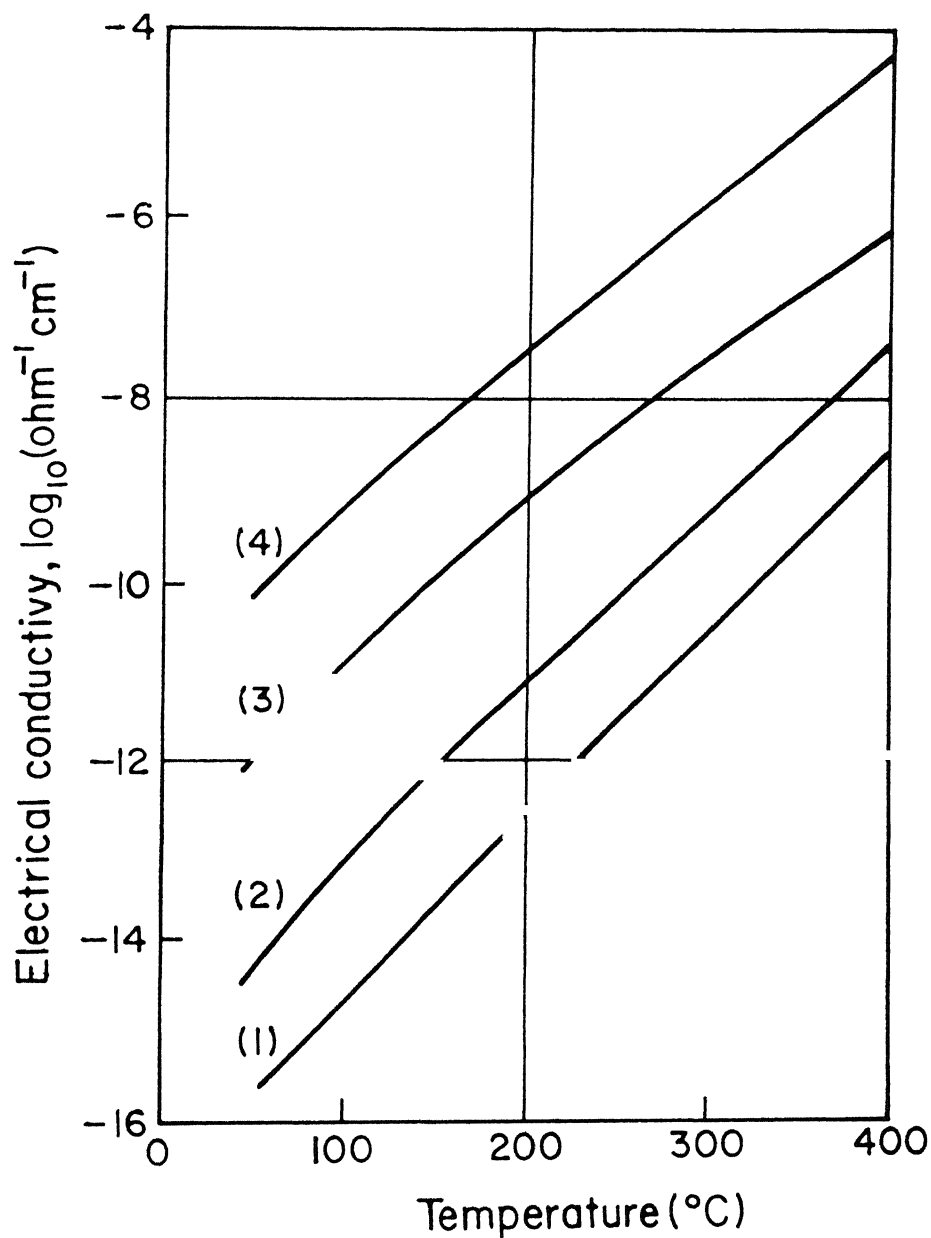


Fig.3.34 Electrical conductivities of glass
 (1) Fused silica, (2) 96 % silica,
 (3) Borosilicate, (4) Soda-lime silica [39]

conduction after boiling of electrolyte is difficult to visualise, as the current cannot exceed few milli-amperes.

To put this aspect of surface conduction on firm footing similar experiments were conducted for a variety of materials. These experiments showed that all types of glass, porcelainware, marble, stone, mica, bakelite and bone behave like soda lime glass. In fact a pyrex glass rod of about 2 mm diameter was able to be drawn to a thin long wire at the section between the electrodes, when the surface was glowing. This indicated that the temperature at the section was quite high. Results of further experiments showed that perspex, PVC, sun mica, rubber, anabond resin sheet and wax behave like plastic. After extensive thinking the author was able to conclude that the aforesaid behaviour of the two class of materials correlates with their moisture adsorption property indicated by the wetting angles as given in Table 3.2. Materials with low wetting angle showed one type of character and high wetting angle materials (like plastic) showed quite different type of character.

Most of the materials belonging to low wetting angle group, investigated in these experiment, contain silica. Good wetting ability of SiO_2 - based compounds is an established phenomena. Figure 3.35 shows the wetting of silica of glass. Recently [42] it has been reported that SiO_2 - based compounds can result in interfacial layer as thick as 0.1 mm on cemented carbide tools.

Material	Wetting angle (water)
Polytetrafluoro ethylene	113°
Polystyrene	98°
Plastic	86°
Fused quartz	27°
Glass	Low angle

Table 3.2 Wetting angle of materials [40]

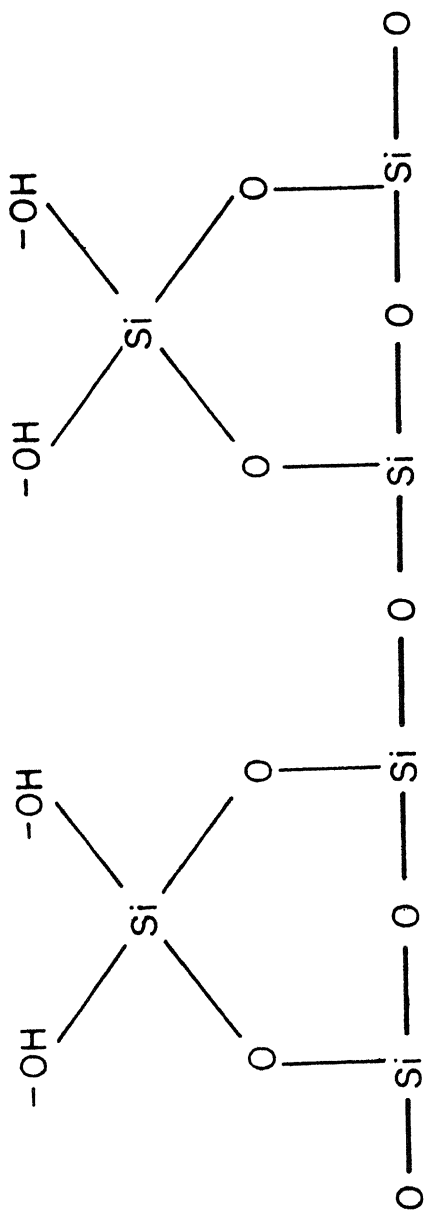
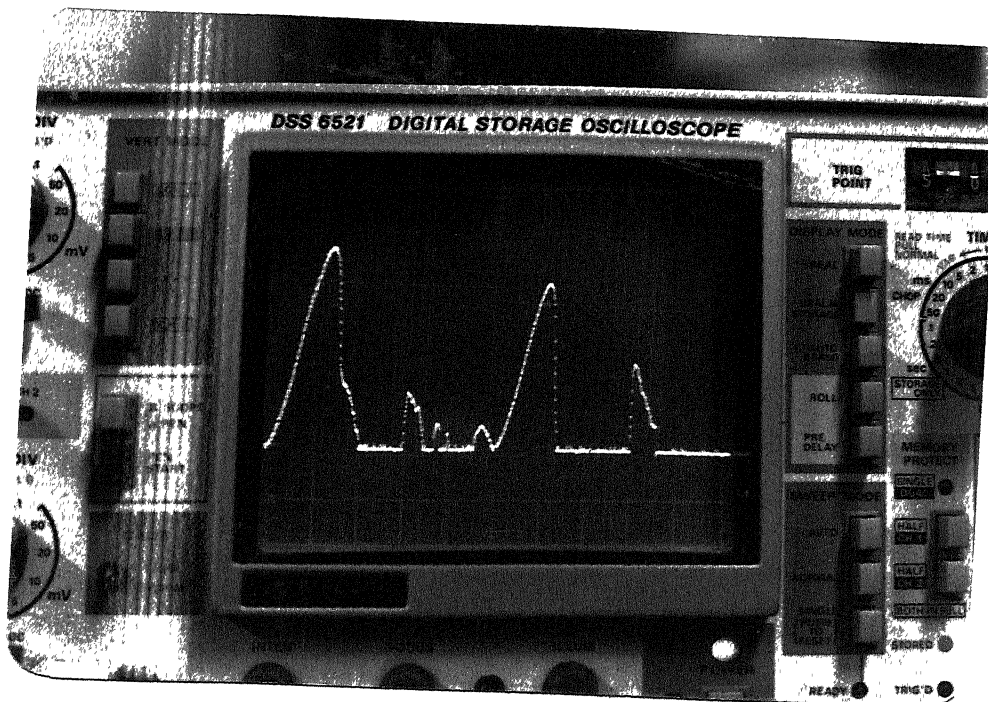


Fig 3.35 Wetting of glass (schematics) [41]

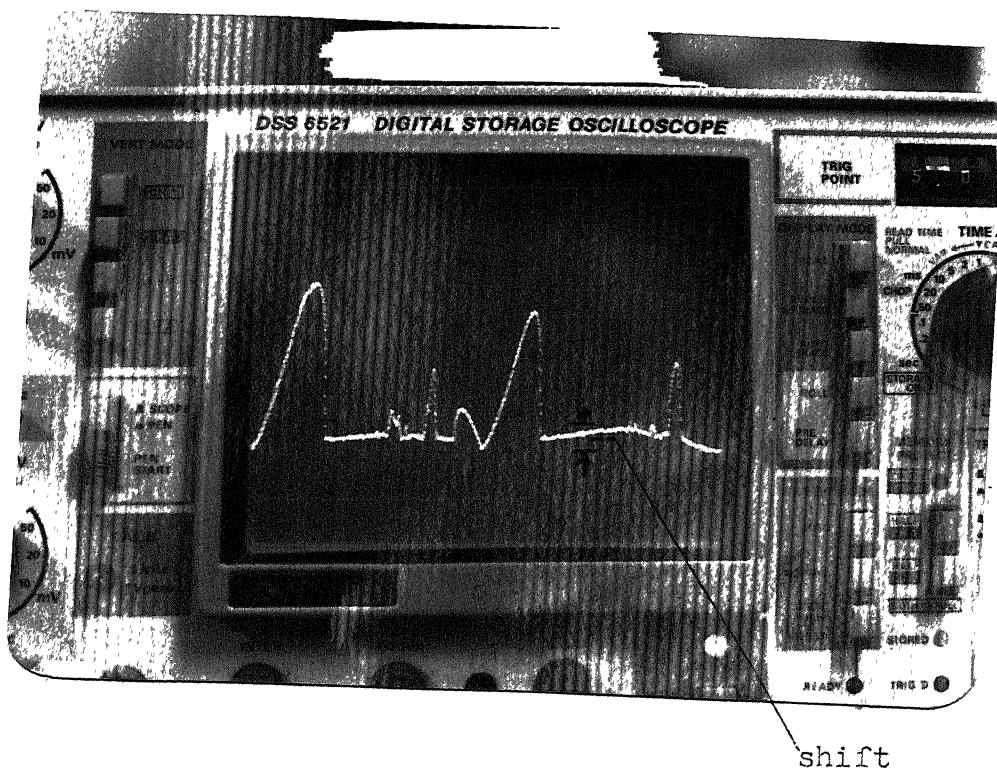
The preceeding experiments clearly demonstrated the difference in the surface phenomena exhibited by glass and plastic. This difference is naturally expected to be reflected in the machining process also. To investigate this aspect author thought it appropriate to observe the current and voltage waveforms, during the machining of these materials. These observations were obtained through appropriate experiments and are given in the next section.

3.8 Studies on Current Waveform during Machining of Glass and Plastic

Figure 3.1 shows the experimental set up used for these studies on machining. In all the previous experiments the tool was stationary with a constant depth of 2 mm in the electrolyte. In the machining experiment, however, tool was given a feed under gravity and the work was kept stationary. A 1 mm diameter steel pin was used as the tool. A voltage was applied between the tool and the non-machining electrode. The penetration was noted from the dial gauge fitted on the set-up. The waveform current and voltage were observed using oscilloscope as already mentioned in Section 3. 4.7 . The waveforms, observed under different machining conditions, are presented in Figure 3.36 a,b,c,d. These waveforms were possible only after the portion of the tool outside the electrolyte was insulated. Without such insulation highly random and unpredictable waveforms were obtained. It can be seen (Figure 3.36a) that the waveform of current while



(a) Machining of plastic (no shift in the waveform) (60 V)



(b) Machining of glass (low Mrr) (negative tool : 55 V)

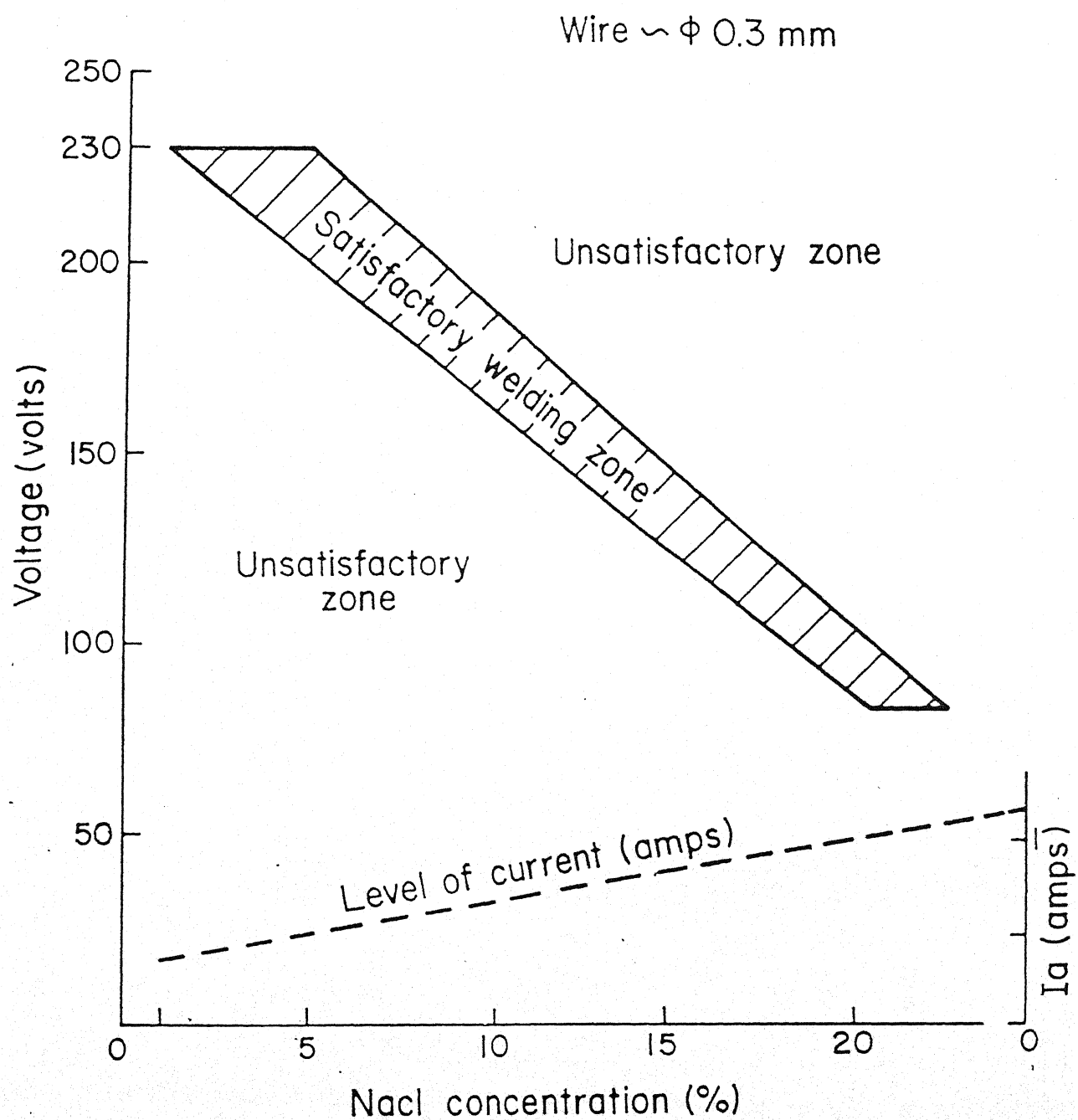


Fig. 5.1 Voltage vs. electrolyte concentration in micro-welding

machining plastic and in free electrolyte showed the same pattern. But while machining glass, shift in the current waveform was observed as shown in Figure 3.36b,c,d. Waveforms only at the beginning of the machining were considered for the study since the penetration of the tool inside the hole caused changes. The difference in the pattern of waveform while machining glass and plastic, clearly shows the participation of the work material during the machining of glass.

Author considers the shift in the current waveform (Figure 3.36) while machining glass as a significant feature of the process. During the discharge the current has not come down to zero unlike the case of plastic, where it is clearly so. It is to be recalled that in the experiment with constricted electrolyte path, discussed in Section 3.6.2 , a similar feature of current shifting was observed, in the case of glass partition only. No such shift was observed with the plastic partition. This indicates the possibility of surface conduction phenomenon at the tool work interface.

The following points emerge from the observations presents in this chapter from the experiments with varied objectives :

- a) The penetration depth of the tool into glass is essentially limited due to the non-availability of sufficient potential at the tool tip.
- b) Removal of material is effected by the combined action of electrochemical discharge across gas bubble and the surface conduction/discharge at the tool-electrolyte-work interface.

CHAPTER IV

PROPOSED MECHANISM OF MATERIAL REMOVAL DURING ECDM OF NON-CONDUCTING MATERIALS

4.1 Introduction

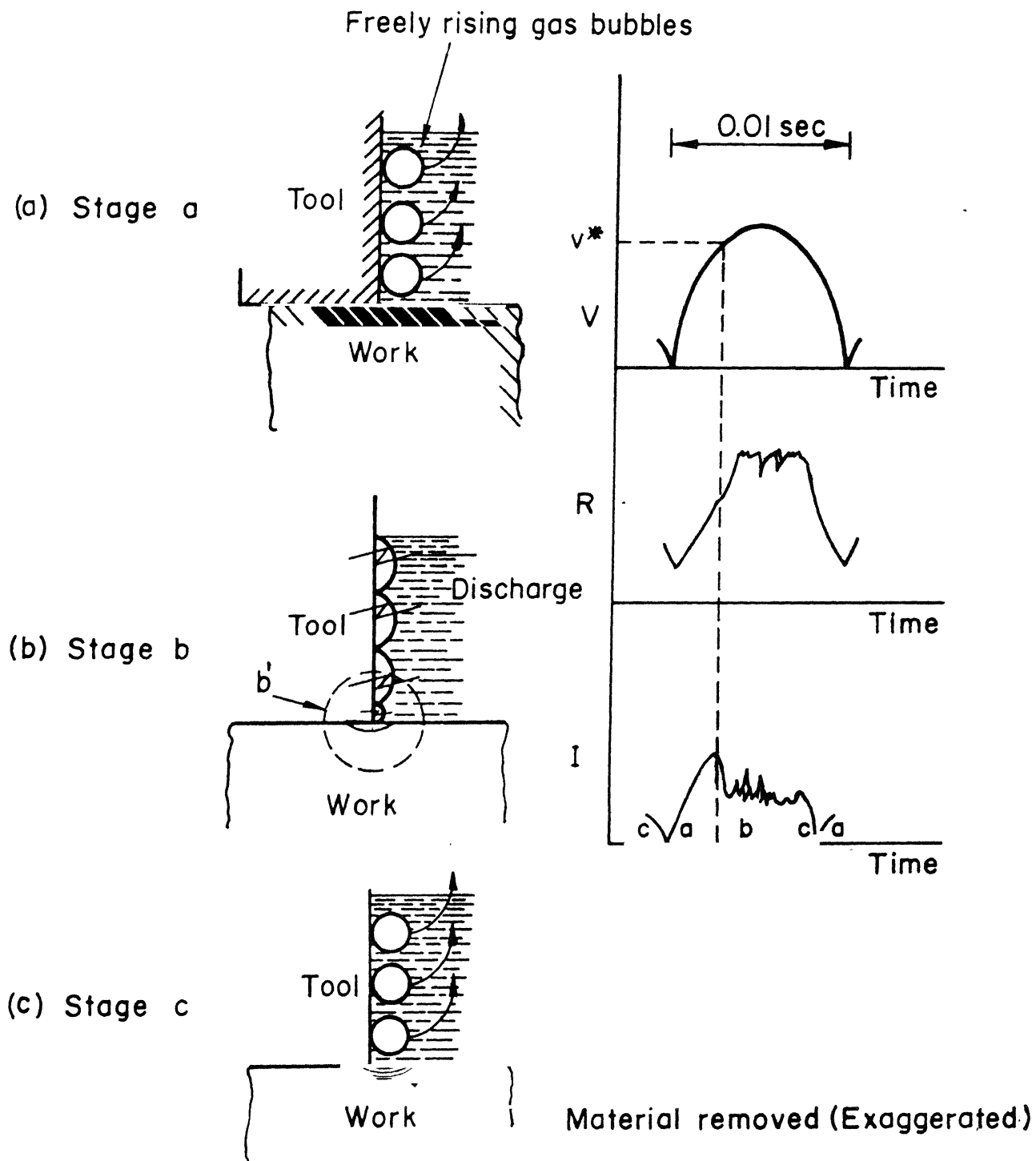
The author has attempted to identify the primary mechanism of material removal during ECDM of nonconducting materials from the results of the experiments discussed in Sections 3.3-3.8. The results of experiments discussed in Sections 3.3-3.8 yielded the primary mechanism for the behaviour observed in ECD machining of non-metals like glass. On the basis of the large number of observations in these multi-directional experiments it is felt that the combined effect of discharge and surface conduction can be identified as the main cause of material removal. This mechanism can be explained with the help of Figure 4.1 (a), (b), (c) and (d).

4.2 Proposed Mechanism

When a voltage pulse is applied, the following phases are identified on the basis of the observed current and voltage waveform during a pulse.

i) First-electrochemical phase (stage a)

The configuration at the tool work interface can be visualized as shown in Figure 4.1 (a). In this phase electrolyte is



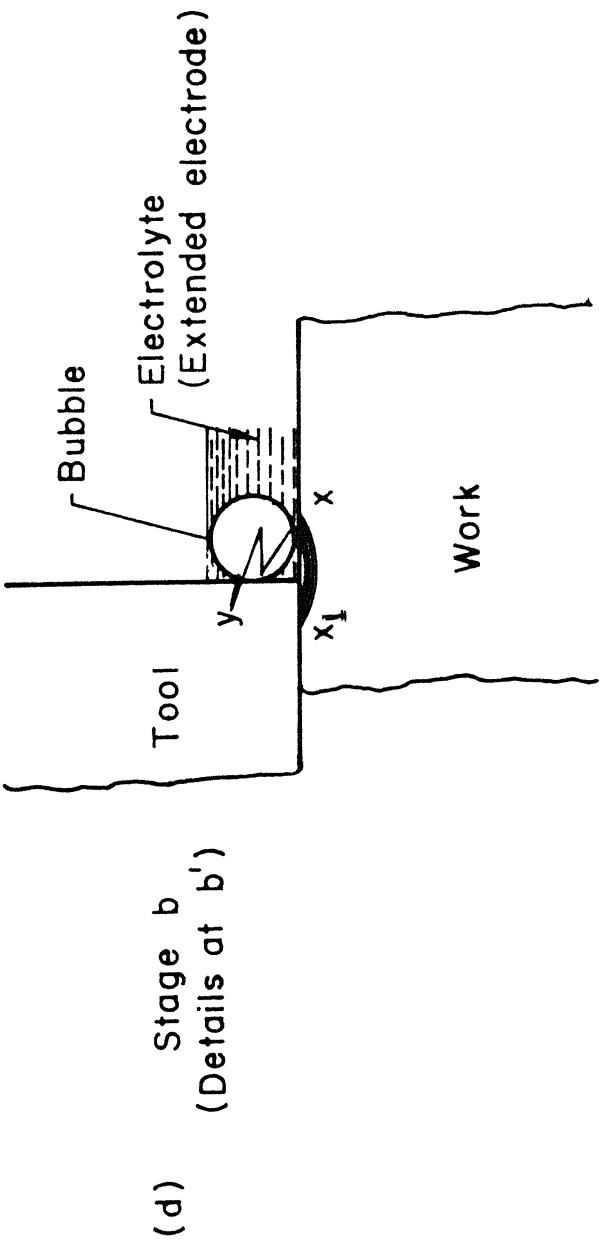


Fig. 4.1 Proposed mechanism of material removal
(Schematic)

in contact with the tool and current is carried by the electrolyte without any discharge.

ii) Discharge phase (stage b)

Electrolyte bridges boil away and vapour phase takes over and discharges occur across the vapour phase/bubbles. Concurrently, the surface activity operates because of the adsorbed electrolyte layer on the work surface. Current flows through the adsorbed layer and also because of the discharge taking place across the gas bubbles. The author wants to propose that the shift in the current profile seen in Figure 3.36 bcd is associated with the current flow through the adsorbed layer alone because, such adsorbed layers are not available with plastics and, thus, no shift was seen in these experiment.

The discharge phase has been shown in Figure 4.1 (b) and (d). It can be seen that conditions conducive to surface conduction along the interface xx_1 and discharge through xy are possible in this configuration. This results in intense heating of the work surface leading to red/orange glow at the interface. Several researchers have reported such a glow but to the best of author's knowledge none has related it to the phenomena of surface conduction. The author strongly feels that the surface conduction plays a significant role in ECD machining.

iii) Second-electrochemical phase (stage c)

When the impressed voltage approaches zero (at the end of the pulse), the electrolyte is back into its original state.

Several things are possible simultaneously :

- a) The hot surface of glass workpiece undergoes quenching leading to thermal cracking or thermal spalling. This is a very common phenomenon affecting ceramic material due to their low thermal conductivity.

Due to heating and quenching cycles, associated with the voltage pulses, the glass surface suffers thermal cracking. The material removal rate consequently increases with greater duration of the discharge phase, as has been seen at high voltage pulse. With high voltage pulses, the critical voltage (V^*) is attained earlier and, hence, for a given pulse frequency more time is available for discharge. Availability of longer discharge phase results in greater effect of surface conduction and, consequently higher material removal rate. Longer discharge phase should be available at lower frequency also and hence MRR should be higher at low frequency if surface conduction is playing a significant role. This has indeed been observed by another researcher [4]. Along with thermal cracking, leading to spalling, the higher temperature dissolution reaction of silica with sodium hydroxide can also occur resulting formation of water glass and, hence, loss of work material. This is shown by the reaction



But this reaction alone cannot account for the rate of glass removal reported by researchers and hence it is concluded that

several effects acting simultaneously are responsible for material removal. Figure 4.2 shows the contribution of several possible mechanisms for the overall material removal. Using the proposed mechanism author has found it possible to explain almost all the available observations and characteristics of various researchers particularly related to ECD machining of glass. These may be grouped as; Dependence of MRR on

- electrolyte concentration and bulk temperature,
- type of electrolyte,
- tool electrode polarity, and
- tool electrode, shape and size.

These are explained in the following sections.

4.2.1 Influence of electrolyte concentration and bulk temperature

MRR has been observed to be increasing with electrolyte concentration and bulk temperature as already seen in Figures 1.5, 1.6, 1.9 and 1.10. This behaviour can be explained as follows:

With the increase in electrolyte concentration the number of ions at the surface in the machining zone increases. Thus ionic concentration would be a function of surface adsorption property. Larger current flow can occur leading to greater heating effect and hence to increased MRR. It is interesting to see that the conductivity of an electrolyte goes through a maximum when estimated as a function of concentration (Figure 3. 16). Experimental results have shown that at very low

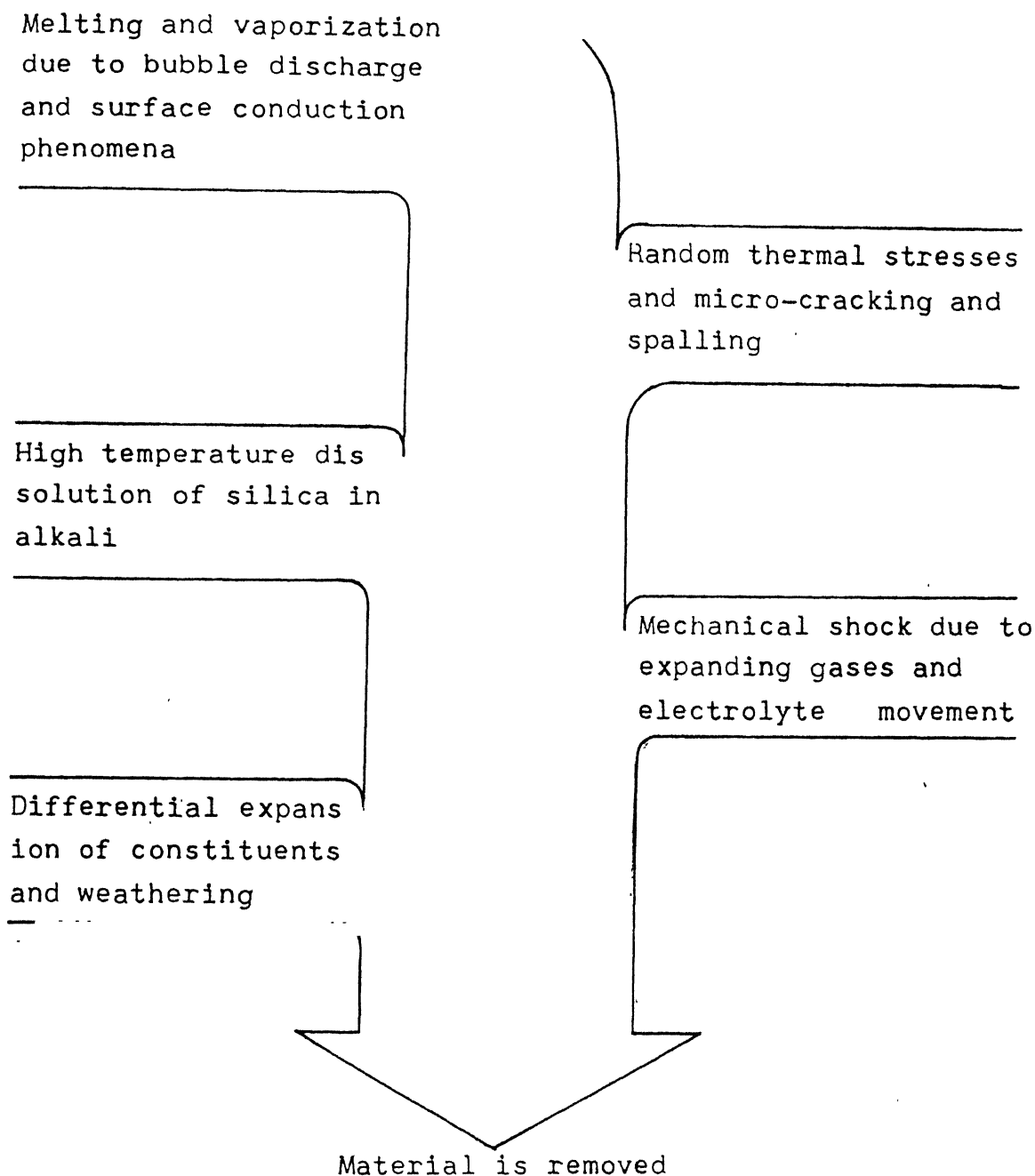


Fig. 4.2 Process of material removal in machining non-conducting materials using ECD phenomena.

concentration MRR is very low. If low conductivity of electrolyte is the cause of low MRR, similar low MRR should be observable even at higher concentrations. But the experimental results have shown otherwise. This anomaly can be explained easily by the mechanism proposed by the author in the preceding section.

Glass surface temperature being quite high in the machining zone, the conductivity of the local electrolyte is naturally very high. Consequently, the number of ions adsorbed will also be very high. On both these counts the larger current should be feasible, a feature already reported by the author (Figure 3. 16).

The wetting angle decreases with increase in temperature and the surface conduction activity should get enhanced. Hence material removal should also increase. This has been observed by various researchers. Wetting angle is thus influenced by bulk temperature, as well as the local temperature.

4.2.2 Influence of type of electrolyte

Sodium chloride is essentially an electrolyte with low conductivity as compared to say NaOH (Figure 1.12) and concentrations beyond 30% is not possible. According to the mechanism proposed by the author only low MRR is possible since ionic concentration, available for surface conduction is lesser. Adsorption of hydroxyl ions by SiO_2 is an established fact. With NaCl as the electrolyte there will be far less number of hydroxy-

ions available than in the case of NaOH. Consequently, if the phenomenon of surface adsorption is the cause of material removal, it should be lower in case of NaCl. This is indeed the observation of the author as well as of other researchers and falls in line with the proposed mechanism.

Conductivity of KOH is little higher than that of NaOH. But, the machined surface obtained is rougher than the one obtained with NaOH. The main difference which the author sees between the two alkalies is the difference in the radius of sodium and potassium ions, which is 0.097 nm for Na^+ and 0.133 nm for K^+ . Van vlack [38] has proposed how surface structure of a soda-lime glass can be modified with replacement of Na^+ by K^+ . The result is seen as a compressed surface layer on the glass. The situation is equivalent to having regions of compressive residual stresses at the machining zone.

Figure 4.3. shows how larger K^+ substituted for smaller Na^+ result in compressed regions between Potassium ions. This may lead to the production of a rougher surface and could inhibit further machining. Both these characteristics were observable to some extent in the limited experimentation with KOH, conducted by the author.

4.2.3 Tool electrode polarity

At higher voltage (> 65) the negative tool is seen to become red hot like the work and electrochemical phase

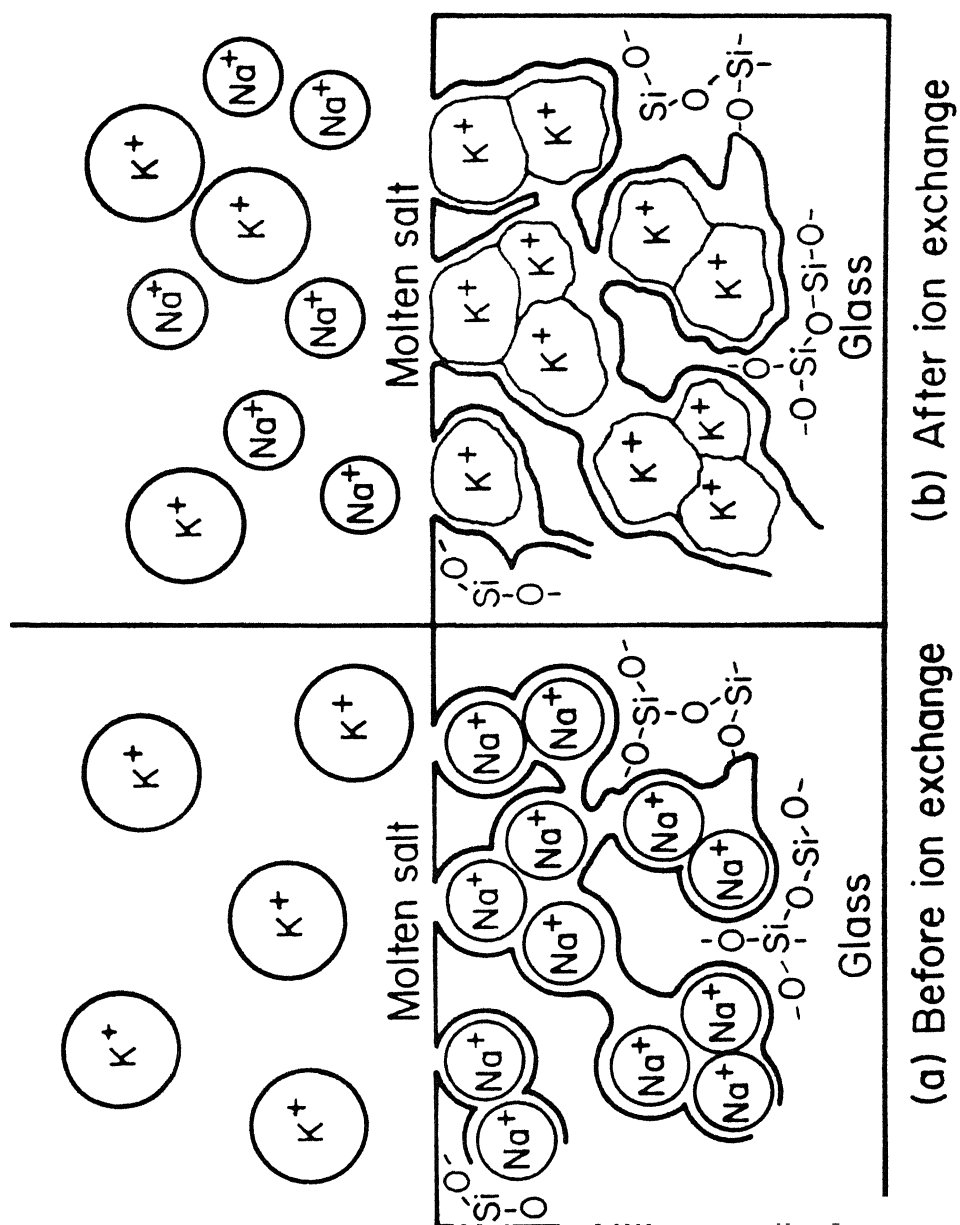


Fig. 4.3 Modification of structure (schematic) by K^+ [38]

as long as sufficient potential for discharge across the surface is available as demonstrated by the results of the study made in Section 3.5.2. With a large tool a substantial unmachined region at centre may be the result of this lack of potential.

On the other hand tools of relatively smaller diameters will be able to drill without hindrance. In particular, pointed tool with a long taper has yielded excellent results. This is in agreement with the proposed mechanism.

CHAPTER V

NON-MACHINING APPLICATIONS OF ECD PHENOMENA

5.1 Microwelding of Wires

The observations described in Section 3.4.2(a), 3.4.8(a) and 3.4.12, on the melting of the cathode tool due to the heat of ECD, induced the author to apply this ECD heat source for microwelding of wires especially for making thermocouples.

In the preliminary experimentation to study the various aspects of the weld formation, the two wires to be welded were twisted together at the end which formed the negative electrode (in place of the tool in machining). As in the machining experiments here also a graphite block was used as the anode. A voltage in the tool melting range was applied between the electrodes and the twisted end of the wires was dipped in the electrolyte for few seconds and withdrawn quickly. It was found that the two wires got welded resulting in a nice bead at the end. In NaOH solution of 20-50% concentration a voltage of 65-75 Volts with full wave rectified DC and 85-100 Volts with smoothed DC were found sufficient to form a satisfactory lead. In NaCl solution of 20% concentration a full wave rectified voltage of 80-90 Volts or a smoothed DC of 120-130 Volts were necessary to form a similar weld of good quality. Chromel-Alumel wires of 0.31 mm diameter were used for most of these experiments. The voltage requirement

was found to vary a little with wire diameters, wires of larger diameter needed higher voltage. However, with wires of larger diameters, it was observed that the bonding lacked soundness. Copper wires of < 0.5 mm diameter were also tested and found to produce good joints. The electrical continuity of these wires was found to be quite good. Thermo-e.m.f. generated by the beads produced in the present method was found to be quite the same as that generated from standard thermocouples.

Experimentation revealed that an AC source also yielded satisfactory joints. Subsequent experiments were then confined to NaCl electrolyte due to its easy availability. Different concentrations of the solution were tried and corresponding operating voltage were found out. Figure 5.1 shows the range of concentration and the voltage in which satisfactory welds were formed. When higher voltages were used with high concentration solution, the ECD was so severe that the breakage of wire occurred frequently near the bead. The average current, momentarily flowing through the circuit was about 1 amp at the upper concentration range, and was about 0.3 amps at the lower range. It was seen that the current in the circuit depends on the surface area of the twisted wire with the electrolyte. Below 2% concentration sparking was observed with 230 Volts AC but adequate melting did not take place to form a weld. The above study clearly demonstrated that 230 Volts line supply from mains can be conveniently used for microwelding, if appropriate concentration of electrolyte is chosen.

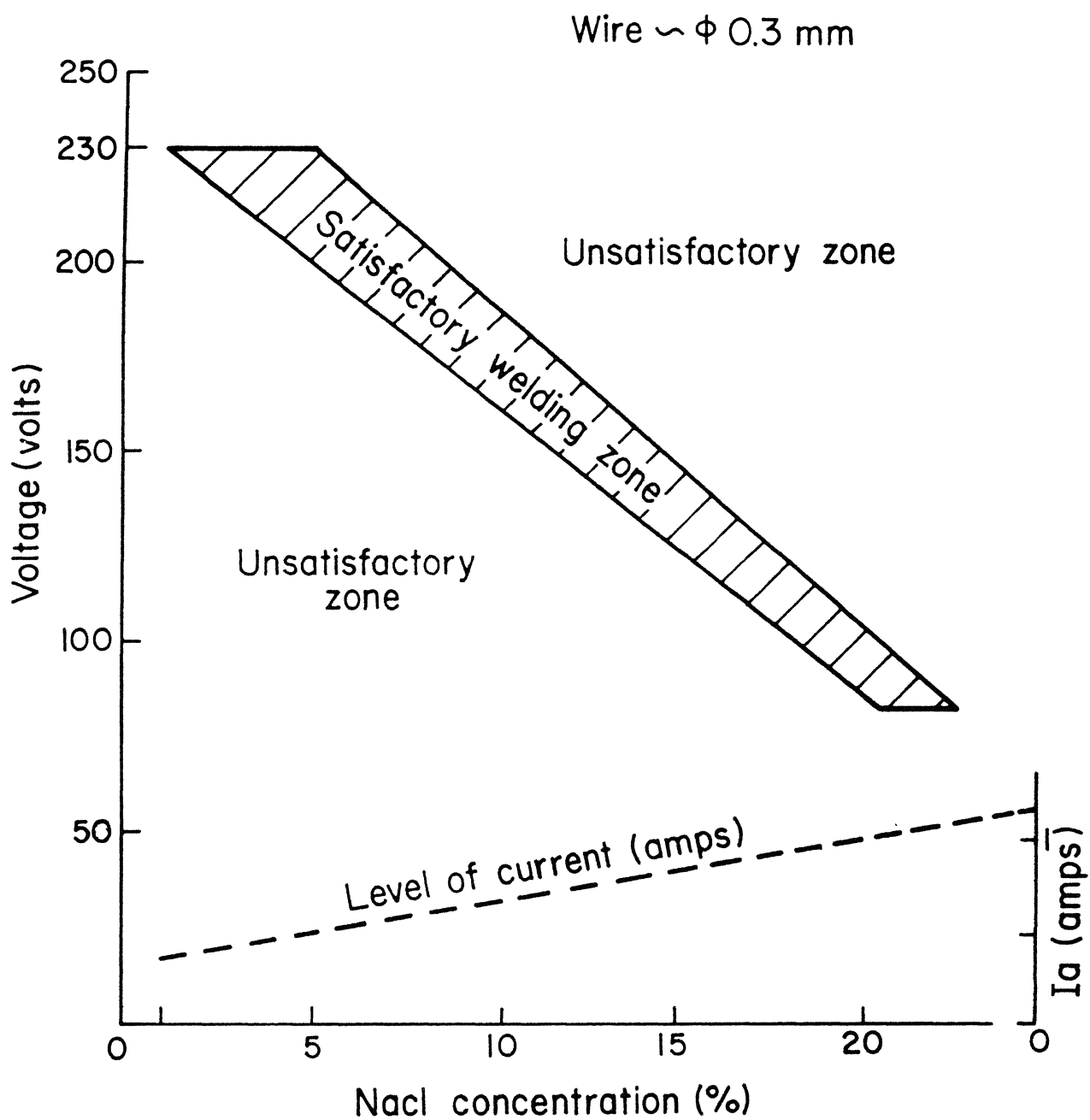


Fig. 5.1 Voltage vs. electrolyte concentration in micro-welding

In the above procedure of micro welding the operator is deciding and controlling the dipping time of the wire. Careful control of the depth of immersion of the wire in the electrolyte and time of immersion are seem to be necessary to achieve a good weld. After a large number of trials, the author could arrive at the final simplified practical method, as indicated in Figure 5.2, as the micro welding set up.

In this micro welding set up NaCl solution (2 to 5%) was used as the electrolyte and the non-sparking electrode was an ordinary insulated wire having its insulation removed at the tip. Sequence involved in micro welding was as :

1. The wire ends were twisted together firmly,
2. The wires were held in the gripper and positioned in the bath, the immersed portion of the wire in the electrolyte adjusted to about 2 mm.,
3. The power was switched on.

Result : The weld was ready within a few seconds.

The novel feature of the process is that there is no need to switch off the power supply since the molten metal at the tip assumes a globular shape and recedes upwards thereby coming out of contact with the electrolyte, switching-off the supply automatically as shown in Figure 5.2. The bead size can be controlled to a certain extent by adjusting the twisted length of the end and the length of the wire that makes contact with the electrolyte. The bead size obtained in this experiment varied from 0.5 mm to

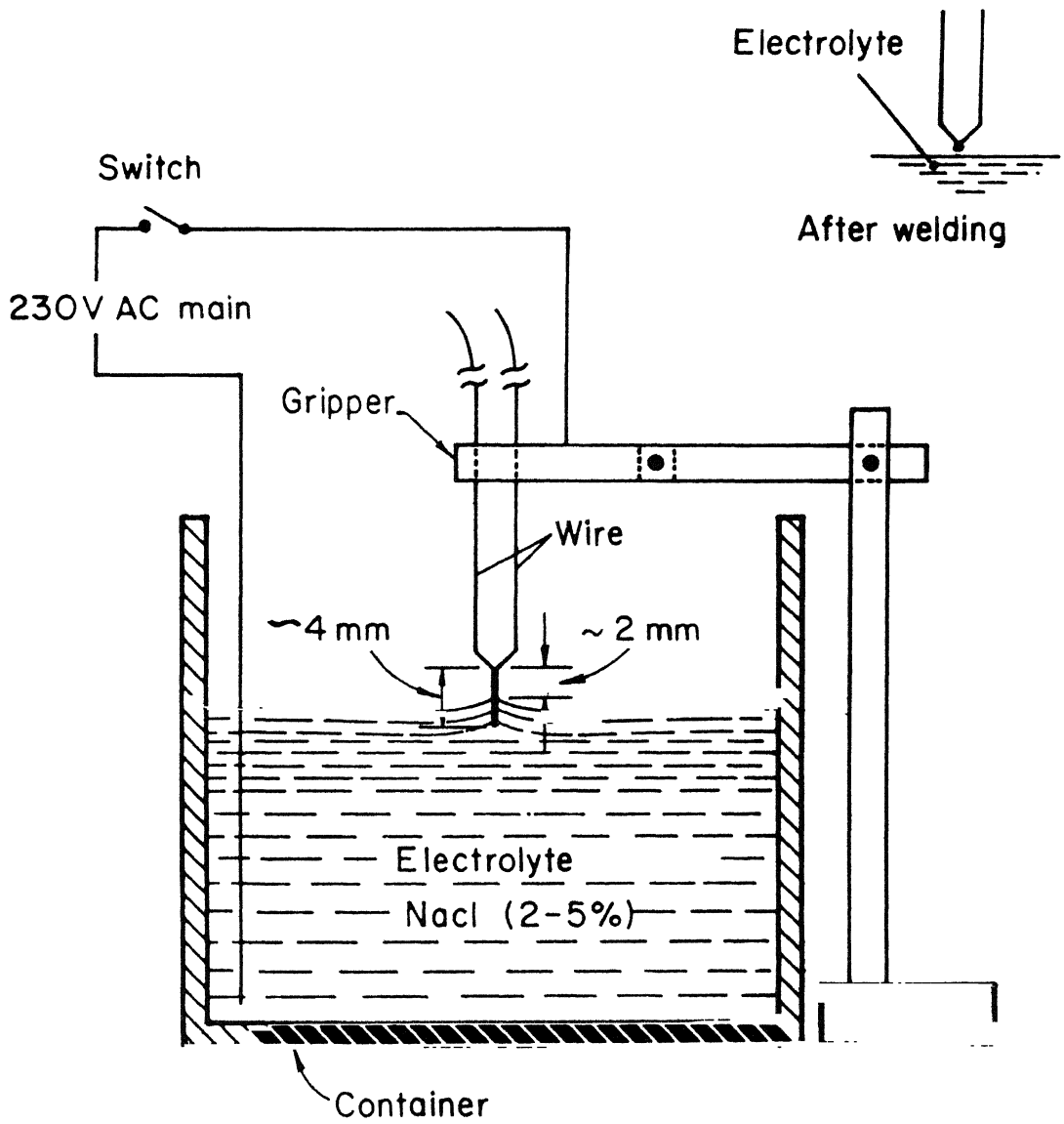


Fig.5.2 Schematics of micro-welding set-up

1.5 mm diameter. Figure 5.3 shows some of such welded joints.

Making a thermocouple joint in an ordinary shop floor involves the following steps : (i) Twisting the wires at the ends (ii) pre-heating the twisted end in an oxy-acetylene flame, (iii) dipping the twisted end in a flux, (iv) keeping the twisted end in the oxy-acetylene flame for few seconds to form the bead.

The method of producing micro welds using ECD is comparatively simpler than the usual shop-floor procedure. But the advantage in using ECD is that it does not need any costly equipment. Also it possesses semiautomatic character.

5.2 Engraving on Glass

Some of the observations related to the machining of glass led the author to devise a pen for engraving on glass surfaces. These observations are :

- (i) The position of the non-machining electrode is not a significant factor; a constant distance from the tool can give consistent results (Section 3.4.3)
- (ii) Pointed tools drill glass easily. A layer of electrolyte is sufficient to obtain a shallow hole (Section 4.2.4)

These observations, in fact, helped to drill small holes in glass using a surface layer of electrolyte and the non-machining electrode kept on the surface of glass. Under this condition, the tool movement produced marks on the surface of glass. Further attempts to improve upon the system helped in incorporating

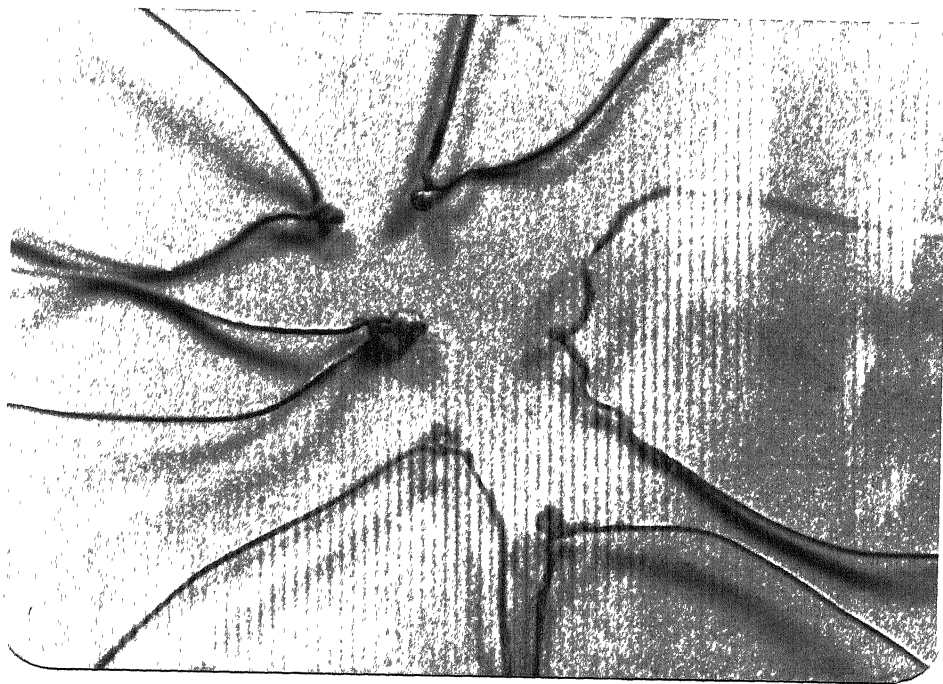


Fig. 5.3 Thermocouple Beads Prepared by ECD Phenomena

the non-machining electrode along with the tool. The tool-non-machining electrode combinations has thus formed a pen for engraving on glass surfaces. These findings actually helped to do away with the electrolyte bath.

Figure 5.4 shows the engraving pen devised by the author. A steel wire of about 0.3 mm diameter with a sharp tip (engraving tip) and approximately 3 mm square graphite rod formed the tool and the non-machining electrode, respectively. The surface of the glass is coated with a layer of NaOH electrolyte 40-60% concentration using a brush or filler, before engraving on it. To impart strength to the sharp tip of the tool, a high strength material is preferred as the tool material. Tool polarity is always negative so that no anodic dissolution of tip occurs. A full wave rectified DC voltage of 50-60 Volts seems to be satisfactory for engraving on glass-ware at the rate of about 60 alphabets per minute. Figure 5.5 shows photographs of some engravings.

5.3 Producing Fine Tapers at Wire Ends

The positive tool in the free (NaCl) electrolyte experiment (Section 3.4.12) showed accelerated dissolutions under discharge condition (at about 40 Volts). The removal rate of the positive tool under discharge condition, resembled the high removal rate of electrochemical arc machining. These feature was employed to produce a taper at wire end.

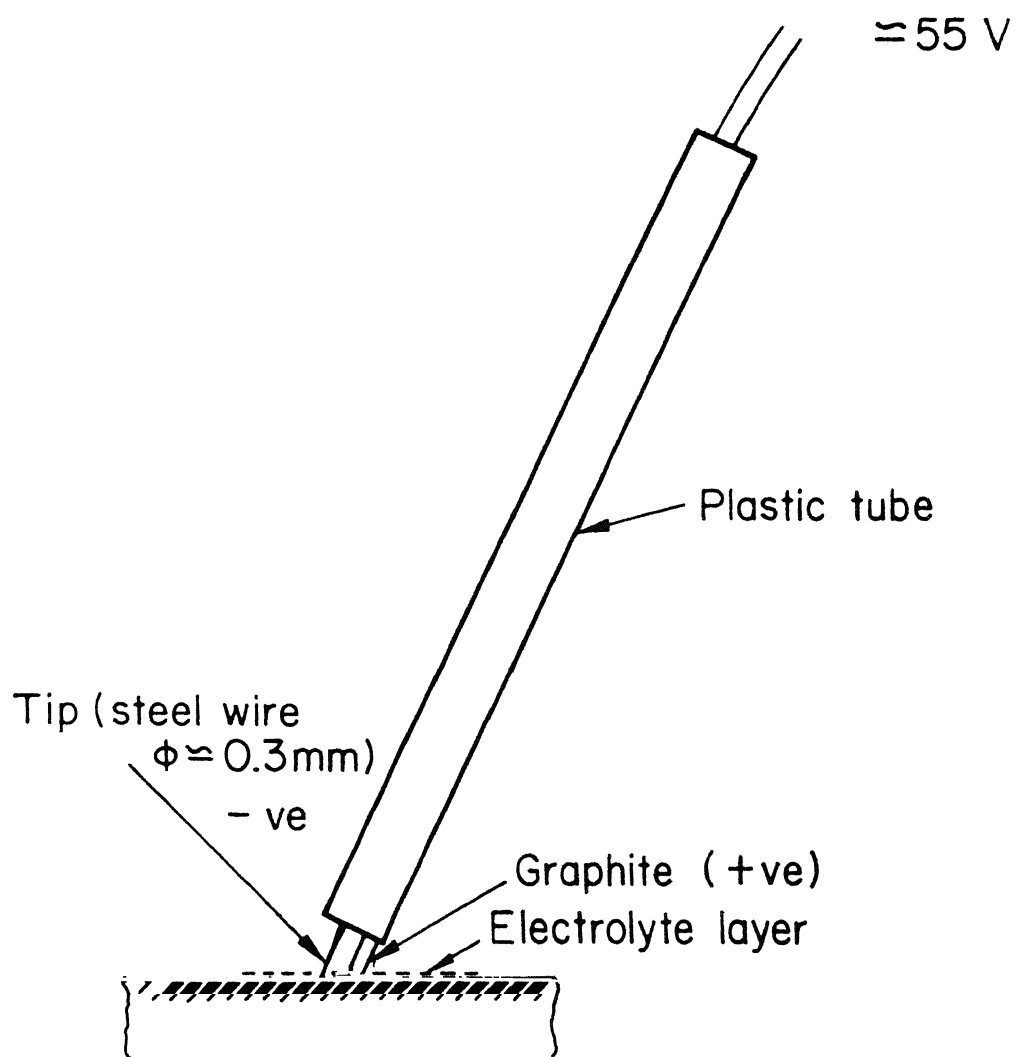


Fig. 5.4 Engraving pen



Fig. 5.5 Engravings on glass slides using ECD Phenomena

The following procedure was adopted for producing fine tips in wires. The wire was made the positive electrode. The cathode can be any wire with large electrolyte interface. By controlling the duration of discharge and imparting suitable movements (slow dipping in and taking out of the electrolyte) it was possible to produce tips with different taper angles. Long tips with very small taper angles (1:30) in wires of about 1 mm diameter were able to produce within a few seconds. The fine tip of the engraving pen (Section 5.2) and pointed tools used for drilling non-conducting materials (Section 4.2.4) were produced by this method.

CHAPTER VI

CONCLUDING REMARKS

Based on the observations and discussions in the preceding chapters the following major conclusions can be drawn :

- 1) The adsorption property of the electrically non-conducting work materials is one of the key factors in deciding the machining characteristics. This is not in accordance with the common hypothesis that bubble discharge is the main cause of erosion.
- 2) The limitation of depth in drilling and the unmachined region at the central portion of larger tools is essentially caused by the non-availability of sufficient potential needed to trigger a discharge and create the surface conduction phenomenon.
- 3) Material removal rate using Sodium hydroxide electrolyte is larger compared to all other electrolyte primarily because the ionic activity with NaOH is more vigorous than with others. Same reason can be attributed for higher material removal rate with higher concentration or temperature.
- 4) A negative tool gives a good finish, while a positive tool consumes itself.
- 5) A positive tool also results in higher material removal rate essentially because it can be operated at much higher voltages.

- 6) Material removal rate in case of materials with low wetting angles is high and it is low for materials with high wetting angles.
- 7) The higher heat generation within the surface of glass can be utilized for the purpose of engraving on its surface.
- 8) ECD phenomenon can be used for non-machining applications like microwelding very conveniently.

References

1. Kurafuji, H. and Suda, K.: 'Electrical Discharge Drilling of Glass-I,' Annals of the C.I.R.P. Vol. XVI 1968, pp. 415-419.
2. Cook, N.H., Foote, G.B., Jordan, P. and Kalyani, B.N.: 'Experimental Studies in Electro-Machining,' Journal of Industry, 1973 pp. 945-950.
3. Umesh Kumar, N.: 'An Experimental Study of Electrical Machining of Non-Conducting Materials,' M.Tech. Thesis, I.I.T. Kanpur, 1985.
4. Tsuchiya, Hachiro, Inoue, Tomoichi and Miyazaki, Makato: 'Wire Electro-Chemical Discharge Machining of Glass and Ceramics,' Bull. Japan Soc. of Prec. Engg., Vol. 19, No.1 1985 pp. 73-74.
5. Allesu, K., Umesh Kumar, N., Muju, M.K. and Ghosh, A.: 'Some Investigations into the Spark Machining of Non-Conducting Materials,' 12th AIMTDR Conference, IIT Delhi: 1986, pp. 521-524.
6. Tandon, Sanjeev: 'Machining of Composites, A New Approach', M.Tech. Thesis, IIT Kanpur, July, 1987.
7. Sreenivasa Rao: 'Application of Travelling Wire-ECSM for Machining of Composites,' M.Tech. Thesis, IIT Kanpur, Oct. 1988.
8. Drake, T.H. and McGeough, J.A.: 'Aspects of Drilling by Electro-Chemical Arc Machining,' Proc. Mach. Tool Des and Res Conference Manchester, 1981, pp. 361-369.

9. McGeough, J.A., Khayry, A.B.M. and Munro, W.: 'Theoretical and Experimental Investigation of the Relative Effect of Spark Erosion and Electrochemical Dissolution in Electrochemical Arc Machining,' Annals of the CIRP Vol. 32/1/1983, pp. 113-117.
10. Crichton, I.M. and McGeough, J.A.: 'Studies of the Discharge Mechanisms in Electrochemical Arc Machining,' Journal of Applied Electrochemistry 15 (1985) pp. 113-119.
11. Khayry, A.B.M. and McGeough, J.A.: 'Modelling of Electrochemical Arc Machining by Use of Dynamic Data Systems,' Proc. 25th Int. Machine Tool Design and Research Conference 1985 pp. 321-328.
12. Silva, de. A. and McGeough, J.A.: 'Surface Effects on Alloys Drilled by Electrochemical Arc Machining,' Proc. Instn. Mech. Engrs. Vol. 200, No. B4 1986 pp. 237-245.
13. Khayry, A.B. and McGeough, J.A.: 'Analysis of Electrochemical Arc Machining by Stochastic and Experimental Methods,' Proc. R. Soc. Lond. A 412 (1987) pp. 403-429.
14. Crichton, I.M., McGeough, J.A., Munro, W. and White, C.: 'Comparative Studies of ecm, edm and ecam,' Precision Engineering, 1981 pp. 155-160.
15. Ghosh, Amitabha and Mallik, A.K.: 'Manufacturing Science' Affiliate East-West Press Pvt.Ltd., New Delhi 1986.
16. Pandey, P.C. and Shan, H.S.: 'Modern Machining Processes,' Tata McGraw-Hill Publishing Company Ltd., 1980.

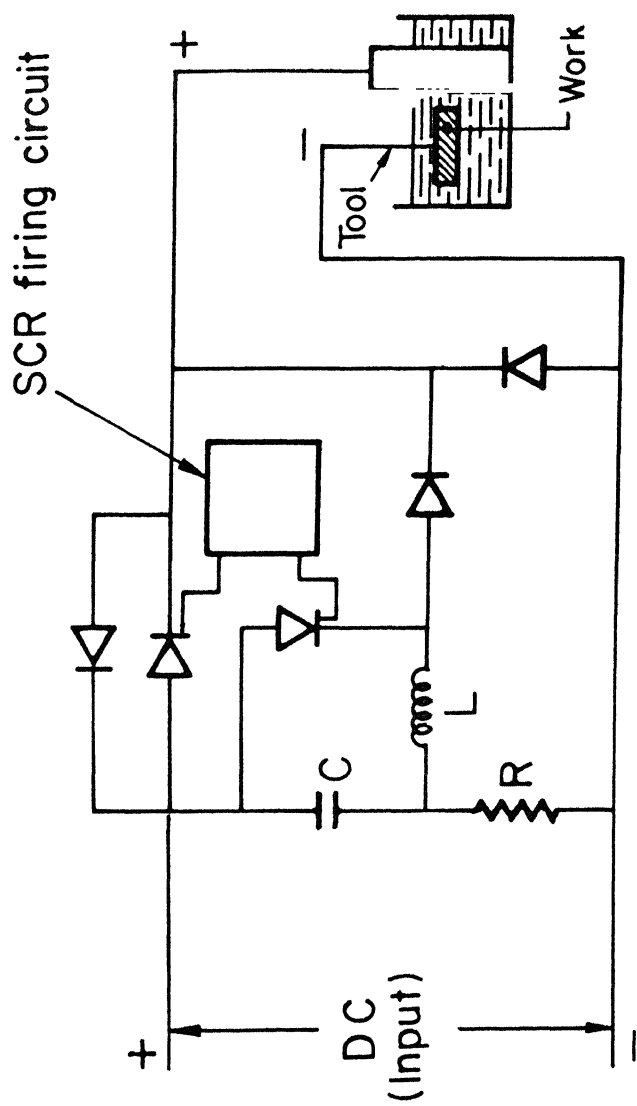
17. Bhattacharyya, Amitabha: 'New Technology,' The Institution of Engineers (India) 1973, pp. 121
18. Kellock, Brian: 'EDM: Controversy Stimulates Progress,' Machinery and Production Engineering, May, 1982, pp. 18-22.
19. Erden, A. and Bilgin, S.: 'Role of Impurities in Electric Discharge Machining:' Proc. 21st Int. Mach. Tool Des and Res. Conference 1980, pp. 345-350.
20. Heuvelman, C.J., Horsten, H.J.A. and Veenstra, P.C.: 'An Introductory Investigation of the Breakdown Mechanisms in Electro-Discharge Machining,' Annals of the CIRP Vol. 20/1 1971, pp. 43-44.
21. Crookall, J.R.: 'Electro-Discharge Machining-the State-of-the-Art,' CIRP, Vol. 20, 1971, pp. 113-120.
22. McGeough, J.A.; 'Principles of Electrochemical Machining,' Chapman and Hall London 1974.
23. Debarr, A.E. and Oliver, D.A.: 'Electrochemical Machining,' American Elsevier Publishing Company, Inc., New York 1968.
24. Loutrel, S.P. and Cook, N.H.: 'High Rate Electrochemical Machining,' Transactions of the ASME November 1973, pp.992-996
25. Krasnyuk, B.A.: 'Electrospark Machining of Metals,' (Volume 3) Consultants Bureau New York 1965, pp. 72.
26. Larsson, C.N. and Baxter, E.M.: 'Tool Damage by Sparking in ECM,' IMTDR, 1977, pp. 499-505.
27. Ebeid, S.J., Baxter, E.M. and Larsson, C.N.: 'Further Effects of Process Parameters on the Incidence of Sparking in Electrochemical Machining,' Proc. 19th International Mach. Tool des. Res. Con. 1978, pp. 511-516.

28. Kubota, Mamoru and Tamura, Yuji,: 'ECDM Drills a Steel Plate with High Feed Rate,' Japan Soc. of Prec. Engg. Vol. 7, No.4 (Dec. 1973), pp. 117-118.
29. Novak, P., Sajdl, B. and Rousar, I.: 'Sparking at Cathode Tools During Electrochemical Drilling,' Electrochimica Acta, Vol. 30, No.1, 1985, pp. 43-49.
30. Ramachandran, K.I.: 'An Experimental Investigation into Electrochemical Arc Machining of HSS,' M.Tech. Thesis, IIT Kanpur, Oct. 1988.
31. Horvath, A.L.: 'Handbook of Aqueous Electrolyte Solutions,' Ellis Horwood Limited, New York, 1985, pp. 270
32. Martin, W.W. and Chandler, G.M.: 'The Local Measurement of Size and Velocity of Bubbles Rising in Liquids,' Applied Scientific Research, Vol. 38, 1982, p. 240.
33. Bhatt, D.B., Krishnamoorthy, R. and Venkatesh, V.C.: 'Performance of Some Electrolytes and Effects of Temperature and Concentration of Electrolyte in the Engraving Application of Electrochemical Machining,' Proceedings of 9th AIMTDR Conference, I.I.T. Kanpur (Dec. 1980), pp. 351-355.
34. James Dillion Cobine.: 'Gaseous Conductors' Dover Publications Inc., New York (1958), p. 163.
35. Dietz H. Gunther, K.G. Otto, K.: 'Electrochemical Machining: Calculation of side gap with respect to hydrogen evolution', Annals of the CIRP, Vol. 23 (1974), pp. 45-46.
36. Robinson R.A. and Stokes, R.H.: 'Electrolyte solutions', London Butterworth (1959), p. 311.

37. Dele Rue, R.E. and Tobias, C.W.: J. Electrochem. Soc. Sept. (1959), p. 827.
38. Lawrence H. Van Vlack.: 'Materials for engineers', Addison-Wesley Publishing Company, Inc., Amsterdam (1982), pp. 525, 364.
39. Lawrence, H. Van Vlack.: 'Physical ceramics for Engineers', Addison-Wesley Publishing Company, Inc., Amsterdam (1964), p. 191.
40. Tareev, B.: 'Physics of dielectric materials', MIR Publishing Moscow (1975), p. 65.
41. Davies, J.T., Rideal, E.K.: 'Interfacial phenomena', NewYork Academic Press (1961) p. 37.
42. Helisto, P., Helle, A.S. and Pietikainen, J.: 'Interface phenomena between oxide layers and cemented carbide tools', Ist International Conference on the Behaviour of Materials in Machining, Stratford-upon-Avon, 8th-10th Nov. 1988, pp. 1-16.
43. Farmer, W.M.: 'Measurement of particle size, number density, and velocity using a laser interferometer', Applied Optics, No. 11, Vol. 11, Nov. 72, pp. 2603-2612.

APPENDIX

Figure A-1 shows the low frequency pulse supply based on silicon controlled rectifier firing circuit and Figure A-2 shows the high frequency pulse supply based on transistor switching circuit used in the course of work.



Pulse frequency : 40 – 125, c/s
On-time : 0 – 100, %

Fig.A-1 Pulsed D.C. circuit

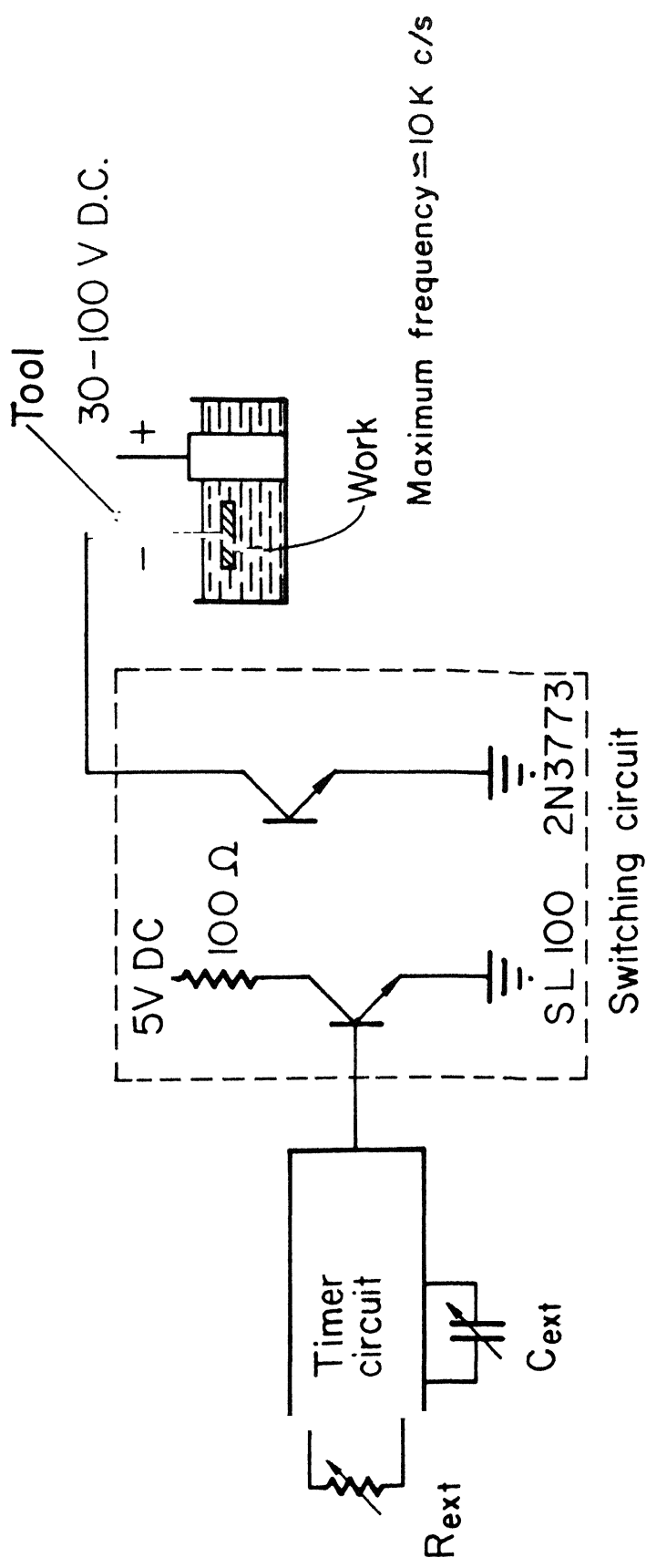


Fig. A•2 High frequency pulse circuit

Bubble size measurement using laser interferometry (Section 3.3.

A method proposed by Farmer [43] has been used to determine the diameter of the bubbles generated at the electrode in a NaOH (35%) solution. The arrangement for the measurement is shown in Figure A.3. The principle of the measurement is based on the non-uniform illumination of a particle by a set of spatially well defined interference fringes generated by two crossed laser beams. The laser beam from the Helium-Neon laser (5 mW) is split into two beams, using a beam splitter, of equal intensity that are brought to a simultaneous cross-focus point by a lens. The bubbles are generated in an electrolytic cell filled with the electrolyte, NaOH (35%), by applying a DC (smoothed) voltage. The diameter of hydrogen bubbles generated at the cathode are measured. The bubbles generated at the anode are conveniently separated from the chamber using a bent tube as shown in the figure. The scattered light from the interaction region with the bubble is focussed on a photo multiplier tube (PMT), output of which is displaced on a CRO. The fringe visibility, S is defined as the ratio of AC to DC of the signal, i.e., Fringe visibility, $S = \frac{AC}{DC}$ of the signal: Interference fringe spacing

$$\delta = \lambda / \beta$$

where λ = wavelength of the light used

β = angle between the beams

S can be approximated as

$$S = 2 J_1 (2\pi a/\delta) / (2\pi a/\delta)$$

where J_1 is a first order - Bessel function and 'a' is the bubble diameter.

Based on this, plots are available for S vs $2\pi a/\delta$

Large number of readings of AC of the signal were noted experimently.

Average AC of the signal = 10 Volts

DC of the signal = 50 Volts

Visibility, $S = \frac{10}{50} = 0.2$

for $S = 0.2$, from [43]

$$\frac{2\pi a}{\delta} = 3$$

Angle $\beta/2 = \frac{2.5}{22.5}$ (from the focal length of lens)

\therefore Bubble diameter, $a = \frac{3\delta}{2\pi}$

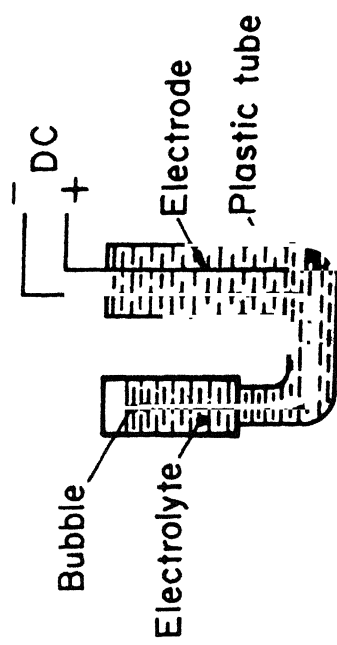
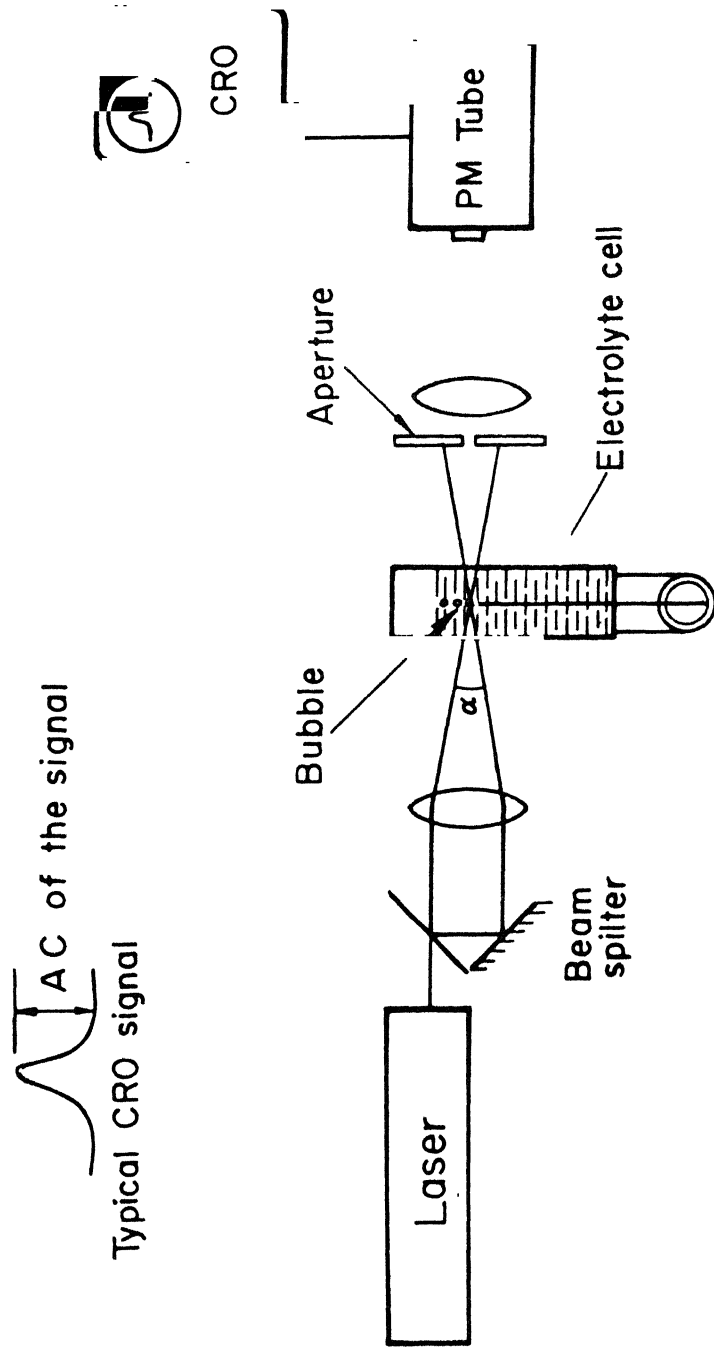
Substituting for δ ,

$$a = \frac{3 \lambda/\beta}{2\pi}$$

Wavelength of the light used, $\lambda = 6328 \times 10^{-10} \text{ m}$

$$\begin{aligned} \therefore a &= \frac{3 \times 6328 \times 10^{-10}}{2\pi \times 2.5 \times 2} \times 22.5 \\ &= 1.36 \times 10^{-6} \text{ m} \\ &= 1.36 \text{ } \mu\text{m} \end{aligned}$$

This value of bubble diameter corresponds to low voltage (< 5 Volts) levels. At higher voltages, since the bubbles were clustering together, it was not able to make reliable measurements.



Electrode connections

Fig. A-3 Schematics of set-up for
Bubble dia. measurement

